CHARACTERIZATION OF FACTORS
CONTROLLING GERMLINE STEM CELL MAINTENANCE
IN *Drosophila melanogaster*

APPROVED BY SUPERVISORY COMMITTEE

_____
Dennis McKearin

_____
Keith Wharton

_____
Eric Olson

_____
Qinghua Liu

CHARACTERIZATION OF FACTORS CONTROLLING GERMLINE STEM CELL MAINTENANCE IN *Drosophila melanogaster*

Joseph Kwang Park

DISSERTATION

Presented to the Faculty of the Graduate School of Biomedical Sciences
The University of Texas Southwestern Medical Center at Dallas, 2007
In Partial Fulfillment of the Requirements
For the Degree of

DOCTOR OF PHILOSOPHY

The University of Texas Southwestern Medical Center at Dallas
Dallas, Texas
July 2007

DEDICATION

For my father and mother, Chon and Kyung Park,
who sacrificed everything to provide me every opportunity,
whose wisdom and guiding hand helped to direct my life,
and whose love and support continually encourage me to succeed.

ACKNOWLEDGEMENTS

The works presented in this dissertation could not have been performed without the constant guidance and encouragement from my research mentor, Dennis McKearin. During my time in the lab, he has always shown great interest in my research and taken time to show me how to think like a rigorous scientist. I have also benefited greatly from the mentoring and interactions with Jean Maines, without whom my development as a researcher would be incomplete. Additionally, my interactions with Qinghua Liu have instilled in me a focused work ethic and an all-encompassing approach to science. I have been lucky to have three wonderful mentors to guide my scientific development and I am forever indebted to them for their time, support, and friendship.

I would also like to acknowledge the members of the McKearin lab who have made my training experience a wonderful one. Senior scientists and lab members – including, but not limited to, Mary Kuhn, Dahua Chen, Jean Maines, Yun Li, and Xiang Liu (Qinghua Liu's lab) – have instructed me in innumerable experimental techniques and provided guidance, friendship, and advice. All of the past and present members of the McKearin lab have made my time spent at the bench both rich and meaningful, through stimulating conversations about science, politics, and current affairs – all against the incessant backdrop of NPR. And, despite their relative indifference toward the national pastime, I also thank the lab for tolerating the occasional baseball broadcast on the radio. Through all this, they provided a wonderful niche in which to conduct science and I thank them for their enduring kindness and friendship.

I would also like to thank the Fly community and the KWAM group at UT Southwestern, especially the contributions of Leon Avery, Scott Cameron, Rene Galindo, and Helmut Krämer. The openness, curiosity, and genuine interest within the KWAM group have provided for critical

analysis of my work and wonderful scientific discussions, forming a crucial component of my training. Similarly, I thank Qinghua Liu's laboratory for engaging with the McKearin lab in a collegial and fruitful collaboration; I hope that the two labs will continue to enrich each other's scientific progress for many more years. Additionally, I extend my gratitude to everyone affiliated with the Medical Scientist Training Program for financial, scientific, and moral support, especially Drs. Mike Brown, Dennis McKearin, Robert Munford, and Rod Ulane, and Ms. Robin Downing and Stephanie Robertson. Lastly, I would like to thank my committee members – Drs. Eric Olson, Qinghua Liu, Keith Wharton, and Dan Garry – who provided me with critical comments about my research and expressed a genuine interest in my scientific development.

Most importantly, I could not have completed my studies without the love and support from my family. My parents, Chon and Kyung Park, sacrificed everything by immigrating to the U.S. to provide my brother, Aaron, and me with unlimited opportunities. Though they are sometimes perplexed by my career choices, my family provides constant support and encouragement to do my best. Finally, my partner, Nancy Srebro, has always believed in my abilities and supported me through difficult times. Though she hasn't always understood the details of my research, she always took a genuine interest in my work and gave me the strength to complete my studies through her encouragement and support.

Submitted to the committee in July, 2007

CHARACTERIZATION OF FACTORS CONTROLLING GERMLINE STEM CELL MAINTENANCE IN *Drosophila melanogaster*

Publication No. _____

Joseph Kwang Park, Ph.D.

The University of Texas Southwestern Medical Center at Dallas, 2007

Supervising Professor: Dennis M. McKearin, Ph.D.

During *Drosophila* oogenesis, a germline stem cell (GSC) divides asymmetrically to produce a renewed stem cell and a differentiated daughter cystoblast (CB) that will progress through the 14 stages of oogenesis to produce a mature egg. A myriad of factors regulate GSC maintenance; extrinsic signals from the somatic niche integrate with intrinsic GSC factors to control CB differentiation pathway. In particular, studies of a key differentiation factor, *bam*, underscored the important paradigm of maintaining GSC by preventing the initiation of the CB differentiation pathway. The Dpp/BMP signaling pathway from the GSC niche promotes quiescence of bam transcription in the GSC. In the differentiating CB, *bam* transcription is initiated and Bam protein, together with its protein partner Bgcn, functions to antagonize the translational repression mediated by Pumilio-Nanos (Pum-Nos) complexes. Repression of Pum-Nos activity by Bam-Bgcn complexes permits CB differentiation, presumably through the derepression of CB-promoting mRNAs.

In this study, I investigated the transcription- and translation-dependent mechanisms controlling the GSC to CB transition. Through genome-wide expression profiling experiments, I showed that there are only minimal transcriptional differences between the GSC and CB. This supports previous studies that highlight the importance of translational repression in maintaining a GSC state. However, some of the transcriptional differences between the undifferentiated GSC and differentiated germ cells were uncovered by expression profiling experiments of germ cells lacking Stonewall (Stwl), a protein required for GSC maintenance through epigenetic regulation of CB-promoting genes. Data from gene profiling experiments of *stwl bam* and *bam* mutant germ cells suggest that a suite of genes is normally repressed by Stwl to maintain a GSC fate.

In addition, I examined whether putative "stemness" genes identified from mammalian systems also affected *Drosophila* GSC fate using a pilot screen in a hypomorphic *bam* background. Components from the COP9 signalosome complex (CSN) and the SCF E3 ubiquitin ligase complex were identified as dominant Suppressors of *bam*, Su(*bam*). Since both the CSN and SCF complexes are involved in protein degradation, the suppression of the *bam* phenotype suggests that they may be involved in stabilizing Bam function through abrogation of Bam turnover. Indeed, though ubiquitinated Bam isoforms were not identified, the abundance of Bam protein was increased in Su(*bam*) heterozygous animals.

In other studies, I examined the requirement for the microRNA pathway in GSC maintenance through the examination of the double-stranded RNA-binding protein Loquacious (Loqs). Loqs enhances Dicer-1's ability to process pre-miRNA hairpin moieties to mature miRNA duplexes. Loqs is required for viability and germline mosaic analysis of *loqs* GSCs indicates an intrinsic, cell-autonomous requirement for the miRNA pathway in GSC maintenance. Loqs localizes to putative RNP complexes and a specialized region of the oocyte

cytoplasm, termed the pole plasm. These data suggest that Loqs is a component of protein-RNA complexes that may be involved in mRNA translational inhibition.

In summary, my studies revealed that GSC maintenance is achieved through the repression of CB-promoting factors; epigenetically through the actions of Stwl and other histone-associated proteins and translationally through the actions of the miRNA pathway via Loqs and Dicer-1. My studies provide insights into the understanding of the CB-promoting factors that are held inactive in the GSC and suggest that other stem cell systems may similarly employ multiple layers of repressive mechanisms to maintain a stem cell state.

TABLE OF CONTENTS

PUBLICATIONS

Park, J.K., Liu, X., Strauss, T.J., McKearin, D.M., and Liu, Q. (2007). The miRNA pathway intrinsically controls self-renewal of *Drosophila* germline stem cells. *Current Biology* **17**, 533-538.

Maines, J.Z., Park, J.K., Williams, M., and McKearin, D.M. (2007). Stonewalling *Drosophila* stem cell differentiation by epigenetic controls. *Development* **134**, 1471-1479.

LIST OF FIGURES

LIST OF TABLES

Chapter 1. Introduction

I. Rationale for investigations

Our lab uses *Drosophila* oogenesis as a model system to examine mechanisms controlling stem cell maintenance and differentiation. The female germline stem cell (GSC) undergoes asymmetric cell divisions to produce a renewed GSC and a differentiated daughter cystoblast (CB), a process that maintains continuous egg production that gives rise to future progeny. Many labs have focused their attention on the multitude of factors that regulate GSC maintenance. These studies have been greatly advanced through the use of immunofluorescence-based histochemistry, allowing for rapid identification of GSCs in their stereotypical position in the ovary. In addition, we can utilize the benefits of *Drosophila* as a genetic model system to uncover additional genes that regulate GSC differentiation.

Recent understanding of the molecular pathways that control GSC maintenance has allowed for a systematic approach to the identification of additional genes that regulate GSCs. Through the combination of global expression profiling and genetic screens, I have identified genes previously uncharacterized as GSC maintenance and differentiation factors.

In addition, detailed understanding of the molecular circuitry controlling GSC fate has provided the framework to examine other factors that regulate GSC biology. In particular, I have been able to broaden our understanding of GSC maintenance and the emerging areas of microRNA-mediated translational control as well as epigenetic regulation through histone modifications.

II. Germline stem cells reside in a niche and are maintained by *bam* transcriptional repression

Stem cells are defined by their ability to undergo self-renewing divisions that produce non-equivalent daughter cells. During *Drosophila* oogenesis, the GSC undergoes asymmetric divisions to produce a renewed GSC and a differentiated daughter cystoblast (CB). Studies from many laboratories demonstrate that GSC maintenance is accomplished by a host of factors that regulate the ability of the GSC to produce a continuous supply of germ cells that will undergo oogenesis. The research examining the *Drosophila* GSCs has provided widespread insights into the mechanisms controlling stem cell populations in other systems. For example, the paradigm of stromal cell microenvironment that supports stem cell biology has its origins from the studies of the somatic cap and hub cells that support the maintenance and differentiation of both female and male *Drosophila* GSCs (Gilboa and Lehmann, 2004; Spradling et al., 2001).

Figure 1.1: Schematic illustration of cell types of the germarium.

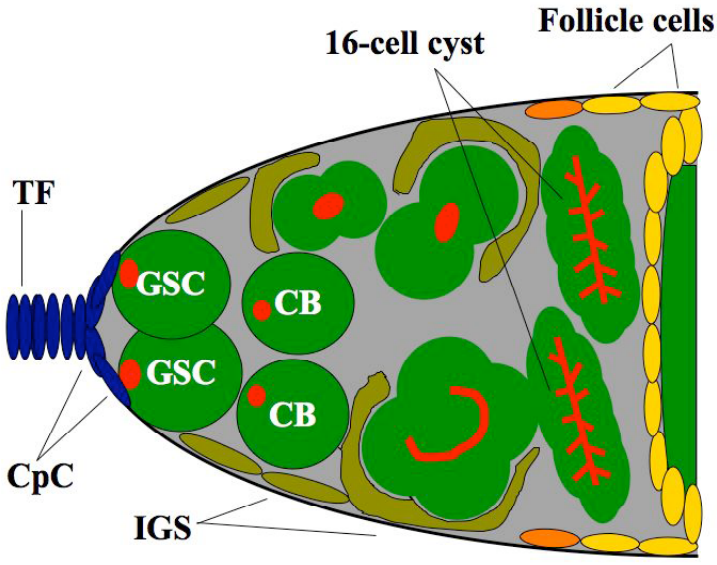

The terminal filament (TF) cells, cap cells (CpC), inner germarial sheath (IGS) cells collectively form the somatic GSC niche. The germline stem cells (GSCs) are located at the anterior end of the germarium, contain round, anteriorly-positioned fusomes (red), and contact the CpCs. The differentiated daughter cystoblast (CBs) are displaced away from the niche, divide four times with incomplete cytokinesis to form a 16-cell syncitial cyst that becomes enveloped by an epithelial layer of follicle cells to form the nascent egg chamber, the defined unit of *Drosophila* oogenesis.

The GSCs are located at the anterior end of the ovary in a specialized structure termed the germarium (Figure 1.1). GSCs are closely apposed to the somatic cap cells and terminal filament cells that form the somatic niche that supports GSC function (Spradling et al., 2001). Key insights from research into GSC maintenance reveals an integrated circuitry in which both extrinsic and intrinsic factors interact to regulate GSC maintenance (Li and Xie, 2005). A key factor regulating GSC maintenance and differentiation is *bam*, a gene required for GSC-to-CB differentiation. In females lacking *bam*, the GSCs are unable to differentiate and instead continue to divide symmetrically producing a germ cell hyperplasia that fills the germarium (McKearin and Ohlstein, 1995). Ectopic expression of *bam* results in the forced elimintation of GSCs from the germarium by precocious differentiation (Ohlstein and McKearin, 1997). Result studies have shown that *bam* transcription in the GSCs is targeted by a Dpp/BMP signal from the cap cells that form the niche. Dpp ligand is secreted from the cap cells and signal to the GSC to repress *bam* transcription (Chen and McKearin, 2003a). In the GSC, the Dpp signal is transduced through the Smad receptors Punt and Thickveins (Tkv), allowing for phosophorylation of Mad (pMad) and subsequent formation of pMad:Medea complexes. Importantly, a discrete silencer element was identified in the *bam* promoter that integrates the pMad:Med signal to silence *bam* transcription (Chen and McKearin, 2003b).

During the asymmetric GSC division, the CB daughter cell is displaced away from the GSC niche along the anterior-posterior axis and, consequently, away from the source of Dpp signal (Kai and Spradling, 2003; Xie and Spradling, 1998). The proposed model of the GSC-to-CB differentiation suggests that as the intermediate precursor to the CB (pre-CB) moves away from the niche, diminished Dpp leads to a drop in pMad levels, a dissociation of pMad:Med complexes and a concomitant derepression of *bam* transcription. This results in the accumulation

of Bam protein, which binds to its protein partner Bgcn (Benign gonial cell neoplasm) and initiates the CB differentiation pathway. Accordingly, the *bam*-dependent transcriptional difference between the GSCs and CBs implies that GSC differentiation is controlled by other transcriptional, translational or post-translational mechanisms that distinguish between their cell fates.

III. Translational control and GSC maintenance

Although the transcriptional repression of *bam* plays a key role in GSC maintenance, key translational repressors also play a critical role in preventing the precocious differentiation of GSCs. Previous studies have shown that the translational repressors Pumilio (Pum) and Nanos (Nos) are both required for GSC maintenance (Forbes and Lehmann, 1998; Lin and Spradling, 1997; Murata and Wharton, 1995). GSCs lacking Nos or Pum differentiate and are not maintained, suggesting that they function to repress the translation of factors that promote GSC differentiation. One possible target for translational repression was *bam*, the critical CB differentiation factor. However, examination of the P{*bam*P-GFP} reporter transgene in *pum* mutant ovaries revealed that *bam* was appropriately silenced in the GSC (Chen and McKearin, 2005). This indicated that *bam* was not the target of Nos-Pum translational repression.

An important insight into the genetic circuitry regulating GSCs was uncovered by epistasis experiments between the GSC maintenance factor *pum*, and the CB differentiation factor *bam*. Germ cells from *pum bam* double mutant females revealed evidence of limited differentiation, such as the presence of polyploid pseudo-nurse cells (Chen and McKearin, 2005; Szakmary et al., 2005). This result indicated that *pum* is epistatic to *bam* function as *bam* mutant GSCs can differentiate if *pum* is also absent. This result also suggests that Bam functions in the

CB to antagonize the function of Nos-Pum complexes to promote CB differentiation. Taken together, these data suggest that as Bam-Bgcn complexes begin to accumulate in the CB, they antagonize the function of Nos-Pum complexes and allow for the translation of factors that promote differentiation.

IV. Su(*bam*) genetic screen identified proteins involved in Bam stability

The identification of factors that stabilize Bam function would provide meaningful insight into the GSC-to-CB differentiation pathway. *bam* transcription is repressed by the Dpp signaling pathway in the GSC, thereby maintaining a GSC fate. As the CB divides away from the somatic niche cells, the source of Dpp ligand, *bam* transcription is activated and both *bam* mRNA and Bam protein accumulate to detectable levels (Chen and McKearin, 2003a; McKearin and Spradling, 1990).

Previous studies from our laboratory have identified a weak allele of *bam*, producing a moderate *bam* phenotype amenable to genetic screens (Ohlstein et al., 2000). Therefore, reducing the dosage of genes involved in appropriate Bam function can modify hypomorphic *bam* alleles. For example, reducing the gene dosage of the Bam-interacting protein Bgcn enhances the hypomorphic *bam* phenotype (Ohlstein et al., 2000). Bgcn, a putative DExH RNA helicase protein, partners with Bam, presumably to antagonize the function of Nos-Pum complexes to promote CB differentiation (Chen and McKearin, 2005; Lavoie et al., 1999) (Y. Li, J.Z. Maines, D.M. McKearin, unpublished). Thus, these studies indicate that the gene dosage of proteins involved in Bam function can be identified through a dominant modifier screen in a hypomorphic *bam* background (Ohlstein et al., 2000).

Bam protein is dynamically expressed in the early germ cells of the germarial regions 1 and 2. Low levels of Bam protein are expressed in the fusomes of GSCs but *bam* mRNA is undetectable in the GSC. In the CB, *bam* mRNA is actively transcribed and readily detectable, leading to the accumulation of Bam protein. In CBs and the maturing 2-, 4-, and 8-cell cysts, Bam protein is detected both in the cytoplasm (BamC) and fusome (BamF) (Figure 1.2) (McKearin and Ohlstein, 1995) Interestingly, similar to Bam expression in the GSC, BamF, but not BamC, is detectable in 16-cell cysts, suggesting that Bam protein is actively shuttled between these two cellular compartments or that active degradation mechanisms promote Bam turnover.

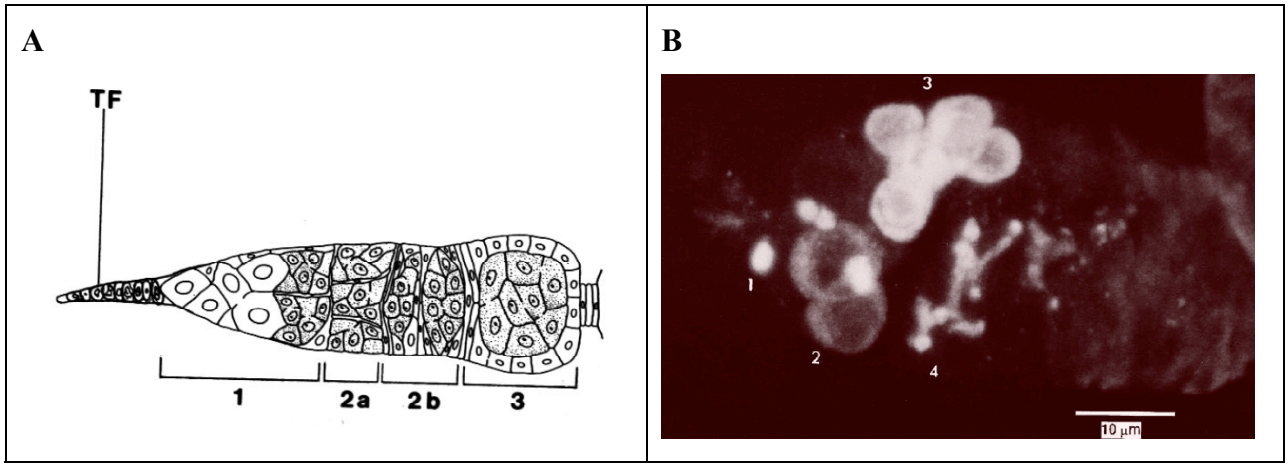

Figure 1.2: Schematic of germarium and dynamic expression of Bam protein.

(Panel A taken from (Mahowald and Kambysellis, 1980); Panel B taken from McKearin and Ohlstein, 1995)

(A) Schematic of germarium illustrating the morphologically-defined regions 1, 2a, 2b and 3. Region 1 contains the GSC, CB and early cysts; region 2a contains the newly-formed 16-cell cysts; region 2b contains the 16-cell cysts immediately prior to envelopment by an epithelial layer of follicle cells in region 3, leading to the formation of the spherical egg chamber. (B) Wild-type germarium immunostained with an anti-Bam antibody that detects both cytoplasmic Bam (BamC) and fusome-associated Bam (BamF). Numbers indicate (1) fusome-assocated Bam staining in a GSC; (2) BamC and BamF in a 2-cell cyst; (3) BamC staining in an 8-cell cluster with BamF staining likely occluded by the strong BamC signal; and (4) branched BamF staining in the fusome of a 16-cell cyst.

Many different protein complexes are involved in protein degradation. Among these include the CSN (COP9 signalosome), a complex consisting of eight subunits (CSN1-8) and fractionating as a 450-550 kD holo-complex (Wei and Deng, 2003). Pairwise homology of CSN subunits with those from the 26S proteasome lid complex (19S regulatory particle) and shared protein domains with the eukaryotic translation initiation factor eIF3 suggest that these three holo-complexes may have a common evolutionary ancestor (Glickman et al., 1998; Hofmann and Bucher, 1998; Wei and Deng, 1998). The eight CSN subunits are defined by their characteristic protein domains, a PCI/PINT (**p**roteasome, **C**OP9 signalosome, **i**nitiation factor 3/**p**roteasome subunits, **I**nt-6, **N**ip-1, and **T**RIP-15) and MPN (**M**pr1-**P**ad1-**N**-terminal) domains.

The major activity of the CSN holo-complex is through the modification of the SCF E3 ubiquitin ligase complex through the removal of the small ubiquitin-like moiety Nedd8 (Cope and Deshaies, 2003). The deneddylation activity of the CSN complex is found within a specialized metalloprotease motif inside the MPN domain of the CSN5 subunit that promotes deneddylation of the Cullin protein of the SCF (Cope et al., 2002; Lyapina et al., 2001). However, previous genetic and biochemical data present conflicting data about whether the CSN holo-complex is a positive or negative regulator of the SCF ubiquitin ligases. Some studies have shown that neddylation of SCF is required for proteolysis of $p27^{kip1}$, IκB, and HIF-1α (Furukawa et al., 2000; Morimoto et al., 2000; Podust et al., 2000; Read et al., 2000). However, genetic studies in *Arabidopsis* have shown a viability requirement for active CSN-dependent deneddylation of SCF ligases (Cope et al., 2002). Taking these disparate data together, others have hypothesized that active cycles of neddylation and de-neddylation are required to maintain SCF activity (Cope et al., 2002; Schwechheimer et al., 2001).

Subunits from both the CSN holo-complex and the SCF ubiquitin ligases have been examined in *Drosophila* development and oogenesis. Studies of the CSN complex have demonstrated that it is required for viability, as mutant animals are lethal at the late larval or pupal stages (Freilich et al., 1999; Oron et al., 2002). Mutations in *CSN4* and *CSN5* result in the delayed cell division and accumulation of Cyclin E (Doronkin et al., 2002; Doronkin et al., 2003). Similarly, mutations in *cul1*, the core cullin component of the SCF E3 ubiquitin ligase, also results in delayed cell division and a concomitant increase in CycE levels (Ohlmeyer and Schupbach, 2003). This suggests that the CSN and SCF E3 ubiquitin ligases may target the same protein for degradation during oogenesis.

Intriguingly, Cullin-1 was shown to localize to the fusome of early developing germ cells (Ohlmeyer and Schupbach, 2003). In addition, this same study showed that Encore (Enc), a novel protein required for executing the proper number of cyst divisions, is also enriched in the fusomes during early oogenesis (Hawkins et al., 1996; Ohlmeyer and Schupbach, 2003; Van Buskirk et al., 2000). Interestingly, *enc* mutant phenotypes were enhanced by mutations in the SCF complex and, in previous studies, *bam* acted as a dominant suppressor of *enc* (Hawkins et al., 1996; Ohlmeyer and Schupbach, 2003). As stated previously, Bam protein is also localized to the fusome (McKearin and Ohlstein, 1995). Taken together, these data suggest that the SCF complex is localized to the fusome during oogenesis and the CSN complex modulates its activity. During early GSC differentiation and cyst development, the fusome-associated SCF complex may play a critical role in protein turnover, including Bam as a putative target.

V. Loquacious and microRNA-mediated translational control

Another form of translational control involves the growing field of microRNAs (miRNAs). miRNA biogenesis is initiated in the nucleus when the primary miRNA (pri-miRNA) transcript is processed by the RNase III Drosha into stem-loop pre-miRNAs of approximately 70 nucleotides (Lee et al., 2003). Drosha requires the dsRNA-binding protein (dsRBP) Pasha/DGCR8 to process pri-miRNAs (Denli et al., 2004; Gregory et al., 2004; Han et al., 2004; Landthaler et al., 2004). The pre-miRNAs are exported from the nucleus by Exportin-5/RanGTP to the cytoplasm (Lund et al., 2004; Yi et al., 2003; Zeng and Cullen, 2004). Once in the cytoplasm, the pre-miRNA hairpin moieties are subsequently cleaved by Dicer-1 into mature 21-22-nt mature miRNA duplexes (Hutvagner et al., 2001; Ketting et al., 2001; Lee et al., 2004).

The requirements for miRNA pathway components have been studied extensively throughout oogenesis. Previous studies of Dicer-1 and AGO1 revealed a cell-autonomous requirement for GSC maintenance (Jin and Xie, 2007) and (D. Chen, personal communication). In addition, studies of *dcr-1* germline mosaic clones suggested that Dcr-1 function is critical for cell cycle progression and cell viability (Hatfield et al., 2005). These data suggest the importance of the miRNA biogenesis pathway in GSC function and promoting GSC maintenance. The GSC requirement for miRNAs is in accordance with previous studies demonstrating the importance of Nos-Pum-mediated translational repression in GSC maintenance.

Other examples of translational repression and protein-RNA complexes during oogenesis are the nuage particles and pole plasm, reviewed in (Williamson and Lehmann, 1996). Greater understanding of pole plasm function during oogenesis has come from studies of maternal effect genes, whose function is required for pole plasm assembly. Females mutant for genes – including *osk*, *vasa*, *valois*, *tudor*, *staufen*, and *aubergine*, among others – are sterile, producing embryos

that fail to form pole plasm and subsequently lack primordial germ cells (Ephrussi et al., 1991; Hay et al., 1990; Lasko and Ashburner, 1990). Importantly, the ectopic anterior localization of *osk*, a critical factor for pole plasm assembly, results in the formation of anteriorly-localized pole cell formation (Ephrussi and Lehmann, 1992). Due to the localization of mRNAs and RNA-binding proteins to the nuage and the pole plasm, the regulation of translational activity is a critical component of primordial germ cell formation.

VI. Aims of project

In these studies, I investigated the mechanisms regulating GSC maintenance and differentiation through the examination of global gene expression profiling, and studies of Loqs requirement in the GSC. First, I showed that the transcriptional profiles between GSC-like cells induced by germline activation of a consitutively-active Tkv receptor are largely similar to that of pre-CB cells that cannot differentiate due to an inactivating *bam* mutation. These data supported the parallel observations that GSCs are prevented from CB differentiation by Nos-Pum mediated translational repression of CB-promoting mRNAs. Thus, to uncover genes that are differentially expressed between GSCs and CBs, we compared the expression profile of pre-CB *bam* mutant cells against that of *stwl bam* mutant germ cells that undergo limited differentiation. These studies reveal that a small pool of mRNAs involved transcriptional and translational regulation, cellular adhesion, and cell signaling are differentially expressed in these two cell populations and that they likely comprise a subset of factors that are repressed by Nos-Pum to regulate GSC maintenance.

Second, I performed a small-scale genetic screen using a subset of stemness genes to identify other factors that are important for the GSC-to-CB transition. Among these factors, I

identified CSN4 as a suppressor of a weak *bam* phenotype, Su(*bam*). CSN4 is a subunit of the multiprotein COP9 signalosome complex that regulates protein degradation through the regulation of SCF E3 ubiquitin ligases. Accordingly, I also found that mutations in *cullin-1* (*cul-1*) also acted as a Su(*bam*) gene, further implicating the importance of these proteins and, by extention, protein degradation in GSC maintenance. Interestingly, I also showed that Bam protein levels are modulated by the dosage of Su(*bam*) genes. These data reveal a critical role for Bam protein turnover or stabilization of Bam protein function mediated by the COP9 signalosome and/or the SCF E3 class of ubiquitin ligases.

Third, I examined the requirement for Loqs protein in GSC maintenance. Loqs is a Dicer-1-associated cofactor that is involved in the processing of pre-miRNA hairpin moieties to mature miRNA duplexes. I showed the Loqs is required in a cell-autonomous fashion to maintain GSCs. Germline mosaics for a *loqs* null allele are lost from the germarium; germline-specific expression of a *loqs* rescuing transgene is sufficient to rescue GSC maintenance. Taken together, these studies demonstrate a cell-autonomous role for Loqs and, by extention, the miRNA biogenesis pathway, in the maintenance of GSCs. These results also support previous studies of Nos-Pum mediated translational repression in GSC maintenance.

Chapter 2. Materials and Methods

Drosophila stocks

All fly stocks were maintained under standard conditions. w^{1118} served as a wild-type control in all immunohistochemical and immunoprecipitation conditions, unless otherwise noted.

Stocks for expression profiling experiments:
bam$^{\Delta 86}$ (McKearin and Ohlstein, 1995);
P{hs-*bam*} (Ohlstein and McKearin, 1997);
P{*bam*P-GFP} (Chen and McKearin, 2003b);
P{*nos*P-Gal4:VP16} (Van Doren et al., 1998); a gift from Ruth Lehmann;
P{UASp-*tkv*^{CA}} (Chen and McKearin, unpublished); constitutively-active Q253D Tkv receptor;
P{lacZ}*stwl*^{z1} (Clark and McKearin, 1996);
stwl$^{\Delta 95}$ (Clark and McKearin, 1996); imprecise excision of P{lacZ}*stwl*^{z1};
P{EPgy2}*stwl*^{EY05697} (Bellen et al., 2004); EP element

Stocks for *bam* modifier screen:
bam$^{Z3\text{-}2884}$ (Ohlstein et al., 2000); amino acid replacement L255F;
bam$^{\Delta 86}$ (McKearin and Ohlstein, 1995);
P{*bam*P-Bam:HA} (D. McKearin, unpublished);
P{lacW}*CSN4*^{k08018} (Oron et al., 2002); P-element insertion 55bp downstream of start codon;
CSN4^{null} (Oron et al., 2002); P-element excision of nt -375 to +55 relative to start codon;
P{EPgy2}*CSN4*^{EY08080} (Bellen et al., 2004); EP element 33bp upstream of start codon;
P{lacW}*CSN5*^{L4032} (Oron et al., 2002); P-element insertion 24bp upstream of gene;
CSN5^{null} (Oron et al., 2002); P-element excision of nt -87 to +1396 relative to start codon;
P{lacW}*lin19*^{k01207} (Doronkin et al., 2003); P-element insertion 55bp downstream of start codon;
lin19^{EX} (Ou et al., 2002); P-element excision corresponding to amino acids 1 to 90

Stocks for *loqs* analysis:
PBac{WH}*loqs*^{f00791} (Jiang et al., 2005);
P{*nos*P-Gal4:VP16} (Van Doren et al., 1998); a gift from Ruth Lehmann;

P{GawB}*bab*$^{Agal4\text{-}5}$ (Cabrera et al., 2002);
P{*c587*-Gal4} (Manseau et al., 1997);
P{*hsFLP*}; P{*ubi*-GFP} P{FRT}40A (a gift from Ben Ohlstein);
r2d2^{1} (Liu et al., 2003); deletion of *r2d2* locus;
P{FRT}82B *dcr-1*^{Q1147X} (Lee et al., 2004); via Dean Smith

Stocks for pole plasm studies:
osk^{6} (Kim-Ha et al., 1991); nucleotide substitution C2506T, amino acid replacement R593W;
stau^{D3} (Ephrussi et al., 1991); absence of pole plasm and pole cells;
P{*osk-bcd*-3′UTR} (Ephrussi and Lehmann, 1992), 1992; via Liz Gavis;
P{UASp-GFP-*aub*} (Harris and Macdonald, 2001); a gift from Paul Macdonald;
P{vasP-GFP-HA-*vas*} (Sano et al., 2002); via Chip Ferguson;
P{vasP-GFP-*me31B*} (Nakamura et al., 2001); a gift from Akira Nakamura;
P{*exu*-GFP} (Wang and Hazelrigg, 1994); a gift from Tulle Hazelrigg

Microarray analysis

Microarray analyses for *tkv*, *bam*, and *stwl bam* ovaries were performed at the UT Southwestern Microarray Core Facility, under the guidance of Dr. Anwu Zhou, using Affymetrix Drosophila Genome 2.0 chips, respresenting ~18,500 transcripts. Briefly, ovaries from each genotype were hand-dissected and placed immediately into a Trizol RNA isolation reagent (Invitrogen) and RNA quality confirmed using Agilent Bioanalyzer analysis. These mutant ovaries provided a yield of approximately 100 ng RNA per ovary. cDNA synthesis, cRNA labeling, probe hybridization and chip scanning were performed according to the manufacturer's instructions (Affymetrix). The data were initially analyzed using the Affymetrix GeneChip Operating Software (GCOS, v1.1). Subsequent data sets were exported to GeneSpring analysis software (Silicon Genetics) and screened to identify signals counted as present and showing at least two-fold change difference between the two genotypes. The data were analyzed using a

parametric t-test and multiple correction method (Benjamini and Hochberg False Discovery Rate; P value < 0.05).

Immunohistochemistry

Ovary dissections were performed as follows, using different fixation conditions as noted. Ovaries were dissected in PBS, with ovariole tips teased apart to improve antibody penetration. Either "standard IHC" (Christerson and McKearin, 1994) or "devitellinizing IHC" (Findley et al., 2003) methods were used as follows.

Standard IHC

Tissue was fixed for 15 minutes with gentle rocking on a nutator in 4% formaldehyde (EM grade) in PBT (PBS + 0.1% Tween-20) under three volumes of heptane. After fixation, ovaries were washed four times in PBT for 10 minutes on a nutator at room temperature. Ovaries were then blocked in PBTA (PBT + 1% BSA) for 1 hour at room temperature. Primary antibodies were used at specified dilutions in PBTA and incubated overnight at 4°C. The next day, ovaries were washed four times with PBT for 10 minutes, blocked in PBTA for 1 hour and incubated for 1 hour with secondary antibodies diluted to 1:500 in PBTA. Ovaries were subsequently washed four times for 10 minutes in PBT and mounted in glycerol or VectaShield Mounting medium with DAPI (Vector Laboratories).

Devitellinizing IHC

Tissue was fixed for 5 minutes with gentle rocking on a nutator in 100 μL devitellinizing buffer under 600 uL heptane. Devitellinizing buffer consists of 1 volume Buffer B (100 mM KH_2PO_4/K_2HPO_4, pH 6.8; 450 mM KCl; 150 mM NaCl; and 20 mM $MgCl_2$), 1 volume 37% formaldehyde (contains 10-15% methanol; Sigma), 4 volumes H_2O. After fixation, ovaries were

rinsed three times in PBS, three times in PBTX (PBS + 0.1% Triton X-100), and washed in PBTX for 2 hours at room temperature with multiple changes every 15-30 minutes. Ovaries were then blocked in PBTX-BSA (PBTX + 1% BSA) for 2 hours at room temperature or overnight at 4°C. Subsequently, primary antibodies were added and incubated in PBTX-BSA overnight at 4°C. The next day, ovaries were washed four times with PBT for 15 minutes, blocked in PBTX-BSA, and incubated for 1-2 hours with secondary antibodies diluted to 1:500 in PBTX-BSA. Ovaries were subsequently washed four times for 15 minutes in PBTX and mounted in glycerol or VectaShield Mounting medium with DAPI (Vector Laboratories).

Immunoprecipitation from ovarian extracts

Lysates were prepared by dissecting 100 wild-type ovaries into ice-cold EBR or PBS and grinding for 30 seconds in 500 µl lysis buffer (50 mM HEPES, pH7.5; 250 mM NaCl; 0.1%NP-40; 0.2% Triton X-100) plus protease inhibitor cocktail (Roche) or 500 µL RISC buffer (110 mM KOAc; 10 mM HEPES, pH 7.4; 2 mM $Mg(OAc)_2$; 5 mM DTT; 0.05% NP-40). The lysate was spun in a microcentrifuge at maximum speed for 15 minutes at 4ºC and the supernatant was added to 40 µL of Protein G beads. After 1hour incubation at 4ºC, the beads were pelleted at 8000 rpm and the supernatant was collected. An optional step involves passing the supernatant through a hand-packed glass-wool column, which removes additional cellular debris from the lysate. Antibodies were added to the cleared lysate and incubated at 4°C for 2 hours. Protein G beads (Roche) were added and incubated with the lysate and immunoprecipitating antibody reagent (e.g., 5 µL anti-GFP; Invitrogen) overnight at 4°C. After 14 hours, the beads were washed 4 times in lysis buffer for 20 minutes, resuspended in an equal volume of protein loading buffer and loaded onto an SDS-PAGE gel. SDS-polyacrylamide gel electrophoresis and transfer

onto nitrocellulose (Hybond ECL, AP biotech) were carried out according to manufacturer's instruction (BIO-RAD). Membranes were blocked in PBST containing 5% milk for 2 h RT, then incubated overnight with rat anti-HA serum at 1:5,000 at 4ºC, washed and incubated with HRP-conjugated anti-goat antibody at 1:5,000. After several washes in PBST, bands were visualized using ECL chemiluminecent detection (Pierce).

For IP experiments with RNase A treatment, 500 μg/mL of RNase A was added to the ovarian extracts and incubated at room temperature for 5-15 minutes at room temperature prior to IP. For eact RNase A-treated sample, a parallel sample was used with 40U of an RNase Inhibitor (SUPERase-In, Ambion; Protector RNase Inhibitor, Roche).

The following antisera were used: antibodies used for IP were rat Monoclonal anti-HA 3F-10 (Roche) at 1:50 dilution and rabbit anti-GFP (Invitrogen) at 1:100 dilution. Primary antibodies used were rat monoclonal anti-HA 3F-10 (Roche) at 1:5,000 dilution, Goat polyclonal anti-GFP (Abcam) at 1:1,000 dilution. Secondary antibodies used were Goat anti-Rat-HRP and Rabbit anti-Goat-HRP (Bio-RAD) at 1:2,000 dilution. Protein G-Sepharose 4 Fast Flow (AP Biotech) was used to immunoprecipitate protein complexes.

7-methyl GTP Sepharose binding assays

Binding assays modified from (Cho et al., 2005). Wild-type ovarian extracts were prepared by dissecting 100 wild-type ovaries into ice-cold EBR or PBS and grinding for 30 seconds in 500 μl Cap Affinity Assay Buffer (50 mM Tris, pH 7.5; 300 mM KCl; 1 mM EDTA; 1 mM DTT) plus protease inhibitor cocktail (Roche). The lysate was precleared for 1 hr at 4°C with 20μL of Protein G Sepharose. The supernatant was immunoprecipitated either 4 hrs or overnight with anti-Loqs serum or 7-methyl-GTP-conjugated Sepharose beads (Amersham). The

resin was washed four times with Cap Affinity Assay Buffer and the bound proteins were eluted with Laemmli loading buffer.

FLP/FRT recombination to generate a *loqs* deletion allele

FLP/FRT recombination mediated deletion of the *loqs* gene locus was conducted by standard protocols (Parks et al., 2004). Two piggyBac transposable elements were identified that flanked the *loqs* gene and a downstream gene, *CG9293*: PBac{WH}*loqs*^{f00791} and PBac{WH}*CG9293*$^{f00384.}$ Crosses were performed to place these two FRT-bearing PBac transposons in *trans* and in the presence of FLP recombinase under the control of a heat-shock promoter, {hsFLP}. FLP recombinase was activated in larvae via heat shock induction, generating deletion events that were detected by PCR. Individual w+ progeny males (n=75) were collected and crossed to females carrying balancer chromosomes to establish lines carrying putative deletions, hereafter Df(2L)*loqs*^{del}.

Screening for putative deletion events used PCR primers designed against transposon-specific sequences and flanking genomic sequences on each end of the deleted region ("two-sided" PCR). Individual heterozygous males from each line were homogenized in a modified single-fly PCR prep (Gloor et al., 1993). In brief, single flies were placed in a 0.5 mL tube and mashed with a pipet tip containing 50 μL homogenizing buffer (10 mM Tris pH 8.2; 1 mM EDTA; 25 mM NaCl; 200 μg/mL fresh proteinase K). The homogenizing buffer is not expelled until the fly is sufficiently squished. The fly homogenates are incubated at 25-37°C for 30 minutes; afterwards, proteinase K is inactivated by heating the samples to 95°C for 2 minutes. Once cooled, 1 μL of the DNA prep can be used in a 25 μL PCR volume.

Ends-out homologous recombination to generate a *loqs* knockout allele

Targeted knockout alleles of *loqs* were generated by ends-out homologous recombination (Gong and Golic, 2003). Genomic sequences 4.4 kb upstream and 2.3 kb downstream of the *loqs* locus were obtained from genomic PCR, subcloned into the pW25 targeting vector (DGRC), and used for generating transformants, hereafter referred to as donor lines. Transgenic lines were generated by DNA injection of w^{1118} embryos at Genetic Services, Inc. under the guidance of Dr. Susan Zusman (Cambridge, MA).

Two independent transgenic donor lines bearing the targeting construct on the 3rd chromosome were crossed to *yw*; {70FLP}{70I-SceI}/TM6 (Bloomington stock #6935) flies and the subsequent F1 progeny were heat-shocked at 38°C for 90 minutes on days 3, 4, 5 after egg laying. The F1 virgin progeny bearing mosaic eye (red/white color) were crossed to *w*; {70FLP} (Bloomington #6938) and subsequent F2 progeny were screened for fully w^{+} (red) eye color, indicating a potential targeting event (approximately 1:450 gametes). A total of 192 candidate targeting events were screened by PCR and confirmed by Southern blotting (primers listed in Table 2.1). A total of 34 independent $loqs^{KO}$ alleles, or ~18% of candidate targeted lines, were identified as being created by homologous recombination between the donor DNA fragment and the *loqs* locus on the 2nd chromosome. Each $loqs^{KO}$ allele was isogenized by backcrossing to a w^{1118} stock and balancing over a 2nd chromosome CyO balancer.

Table 2.1: Primers used for PCR screening of homologous recombination-mediated targeting events and generating probes for Southern blot analysis

5' PCR (4.5 kb)	5'-GGACTAGTTGAGAAACCTATCG-3' and 5'-GGGCATGATAACTTCGTATAGC-3'
3' PCR (2.3 kb)	5'-CAGGTCGACTCTAGAGGATCATAA-3' and 5'-TAGTAGGGCATTAGTGGTCTTTCC-3'
Control PCR (4.4 kb)	5'-GCGGCCGCGGCAATAACAGCTTGGATCAAAGTG-3' and 5'-GGTACCGGTGTTCTTGTTTTGCACGGTTTTC–3'
5' probe	5'-AGAAACGAAAATAGACACCCAGAG-3' and 5'-GGATATCCCACCATTCTGTACTTC-3'
3' probe	5'-ACGTGTTCGAGATCACACTG-3' and 5'-ATGCGCATAAAGAGCGAGAG-3'

Generation of transgenic *loqs* rescuing constructs

Rescuing transgenes were generated for both the *loqs-PB* and *loqs-PA* isoforms. An N-terminal myc_{2x} tag was added to each cDNA prior to subcloning. The P{*ubi*P}-based transgenes were generated by subcloning the P{myc_{2x}:*loqs*} cDNAs into a pCaSpER4 vector with a ubiquitin promoter. The P{*loqs*P}-based transgenes were generated by ligating both P{myc_{2x}:*loqs*} cDNAs to 2.5 kb of upstream genomic DNA, including the promoter and 5′ UTR, and 0.8 kb downstream genomic sequences (3′ UTR) and subsequent subcloning into a pCaSpER4 vector. The P{UASp}-based rescuing transgenes were generated by subcloning the P{myc_{2x}:*loqs*} cDNAs for *loqs-PB* and *loqs-PA* into a pUASp vector.

The P{UASp}-based transgenes with a C-terminal GFP tag were generated using the Gateway system (Invitrogen). Both *loqs-PB* and *loqs-PA* isoforms were cloned into a

pENTR/D-TOPO vector and subsequently shuttled to the pPWG destination vector via Gateway site-specific lambda recombination system (Invitrogen).

Table 2.2: *loqs* rescuing transgenes

Transgene	Promoter	Tag	Isoform
P{w^{+}; *loqs*P-myc$_{2x}$:*loqs-PB*}	*loqs*	N-terminal 2x-myc	*loqs-PB*
P{w^{+}; *loqs*P-myc$_{2x}$:*loqs-PA*}	*loqs*	N-terminal 2x-myc	*loqs-PA*
P{w^{+}; *ubi*P-myc$_{2x}$:*loqs-PB*}	ubiquitin	N-terminal 2x-myc	*loqs-PB*
P{w^{+}; *ubi*P-myc$_{2x}$:*loqs-PA*}	ubiquitin	N-terminal 2x-myc	*loqs-PA*
P{w^{+}; UASp-myc$_{2x}$:*loqs-PB*}	UASp	N-terminal 2x-myc	*loqs-PB*
P{w^{+}; UASp-myc$_{2x}$:*loqs-PA*}	UASp	N-terminal 2x-myc	*loqs-PA*
P{w^{+}; UASp-*loqs-PB*:GFP}	UASp	C-terminal GFP	*loqs-PB*
P{w^{+}; UASp-*loqs-PA*:GFP}	UASp	C-terminal GFP	*loqs-PA*

Analysis of germline mosaic clones

To assay *loqs* requirement in GSCs, two independently derived *loqs*^{KO} alleles (*loqs*$^{KO1-53}$ and *loqs*$^{KO2-49}$) were recombined onto P{FRT}40A chromosomes. Clonal analyses were conducted by crossing the *loqs*^{KO} P{FRT}40A females to flies of the genotype *yw* P{*hsFLP*}; P{*ubi*-GFP} P{FRT}40A/CyO. Adult F1 females were collected, fed on wet yeast overnight, transferred to empty vials and subjected to heat shock in a 37°C water bath for 1 hr three times per day for three consecutive days. Heat-shocked animals were kept on wet yeast and aged for the appropriate number of days prior to dissection and IHC. GSC maintenance was determined as the percentage of germaria with negatively marked clonal GSCs at 4, 6, 10, 14, and 21 days after heat shock (n > 100 germaria per genotype per time point).

Chapter 3. Expression profiling of germline stem cells

I. Summary

Drosophila female GSCs are located at the anterior end of the germarium, a specialized structure at the anterior end of each ovariole. GSCs are prevented from differentiating by a Dpp signal secreted from the somatic cap cells that contact the GSCs and form the supportive GSC niche. The primary target of Dpp signaling in the GSC is key differentiation factor *bam*, which is required for GSC to CB differentiation. Germ cells from *bam* mutant ovaries fail to differentiate, continue to divide, and produce germ cell hyperplasia (McKearin and Ohlstein, 1995). These undifferentiated *bam* mutant germ cells represent a "pre-CB" state, poised between a GSC and a fully differentiated CB that will proceed through the later stages of oogenesis.

I designed a series of expression profiling experiments to identify differentially expressed transcripts between the undifferentiated GSC and the differentiated CB. My initial efforts focused on the comparison of *bam* mutant germ cells trapped as pre-CBs against germ cells trapped as GSC-like cells due to the germline-specific expression of a constitutively active *tkv* receptor, tkv^{CA} (Casanueva and Ferguson, 2004). Comparison of these two expression profiles failed to uncover a significant sample of differentially expressed transcripts. Accordingly, concurrent studies of the relationship between *pum* and *bam* indicated that *bam* was dispensable for germ cell differentiation if *pum* function was also abrogated (Chen and McKearin, 2005; Szakmary et al., 2005). This suggested that *bam* normally functions to antagonize *pum* function to allow for GSC differentiation. Since *pum* function has been studied previously as a translational repressor, we speculated that GSCs are maintained by preventing the translation of mRNAs that promote CB differentiation (Murata and Wharton, 1995; Zamore et al., 1997).

Taken together, I have concluded that the mRNA profiles of GSCs and pre-CB cells are likely to be very similar and that translational repression, not transcriptional control, is key for GSC maintenance.

A modified approach to uncovering GSC-enriched mRNA transcripts used a *stwl bam* double mutant background in which germ cells are able to differentiate in the absence of *bam*. Similar to the genetic epistasis tests performed with *bam* and *pum*, *stwl bam* double mutant ovaries can form differentiating germ cell cysts, indicating that *bam* function is dispensable when *stwl* is also absent (Maines et al., 2007). Like *pum*, *stwl* is required in the GSC to repress targets that promote CB differentiation. Whereas *pum* is a translational repressor, *stwl* is a DNA-associated protein that likely controls transcription through histone interactions. Therefore, the profile of mRNA transcripts in a *stwl bam* double mutant ovary should be enriched for those transcripts that are associated with germ cell differentiation. In addition, a small but significant number of transcripts that were upregulated in *stwl bam* mutant ovaries also shared consensus sequences that suggest an overlap with mRNA targets repressed by Nos-Pum function. Taken together, these sets of experiments designed to identify GSC-enriched transcripts highlighted the paradigm that GSCs are maintained by preventing the translation of CB-promoting mRNAs.

II. Subtractive hybridization to reveal GSC-enriched transcripts

Our lab was interested in the transcriptional controls that regulate GSC maintenance and differentiation. From previous work in our lab, *bam* was identified as a key factor that was both necessary and sufficient for GSC differentiation (McKearin and Ohlstein, 1995; Ohlstein and McKearin, 1997). Without Bam, the GSCs cannot differentiate into CBs and instead divide symmetrically, producing hyperplastic ovaries filled with GSC-like cells. Conversely, ectopic expression of *bam* results in the forced elimination of GSCs from their niche. Based upon our ability to genetically manipulate GSC states, I used gene expression profiling experiments to uncover additional transcriptional changes associated with GSC maintenance and differentiation.

Concurrent to these studies, work from Dahua Chen in our lab showed a direct role for the Dpp/BMP signaling pathway in the transcriptional silencing of *bam* in the GSC (Chen and McKearin, 2003a). This demonstrated a direct role for transcriptional control in the maintenance of GSCs. I designed a series of expression profiling experiments to exploit the different transcriptional profiles of the GSCs and their CB daughters and to identify transcripts associated with GSC maintenance and/or differentiation.

Our first approach utilized a modified subtractive hybridization protocol to identify GSC-specific transcripts. Subtractive hybridization compares two mRNA populations, termed the tester and driver, and specifically enriches for those transcripts that are differentially expressed in the tester sample but not the driver sample (Diatchenko et al., 1996). Our application of the modified subtraction strategy compares a single GSC-negative driver sample, derived from P{hs-*bam*} germaria, against two different GSC-positive tester samples, derived from wild-type germaria and $bam^{\Delta 86}$ ovaries. The germaria from both P{hs-*bam*} and wild-type ovaries were

hand-dissected to limit the inclusion of late-stage polyploidy egg chambers that would introduce a large pool of undesired mRNA transcripts.

Table 3.1: Clones isolated from subtractive hybridization of wild-type and *bam*$^{\Delta 86}$ ovaries against P{hs-*bam*} ovaries

Gene name	Differential expression by dot-blot analysis	Description
bobbed	No	18S/28S rRNA
Tsp42Ee	Yes	tetraspanin; cell signaling
CG10417	Yes	protein Ser/Thr phosphatase
14-3-3ζ	Yes	epithelial polarity
RpS11	No	ribosomal protein
Hsr omega	No	heat-shock protein
PRL-1	No	protein phosphatase
CG5021	No	unknown
Uch	No	ubiquitin carboxy-terminal hydroxylase
CG1542	No	unknown

Unfortunately, subtractive hybridization did not reveal a large number of transcripts that were differentially expressed between the tester and driver samples. Approximately 50% of the sequenced clones corresponded to sequences from the *bobbed* gene, associated with 18S and 28S ribosomal RNAs. However, subsequent dot blot analyses of *bobbed* levels in the subtraction sample against an "unsubtracted" sample did not reveal a marked differential expression. This suggests that the experimental methodology was unsuccessful in filtering both non-specific and

undesired transcripts. In fact, most of the recovered clones were not differentially expressed between a subtracted and unsubtracted sample (Table 3.1).

Due to the relative inability to isolate large numbers of clones that were differentially expressed in a subtracted sample, I decided not to pursue further characterization of the clones that were identified. In addition, to robustly identify transcripts that might be differentially expressed in GSCs and CBs, I felt it necessary to compare two homogenous cell populations and compare their global expression profiles. Despite efforts to collect hand-dissected germaria, the inclusion of late-stage germ cells in the wild-type and P{hs-*bam*} samples might have complicated the ability to recover differentially expressed transcripts. To address this possibility, I modified our approach to examine homogenous populations of GSC-like cells and pre-CB cells using a genome-wide microarray-based platform.

III. Microarray-based expression profiling of *dpp*-induced GSCs and *bam* mutant germ cells

The major limitations of a subtractive hybridization-based expression profiling of GSC-enriched transcripts included the possibility of missing low abundance transcripts as well as the relative difficulty of isolating hand-dissected germaria from wild-type and P{hs-*bam*} ovaries. However, at the time that these experiments were initiated, I was restricted by the inability to efficiently isolate pure populations of GSCs.

During this time, Dahua Chen developed a powerful reagent that provided an entry point for a genome-wide expression profiling approach. Specifically, he exploited our understanding of Dpp-mediated repression of *bam* in the GSC to generate a constitutively-active Tkv receptor, P{UASp-tkv^{CA}}, hereafter simply tkv^{CA} (Chen and McKearin, unpublished). Expression of this transgene at high levels in the germline, using the P{*nos*P-Gal4:VP16} driver, resulted in the

production of *bam*-like ovaries that were devoid of differentiated egg chambers. IHC analysis of germ cells in both the tkv^{CA} and $bam^{\Delta 86}$ mutant ovaries contained round fusomes or paired cells undergoing symmetric cell division (Figure 3.1). In addition, using an anti-phospho-histone H3 antibody revealed that germ cells in both genotypes were equally capable of mitotic progression (not shown). These observations demonstrated that germline expression of a constitutively-active Tkv receptor produced ovaries filled with GSC-like cells that are morphologically similar to *bam* mutant GSC-like cells.

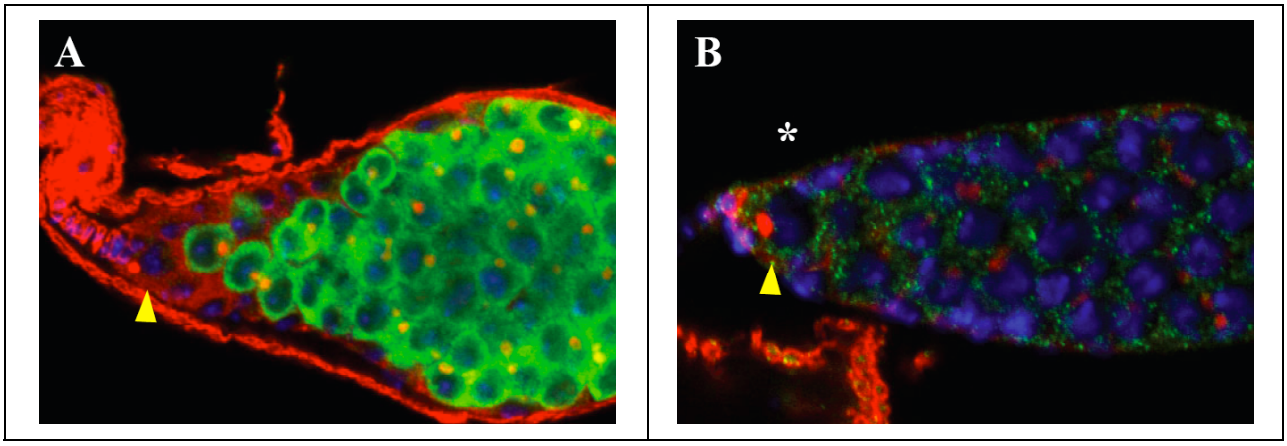

Figure 3.1: *bam* transcription silenced by Dpp signaling pathway. (A) Germ cells from *bam* mutant ovaries contain spherical fusomes (stained with anti-Hts in red) indicating a failure to differentiate. The GSC is unable to activate the P{*bam*P-GFP} transcriptional reporter (yellow arrowhead) whereas the hyperplastic *bam* mutant germ cells that fill the germarium are GFP-positive. (B) Germline specific expression of a constitutively-active *tkv* receptor, P{UASp-tkv^{CA}}, produces undifferentiated germ cells containing spherical fusomes (anti-Hts, red). However, these germ cells are unable to activate the P{*bam*P-GFP} transcriptional reporter. Yellow arrowheads in both panels indicate the GSC.

*Note: the collection gain was increased in tkv^{CA} ovaries (B) to highlight the absence of signal from the P{*bam*P-GFP} transgene. Consequently, increased background is observed in the FITC channel.

However, a key difference between tkv^{CA} and $bam^{\Delta 86}$ mutant genotypes was in the ability to activate a P{*bam*P-GFP} reporter transgene. Except for the anteriormost GSCs in a *bam* mutant ovary, all of the hyperplastic *bam* mutant germ cells activate the P{*bam*P-GFP}

transcriptional reporter (Figure 3.1A) (Chen and McKearin, 2003a). Presumably, these GFP-positive cells are sufficiently removed from the source of Dpp ligand that acts to silence *bam* transcription via the Smad signaling cascade. However, in a tkv^{CA} ovary, all of the germ cells are unable to activate the P{*bam*P-GFP} transcriptional reporter and are GFP-negative (Figure 3.1B). Because these cells express a constitutively-active Tkv receptor, this broadens the source of Dpp signal and effectively mimics an expansion of the GSC niche. Thus, the P{*bam*P-GFP} transcriptional reporter highlights the functional difference between hyperplastic germ cells from tkv^{CA} and $bam^{\Delta 86}$ mutant ovaries; that is, tkv^{CA} germ cells are more "GSC-like" than $bam^{\Delta 86}$ mutant "pre-CB" germ cells.

Using this paradigm, I could perform a genome-wide expression profiling experiment. Comparing the "GSC-like" tkv^{CA} germ cells against the $bam^{\Delta 86}$ mutant "pre-CB" germ cells should uncover transcripts that are enriched in GSCs. Any transcripts that were identified by this approach would be verified by RNA *in situ* hybridization in wild-type ovaries to validate a differential expression pattern. To nullify the possible effects of Gal4 mosaicism in females carrying the P{*nos*P-Gal4:VP16} and P{UASp-tkv^{CA}} transgenes, the tkv^{CA}-induced GSC-like cells were also *bam* null. Therefore, any germ cells in which the Gal4-mediated tkv^{CA} expression was insufficient to trap germ cells as GSCs would not be able to differentiate beyond the pre-CB state. This is an important consideration because the inclusion of maturing egg chambers replete with mRNA transcripts from polyploid nurse cells would confound subsequent analyses.

RNA was extracted from both tkv^{CA} and $bam^{\Delta 86}$ germ cells and prepared without RNA amplification for Affymetrix oligonucleotide arrays (Affymetrix GeneChip Drosophila Genome 2.0 Array; 18,500 transcripts). Raw data was analyzed using both Affymetrix GeneChip Operating Software which determined whether a given gene is likely to be present or absent, and

also provided a quantitative expression value (e.g., present or absent calls). Three separate arrays were used for each genotype and the results were reproducible.

To determine whether both samples expressed a representative collection of transcripts, I examined the expression values and present/absent calls for a subset of genes known to affect GSC function. Since both cell types are very similar to in vivo GSCs, I examined the expression levels of genes involved in the Dpp signaling, CB differentiation, translational regulation, miRNA/siRNA factors and adhesion proteins (Table 3.2). This comparison reveals that many of these genes are present and expressed at comparable levels in both *tkv*^{CA} and *bam*$^{\Delta 86}$ germ cells.

Table 3.2: Observed average expression of genes relevant to GSC-related biology in *tkv*^{CA} and *bam*$^{\Delta 86}$ germ cells

Gene	Function	*tkv*^{CA}	*bam*$^{\Delta 86}$
Dpp pathway components			
tkv	Dpp Type I receptor	746	763
punt	Dpp Type II receptor	690	801
sax	Dpp Type I receptor	1180	1180
Mad	Smad protein	490	545
Med	Smad protein	*57	*41
Dad	Inhibitory Smad protein	619	741
shn	Mad interacting txn factor	562	602
dpp	BMP ligand	183	206
gbb	BMP ligand	682	745
activin-B	BMP ligand	28	30
CB differentiation			
bam	CB differentiation factor	71	97
bgcn	DExH-box helicase	851	801
otu	Tudor domain	471	440
ovo	Zn finger txn factor	2278	2216
Translation factors			
nos	Translation repressor	1416	1378

pum	Translation repressor	192	156
brat	Translation repressor	189	194
orb	CPEB	566	573
hrg	poly(A) polymerase	750	781
Pabp2	poly(A) binding protein	579	643
dPaip2	PABP interacting protein	283	299
cup	eIF4E interacting protein	1807	1728
vasa	eIF4A-like protein	22	22
stau	RNA binding protein	776	682
RNAi/miRNA associated proteins			
loqs	dsRNA binding protein	387	383
Dicer-1	ds RNase-III; miRNA	214	185
Ago-1	miRISC activity	323	327
r2d2	dsRNA binding protein	446	509
Dicer-2	ds RNase-III; siRNA	1004	1171
Ago-2	siRISC activity	1326	1255
piwi	AGO family; piRNA	2728	2396
aub	RNAi; translation	2289	2079
spn-E	DEAD-box helicase	2525	2559
armi	siRISC assembly	2675	2808
tud	Tudor domain	836	797
Protein degradation			
enc	novel protein	1463	1564
CSN4	COP9 signalosome subunit	1043	1061
CSN5	COP9 signalosome subunit	1386	1353
Cul1	Cullin; SCF E3 Ub ligase	1257	1297
Other			
stwl	transcription factor	95	75
shg	DE-cadherin	247	250
arm	adherens junction	2743	2535
zpg	innexin	716	926

* indicates genes scored as absent

I identified less than 60 genes that were differentially expressed two-fold or more (P value <0.05) in *tkv*^{CA}-induced GSC-like cells relative to *bam* mutant pre-CBs in at least one of three comparisons. Of these transcripts, 21 were upregulated in *tkv*^{CA} relative to *bam* and 36 were upregulated in *bam* relative to *tkv*^{CA}. Differentially expressed transcripts enriched in the *tkv*^{CA} population, including a few that are differentially expressed less than two-fold, are listed in Table 3.3 and annotated as having a function in mRNA processing, transcription, cell adhesion, cell signaling and metabolism. Conversely, selected transcripts enriched in *bam* mutant cells are listed in Table 3.4.

Table 3.3: Selection of transcripts whose abundance increased in *tkv*^{CA}-induced GSCs relative to *bam*$^{\Delta 86}$ mutant pre-CBs

Gene	Function	*tkv*^{CA}	*bam*$^{\Delta 86}$	Fold Δ	P-value
mRNA Processing/Translation					
pst	learning/memory	1120	637	1.8	4.2E-05
eIF4E-3	translation initiation factor	760	411	1.8	2.3E-06
Transcription					
fs(1)K10	DNA binding domain	1216	355	3.4	3.7E-06
CG17462	sigma DNA pol	112	69	1.6	3.8E-04
Adhesion/Signaling					
CG7060	FnIII repeat	72	*18	4	3.6E-04
CG3105	S/T kinase	111	64	1.7	3.2E-04
Metabolism					
CG8563	metalloprotease	118	*16	7.4	4.7E-06
grappa	SAM methyltransferase	136	60	2.3	5.0E-05
GstD3	glutathione transferase	563	343	1.6	2.0E-06
CG1906	S/T phosphatase	57	33	1.8	1.7E-04
Unknown/Other					
CG32368	unknown	1474	168	8.8	2.3E-06
Hsp67Bc	heat shock protein	157	76	2.1	3.7E-04
CG10063	unknown	473	291	1.6	5.4E-05

* indicates genes scored as absent

Table 3.4: Selected transcripts whose abundance decreased in *tkv*^{CA}-induced GSC-like cells compared with *bam*$^{\Delta 86}$ pre-CBs

Gene	Function	*tkv*^{CA}	*bam*$^{\Delta 86}$	Fold Δ	P-value
mRNA Processing/Translation					
nemy	memory defective	440	1077	2.4	2.0E-06
Adhesion/Signaling					
Nplp4	Neuropeptide-like precursor	138	367	2.7	3.1E-04
IM10	Toll signaling pathway	35	76	2.2	4.1E-04
TpnC4	Calcium binding	23	58	2.6	2.0E-05
Metabolism					
CG10175	carboxylesterase	*8	65	8.4	4.6E-05
Pepck	gluconeogenesis	153	381	2.5	2.0E-06
CG13903	Ub protease	415	1247	3.0	9.0E-06
Unknown/Other					
CG16772	unknown	*33	114	3.4	4.3E-04
CG7695	unknown	391	1520	3.9	2.0E-06
CG18064	Met75Cb/unknown	113	414	3.7	3.0E-06
CG8066	unknown	168	348	2.1	2.0E-06

* indicates genes scored as absent

To determine whether the differentially expressed transcripts uncovered by microarray analyses also displayed a differential expression pattern in wild-type germ cells, I performed RNA in situ hybridization experiments on wild-type ovaries. Using a *bam* RNA probe served as a control both for the detection of low abundance transcripts as well as the identification of differential gene expression (Figure 3.2, panel A). The gene encoding *fs(1)K10* was identified as one that was enriched greater than 3-fold in *tkv*^{CA} germ cells relative to *bam* mutant germ cells. The function of *fs(1)K10* has been examined in the later stages of oogenesis, where it plays a role in the localization of *grk* mRNA to the anterior-dorsal border of the oocyte (Serano et al., 1995). However, *fs(1)K10* did not have a defined role during the early stages of oogenesis, including

early GSC differentiation. As previously noted, RNA in situ hybridization did indicate that *fs{1)K10* was expressed in the developing oocyte, but I detected *fs{1)K10* in the germarium (Figure 3.2, panel B). Unfortunately, expression was not detected in the GSCs at the anterior of the germarium and only in differentiated cyst cells, which is inconsistent with the data from the array analyses.

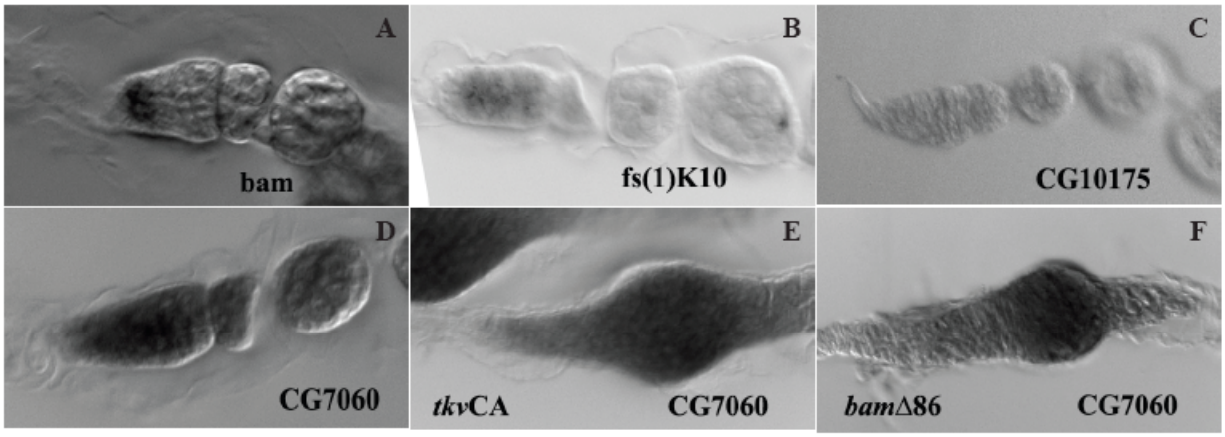

Figure 3.2: RNA *in situ* hybridization of selected transcripts identified by *tkv*^{CA} and *bam*$^{\Delta 86}$ microarray analysis. RNA probes were tested on ovaries from wild-type (A-D), *tkv*^{CA} (E) and *bam*$^{\Delta 86}$ (F).

Many other probes were not successful in RNA *in situ* hybridization experiments (as an example, Figure 3.2, panel C). Alternatively, other probes were expressed uniformly throughout the germarium, as shown in Figure 3.2, panel D. To determine whether in situ hybridization could be used to confirm differential expression, I used the RNA probes on ovaries *tkv*^{CA} and *bam*$^{\Delta 86}$ mutant ovaries. For example, the RNA probe for CG7060 showed uniform expression in wild-type germaria. However, in *tkv*^{CA} and *bam*$^{\Delta 86}$ ovaries, the probe was unable to reveal a difference between the two genotypes, despite the observations that the CG7060 transcript was flagged as absent in *bam*$^{\Delta 86}$ mutant ovaries (compare Figure 3.2E versus 3.2F; Table 3.3). Thus,

based upon the relatively marginal differences in the number of genes that were two-fold change different between the *tkv*^{CA} and *bam*$^{\Delta 86}$ arrays, as well as the relative inconsistencies of RNA in situ hybridizations, I concluded that there were few transcriptional differences between the two populations.

Concurrent studies from our lab determined that *pumilio* (*pum*), a gene involved in translational repression, is required for GSC maintenance by repressing *bam*-independent differentiation pathways. Specifically, studies demonstrated that *pum bam* double mutant ovaries displayed evidence of differentiation unlike *bam* mutant ovaries (Chen and McKearin, 2005; Szakmary et al., 2005). This allowed us to propose a mechanism for controlling GSC maintenance, in which GSC are maintained by preventing the translation of differentiation promoting mRNAs. Genetic epistasis experiments between *pum* and *bam* indicated that *pum* functions downstream of *bam* function. Since *pum* is required in the GSC and *bam* function is required for CB differentiation, we proposed that the function of Bam protein is to antagonize Pum translational repression. Therefore, my gene expression analyses of *tkv*^{CA} and *bam*$^{\Delta 86}$ mutant germ cells is predictably unrevealing because GSCs and pre-CB cells likely share the same pool of mRNAs.

IV. Expression profiling of *bam* and *stwl bam* mutant ovaries

The limitations of comparing the expression profiles of *tkv*^{CA} and *bam*$^{\Delta 86}$ germ cells are that the mRNA profiles of these two cell types are likely very similar. To utilize this set of data effectively, I needed to compare these expression profiles against that of germ cells that experience a limited amount of germ cell differentiation. I could use wild-type ovaries to compare the expression profiles. However, with whole ovaries, the inclusion of egg chambers

with polyploid nurse cells would distort our subsequent analyses and dilute the relative concentration of GSCs relative to total ovarian tissue mass.

In order to keep the genetic backgrounds relatively homogenous, it is important to compare the *bam*$^{\Delta 86}$ mutant ovaries with a genotype that is not substantially different in the composition of cell types. Toward that end, we decided to compare the expression profiles of *bam* mutant ovaries with *stwl bam* double mutant ovaries. In the following series of experiments, detailed in greater depth in Maines et al., 2007, I will present the accumulated genetic analysis of *stwl* that helped us to establish the *stwl bam* double mutant genotype as a suitable one for microarray anaysis.

IV.A. *stwl* mutant GSCs are lost

Defects in GSC maintenance typically result in the progressive loss of egg chamber progression and overall germ cell number. Ovaries from *stwl* mutant females are typically smaller than wild-type controls, primarily because of a gradual age-dependent loss of egg chamber number. To examine the role that *stwl* may play in GSC maintenance, we examined ovaries from wild-type and *stwl*^{z1}/*stwl*$^{\Delta 95}$ mutant females at 4- and 10-days after eclosion. Whereas wild-type females retained their GSCs and germ cells for more than 3 weeks, *stwl* mutant females displayed a rapid loss of germ cells, with approximately 50% of ovarioles completely devoid of germ cells (Figure 3.3). These data, in addition to a previously published study, suggest that *stwl* mutant females fail to maintain GSCs (Akiyama, 2002; Maines et al., 2007).

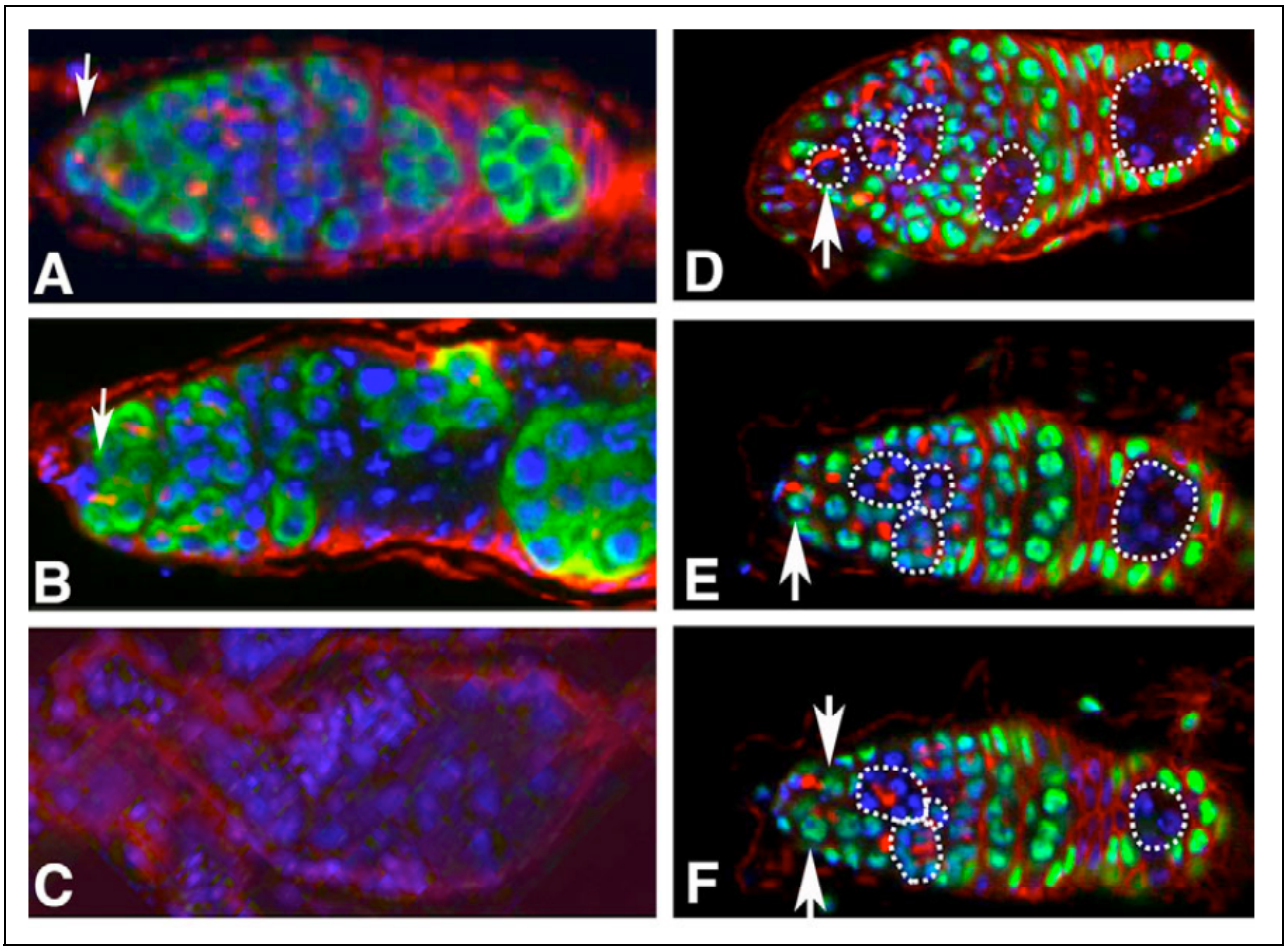

Figure 3.3: Stwl is required for GSC maintenance (Image taken from Maines et al., 2007). (A-C) Ovaries from heterozygous control animals (A) were dissected at 10 days post-eclosion and labeled with anti-Vasa (germ cells; green), anti-Hts (fusome; red) and Hoechst (DNA; blue). Ovaries from $stwl^{Z1}/stwl^{\Delta 95}$ mutant females were dissected at 4 days (B) and 10 days (C) post-eclosion. (D-F) GSC clones were induced in adult animals and identified by the absence of nuclear GFP. GSC clones induced in control FRT background (D). Arrows indicate GSCs. Clones are outlined by dotted lines. (E-F) *stwl* mutant GSC clones examined 7 days after clonal induction. The presence of negatively marked and clonally related germ cell clusters indicate that they arose from a mutant GSC. The stem cell region of this germarium contained only wild-type GSCs (arrows). **(Clonal analyses (D-F) performed by Jean Maines)**

A specialized microenvironment, or niche, regulates GSC maintenance by producing factors that regulate cell survival and differentiation. Since Stwl is expressed in both the somatic and germline cells of the ovary, it could be required extrinsically in the somatic niche cells or intrinsically in the germline to promote GSC maintenance. To distinguish between these two

possibilities, mitotic recombination can be used to specifically eliminate *stwl* in germ cells. While wild-type clones were maintained over a two-week period after clonal induction, *stwl* mutant clones were rapidly depleted from the germarium (Figure 3.3, panels D-F). These data indicate that *stwl* plays a cell-autonomous role in GSC maintenance.

IV.B. *stwl bam* double mutant ovaries display *bam*-independent differentiation

Genetic epistasis experiments between *bam* and *pum* revealed that double mutant ovaries were capable of forming differentiating germ cell cysts, suggesting that *bam* is dispensable for differentiation when *pum* is also absent (Chen and McKearin, 2005; Szakmary et al., 2005). Similar genetic epistasis experiments were conducted with *stwl* and *bam* to determine whether double mutant ovaries also display evidence of *bam*-independent differentiation. In approximately 80% of *stwl bam* double mutant germaria, we could identify germ cells with elongated fusomes indicative of cyst formation (Figure 3.4). These experiments were also recapitulated with *stwl bgcn* double mutant ovaries, further suggesting that the Bam-Bgcn complex and Stwl form an antagonistic genetic relationship. Importantly, this establishes that Stwl+ promotes GSC maintenance and acts downstream of Bam-Bgcn complexes.

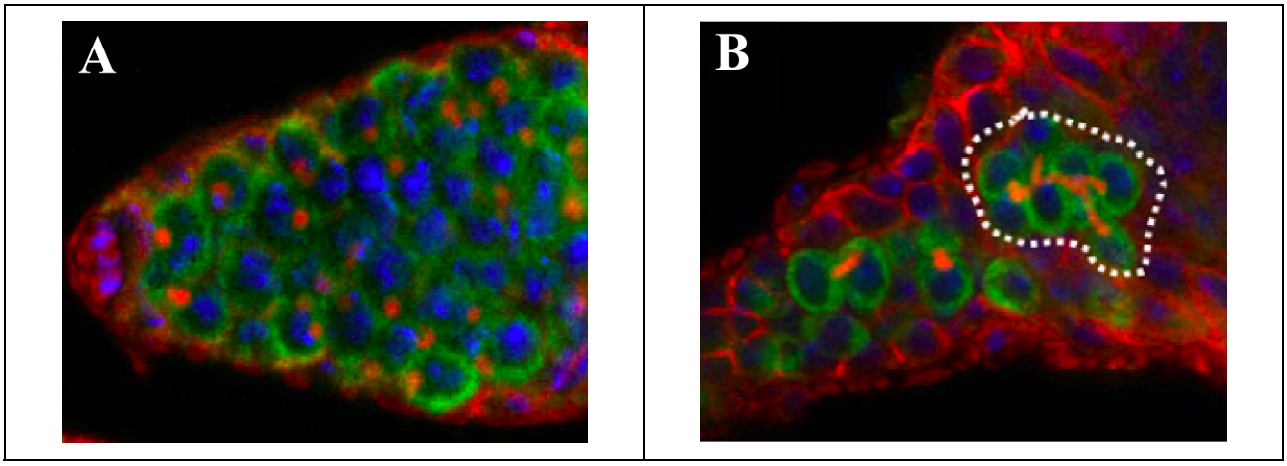

Figure 3.4: *stwl* suppresses GSC differentiation independent of *bam* function. (Image taken from Maines et al., 2007). (A) *bam* mutant ovaries stained with anti-Vasa (green) reveal germ cells containing spherical fusomes (anti-Hts; red). (B) Elongated fusomes (circled by dotted line) indicate cyst formation in *stwl bam* double mutant ovaries. **(Analysis performed by Jean Maines)**

IV.C. Expression profiling experiments of *bam* and *stwl bam* ovaries

To identify targets of Stwl whose transcriptional silencing is required for GSC maintenance, we carried out microarray analysis of undifferentiated germ cells that lack *bam* and compared them to *stwl bam* mutants. Both of these genetic backgrounds provided a nearly homogeneous population of cell types since *bam* mutant cells failed to differentiate into CBs and *stwl bam* germ cells arrested as partially formed cysts. The homogeneity and early arrest of the mutant germ cells improved the quality of microarray data by eliminating late stage egg chambers that produce complex and abundant populations of mRNA, which can distort microarray analysis.

We identified 501 genes that were differentially expressed two-fold or more (P value <0.05) in *stwl bam* mutants relative to *bam* mutant ovaries. 235 of these candidate transcripts were upregulated in *stwl bam* versus *bam*. Differentially expressed transcripts designated as

having functions in mRNA processing, transcription and others are listed in Table 3.5 and those with the largest differential change in expression are highlighted.

Table 3.5: Transcripts whose abundance increased in *stwl bam* double mutant ovaries relative to *bam* mutant ovaries

Gene	Function	*stwl bam*	*bam*	Fold difference	*P*-value
mRNA processing/translation					
CG8335	eIF-3	816	72	11.3	0.000371
CG14443	RNA helicase	155	22	7.0	0.00131
B52	mRNA splicing	1631	363	6.7	0.0165
aret	Bruno: RNA binding	1481	405	3.7	0.0155
CG10630	ds-RNA binding	4049	1199	3.4	0.00964
CG8023	eIF-4e like	953	411	2.3	0.00738
Transcription					
CG10102	Zn finger	291	11	26.5	0.000255
CG31601	Zn finger	216	17	12.7	0.0103
CG16898	Zn finger, bHLH	132	16	8.3	0.0482
east	Nucleoskeleton	356	76	4.7	0.0361
CtBP	Co-repressor	1756	460	3.8	0.0115
CG8119	SANT domain	187	56	3.3	0.00445
lola	BTB/POZ domain	350	105	3.3	0.0134
His3.3B	Histone 3.3	5137	2136	2.4	0.0357
CG12054	Repressor	158	70	2.3	0.0128
Smr	Co-repressor	772	348	2.2	0.043
Signaling					
CG31187	Diacylglycerol kinase	188	6	31.3	0.00077
Rala	Ras-related	988	128	7.7	0.00449
Pi3K21B	PI-3 kinase	330	71	4.6	0.00339
Tob	Dpp antagonist	77	19	4.1	0.00498
Src64B	Src tyrosine kinase	219	82	2.7	0.00455
Adhesion					
CG8563	Metalloprotease	266	16	16.6	0.00512
Fas2	Homophilic cell adhesion	1185	310	3.8	0.00224
CG12497	Laminin	80	37	2.2	0.0371
Structural/other					
Act88F	Actin filament	531	17	31.2	0.0116
Acp1	Cuticle protein	269	24	11.2	0.0107
up	Tropomyosin binding	3022	302	10.0	0.000511
RfaBp	Fatty acid binding	1004	350	2.9	0.0416

Bold indicates genes with the largest differential change in expression.

Since Stwl is predicted to function as a transcriptional inhibitor, initial studies focused on those transcripts that were upregulated in the *stwl bam* double-mutant ovaries relative to *bam* ovaries (Table 3.5), as this would include the genes that comprise the set of "CB differentiation-promoting mRNAs". Among these genes, we expected to find some whose expression was directly influenced by the absence of *stwl* and others whose expression increased secondarily as a

consequence of early cyst development. For example, examination of *aret* (also known as *bruno*, a translational repressor) revealed that its protein accumulation was not markedly altered in *stwl*$^{+/-}$ versus *stwl*$^{-/-}$ germline clones; however, Aret protein is more abundant in *stwl bam* ovaries relative to *bam* ovaries (Maines et al., 2007; Parisi et al., 2001). This indicates that *aret* is not a direct target of Stwl action but rather that *aret* is upregulated in *stwl bam* double mutants due to cyst differentiation. Conversely, examination of *lola* reveals a different reason for upregulation in *stwl bam* double mutants. Lola, a protein implicated in chromatin organization, is expressed in greater abundance in *stwl*$^{-/-}$ germline clones, whereas most *stwl*$^{+/-}$ germ cells were Lola-negative (Maines et al., 2007; Zhang et al., 2003). Therefore, the examination of *aret* and *lola* accumulation in *stwl bam* versus *bam* mutant ovaries indicates that the list of differentially expressed genes will include both direct targets and indirect consequences of *stwl*+ function.

V. Discussion

The data presented above highlight the importance of translational control in regulating GSC fate as well as the emerging importance of epigenetic regulation through histone-associated proteins. Toward that end, I will examine two genes highlighted by my data, *pastrel* (*pst*) and *His3.3B*, that might yield further insights into translation and epigenetic control of GSC fate.

V.A. Translational control critical for GSC fate

Data collected from expression profiling studies of *tkv*^{CA} and *bam*$^{\Delta 86}$ germ cells reinforce the critical role for translational control of GSC fate. The two sample populations expressed a very similar transcriptional profile of genes involved in GSC function. Direct comparison of "GSC-like" *tkv*^{CA}-induced germ cells against *bam*$^{\Delta 86}$ mutant "pre-CB" cells revealed that only a

small number of genes are differentially expressed in a reproducible and significant degree. Due to the similarity of the two expression profiles, I believe that I have a comprehensive catalog of GSC transcripts but not necessarily the much-desired subset of "stemness" genes.

However, one intriguing prediction of the translationally-repressed GSC is that a differential protein profile of GSCs and CB cells could provide a unique insight into the key factors required for GSC differentiation. Bam accumulation would serve as a positive control; a negative control would be Nos protein, which appears to be downregulated in the presence of Bam protein. This experiment, detailed later in Chapter 9, could provide key insights into the functional proteomic changes that accompany the GSC to CB transition.

However, gene expression profiling of tkv^{CA} and $bam^{\Delta 86}$ germ cells may have uncovered a few candidate genes that might play an as yet undefined role in GSC maintenance. An intriguing upregulated transcript in tkv^{CA} germ cells encodes *pastrel* (*pst*), a gene identified in a screen for learning and memory defective mutants (Dubnau et al., 2003). Intriguingly, a large number of factors known to play a role in GSC maintenance and oogenesis were also recovered in this screen, including *pum*, *orb*, *stau*, *lin19*, *slbo*, and *lola* (Chen and McKearin, 2005; Christerson and McKearin, 1994; Dubnau et al., 2003; St Johnston et al., 1991; Szakmary et al., 2005) and (E. Davies and M. Fuller, personal communication). This raises the intriguing hypothesis that similar mechanisms may be playing a role in oogenesis as well as learning and memory. Indeed, such a role has been proposed for Staufen, a RNA binding protein, in the polarized transport of RNA in both neurons and oocytes, reviewed in (Roegiers and Jan, 2000). Since *pum* has been identified as critical for both GSC maintenance and learning/memory, it is tempting to speculate that *pst* might also have a function in both compartments as well. In fact, another study of GSC expression profiling also revealed that *pst* is enriched in "GSC-like" cells

induced by ectopic Dpp expression (Kai et al., 2005). Therefore, it would be worthwhile to examine *pst* mutant animals to determine whether they display phenotypes associated with GSC maintenance defects. Similar to *pum* mutant, I predict that *pst* might also display a GSC loss defect.

Table 3.6: Comparison of GSC-enriched genes from Kai and Spradling, 2005.

Gene	Function	Fold Δ		P-value[1]
"GSC" enriched		***dpp/bam****	***tkv^{CA}/bam^{Δ86}***	
pastrel	learning/memory	8.7	1.8	4.2E-05
CG13603	FnIII repeat	5.7	0.99	0.43
CG5028	S/T kinase	4.8	1.0	0.5
CG10191	heat shock protein	4.2	1.6	9.3E-06
CG2006	unknown	3.5	0.96	0.54
CG7900	fatty acid amide hydrolase	3.4	2.5	6.7E-06
TM4SF**	Tetraspanin	3.1	0.86	0.69
SP1029/CG11956		3.0	1.3	0.05
"pre-CB" enriched		***bam/dpp****	***bam/ tkv^{CA}***	
CG15390		18.2	0.99	0.5
dhd	deadhead	8.3	0.76	0.20
egr/CG12919		4.1	1.3	2.2E-03
CG11899		3.8	1.1	0.73
Paip2/CG12358		3.7	1.1	0.59
klu	klumpfuss	3.5	*0.71	0.25

[1] P-values are from comparisons of *tkv*^{CA} and *bam*^{Δ86} data

* *dpp* and *bam* ratios are taken from Kai and Spradling, 2005

** CG10106 was chosen as a representative tetraspanin for these comparisons

Comparisons of our analysis of *tkv*^{CA} and *bam*^{Δ86} germ cells with the analyses from Kai and Spradling's analysis of flow-sorted *dpp*-induced and *bam*^{Δ86} mutant germ cells did not reveal a large concordance of data (Table 3.6). This discordance could be attributed to experimental design (flow-sorted cells vs. mutant ovaries) or the different gene chip platforms (Affymetrix

Drosophila Genome, Version 1.0 vs. Version 2.0, representing 13,500 transcripts versus 18,500 transcripts, respectively). As mentioned previously, *pst* represents an intriguing transcript that was uncovered by both array experiments. Additionally, the tetraspanin family of proteins might also play a key role in GSC maintenance. Although my analyses with tkv^{CA} and $bam^{\Delta 86}$ germ cells did not reveal a differential expression of tetraspanins between these two samples, my previous results from subtractive hybridization did reveal this transcript as a possible GSC-enriched transcript. This suggests that tetraspanins may be involved in the organization of signaling networks and adhesion of GSCs to cap cells.

V.B. Epigenetic regulation of GSC fate

Unlike the analyses of tkv^{CA} and $bam^{\Delta 86}$ germ cells, the comparison of *stwl bam* and *bam* mutant ovaries provides a unique insight into the transcriptional changes that underlie the GSC. Stwl contains two modified SANT domains, the MADF and BESS domains, which have been studied in several *Drosophila* proteins, Myb, Adf1 and Dip3 (Bhaskar and Courey, 2002; Cutler et al., 1998). Previous studies have shown that SANT-domain proteins are associated with chromatin-remodeling and histone-modifying functions (Boyer et al., 2002). The MADF domains were essential for sequence-specific DNA-binding activity and the BESS domains mediate protein-protein interactions. In particular, due to observations that *stwl* mutations are dominant suppressors of position-effect variegation, *Su(var)*, we speculate that Stwl functions as a histone-interacting protein (Maines et al., 2007).

One of the most interesting aspects of Stwl+ transcriptional function in the GSC is that it might converge with the function of Nos-Pum complexes as translational repressors. Work from the McKearin lab has demonstrated that reducing the gene dosage of Nos and Pum suppressed

the expanded GSC phenotype observed by ectopic germline expression of Stwl (Maines et al., 2007). This indicates that the mechanism of Stwl action in controlling GSC fate relies heavily upon the function of Nos-Pum function. Indeed, an examination of upregulated gene targets in *stwl bam* ovaries revealed a higher than random occurrence of transcripts containing multiple Pum-binding sites (termed Nanos reponse elements, or NRE) in their 3′-UTR (Murata and Wharton, 1995; Sonoda and Wharton, 1999). This observation led us to speculate that Stwl represses a suite of CB-promoting differentiation factors, which are also targeted for translational repression by Nos-Pum complexes (Maines et al., 2007).

One particularly interesting transcript upregulated in *stwl bam* double mutants is the gene encoding for His3.3B, a histone variant that marks active chromatin (Ahmad and Henikoff, 2002). Since His3.3B is upregulated in the absence of *stwl*, this suggests that His3.3B is deposited into regions of active genes that promote GSC differentiation or are involved in cyst formation. As current efforts in the McKearin lab have focused on the pattern of expression of covalently modified histones, I predict that the dynamic expression of histone variants, including His3.3B, will play a critical role in modulating the turnover and redistribution of the GSC histone code.

Taking the requirements for Stwl in GSC maintenance together with the data supporting Stwl function in histone modification, expression profiling of *stwl bam* double-mutant ovaries against *bam* mutant ovaries uncovers genes whose expression is directly controlled by Stwl and/or upregulated in cyst development. In particular, Stwl negatively controls the transcription of mRNAs that promote CB differentiation. Thus, in the absence of *stwl* function, the abundance of CB-promoting mRNAs increases and permits the premature differentiation of GSCs to CBs.

Chapter 4. Identification of CSN4 as a dominant Suppressor of *bam*, Su(*bam*)

I. Summary

Bam protein is necessary and sufficient for GSC differentiation. Previous studies from our lab established that *Drosophila* females lacking *bam* are sterile produce hyperplastic ovaries filled with undifferentiated pre-CB cells (McKearin and Ohlstein, 1995; McKearin and Spradling, 1990). In addition, the ectopic expression of *bam* in GSCs forces them to differentiate into daughter CB cells (Ohlstein and McKearin, 1997). Accordingly, *bam* is a key factor regulating the process of GSC-to-CB transition.

Our lab has utilized genetic screens to identify factors that modulate bam function in the critical GSC-to-CB transition. Using a sensitized *bam* genotype that produces females with a reduced fecundity, I can screen for genes that modify bam function as measured through an increase or decrease in fertility. Enhancers of bam, E(*bam*), are predicted to diminish *bam* function and result in a stronger bam phenotype, as measured by female sterility and fully tumorous ovaries reminiscent of a strong *bam* phenotype. Using this approach, previous studies in our lab have demonstrated that Bgcn, a Bam-interacting protein required for Bam function, predictably acts as an enhancer of the sensitized *bam* genotype (Ohlstein et al., 2000).

Taking a candidate gene approach, I utilized a cross-references list of "stemness" genes identified from expression profiling of mammalian stem cell systems (Ivanova et al., 2002; Ramalho-Santos et al., 2002). Of note, CSN4, a subunit of the COP9 signalosome holoenzyme, was identified as a strong dominant Suppressor of *bam*, Su(*bam*). The COP9 signalosome has been studied as a multi-functional protein complex that is thought to play a role in the regulation of protein turnover through the SCF class of E3 ubiquitin ligases (Wei and Deng, 2003). As

such, I hypothesized that CSN4 and, by extention, the COP9 signalosome and SCF E3 ubiquitin ligases may play a role in Bam turnover during oogenesis. This prediction is consistent with the finding that multiple CSN4 alleles recapitulate the Su(*bam*) phenotype and that germline specific expression of CSN4 reverted the Su(*bam*) phenotype to the weak bam levels. Additionally, the core Cullin component of the SCF E3 ligase also acted as a dominant Su(*bam*).

Further studies of CSN4 and Bam function have revealed two additional pieces of data that may provide insight into Bam regulation during GSC-to-CB transition. First, work from our collaborators has identified CSN4 as a Bam-interacting protein by Y2H analysis (Ting Xie, personal communication). Second, I have found that the levels of Bam protein are sensitive to the gene dosage of both COP9 and SCF components that were isolated as Su(bam) genes. Taken together, these observations suggest that Bam protein levels are tightly regulated during the GSC-to-CB transition and that active mechanisms of Bam degradation are critical for maintaining GSCs.

II. Hypomorphic *bam* background for modifier screens

Our lab identified a weak allele of *bam*, bam^{BW} or $bam^{Z3\text{-}2884}$, and established a sensitized genetic background suitable for genetic modifier screens (Ohlstein et al., 2000). Females with the genotype $bam^{Z3\text{-}2884}/bam^{\Delta 86}$ are poorly fertile, presumably because they lack sufficient Bam activity. Additionally, it was demonstrated that this "weak *bam*" genetic background could be used to screen for factors that modify Bam function. Since our lab has demonstrated that Bam and Bgcn may function together in a complex to promote cystoblast differentiation, testing *bgcn* in the sensitized *bam* background serves as a standard enhancer of *bam*, E(*bam*). Reducing the dosage of *bgcn* (*bgcn*/+; $bam^{Z3\text{-}2884}/bam^{\Delta 86}$) enhances the phenotype of the sensitized genetic background and the females become completely sterile, phenocopying a strong *bam* mutations (Ohlstein et al., 2000). Thus, I can use the sensitized *bam* background to screen for mutations that increase or decrease female fecundity and identify genes that dominantly modify *bam* function.

Previous efforts in the McKearin lab focused on P-element, deficiency or EMS based screens for E(*bam*) genes, scoring for decreased fecundity as a primary screen. Using this paradigm, I used the sensitized *bam* background to employ a candidate gene screen for *bam* modifiers. I selected available mutant alleles of *Drosophila* genes that appeared as "stem cell" genes on microarray analyses (Ivanova et al., 2002; Ramalho-Santos et al., 2002). Mutant alleles were put into the sensitized *bam* background and fecundity scored on a scale of 1-5 relative to the sensitized background alone (1 = no enhancement; 5 = strong enhancement, e.g., *bgcn*). In addition to the "stemness" genes, I also tested a series of mutant alleles of various kinases and signaling molecules (Table 4.1).

Table 4.1: Selected list of genes tested as *bam* modifiers

Genes/deficiencies tested as *bam* modifier (Stock number)	**Mammalian orthologue**	**Fecundity score**
bgcn[1] **(Positive control)**	DExH helicase domain	5
CyO balancer **(Negative control)**	---	2
Df(1)mal3 (#899)	TAK1	2
Dsor1 (#5545)	MAPKK	2
Df(1)N12 (*hep* and *lic*; #966)	MAPKK	2
mys (#12881)	PS integrin β-subunit	1
Df(2R)rl10a (*rolled*; #742)	MAPK	2
CSN4 (#10765)	CSN4	SUPPRESSION
emb (#11195)	Exportin-1	1
Rho1 (#12185)	Rho-GTPase	2.5
zfrp8 (#12199)	Pdcd2	3.5
bsk (#3088)	MAPK	2
Df(3L)AC1 (#997)	Sialomucin	3.5
awd (#12167)	Nucleotide diphosphate kinase	3.5
Ras85D (#11694)	Ras	3

It is important to note that between 15-20 other "stemness" genes chosen for the pilot screen for *bam* modifiers uncovered no genetic interactions. While there were a few genes that were identified as putative E(*bam*) genes (e.g., *zfrp8* or *awd*), I decided to focus my efforts on CSN4 which was identified as a strong dominant Su(*bam*). The reasons were two-fold: first, none of the putative E(*bam*) genes showed strong enhancement as observed with *bgcn*. Multiple

factors, including non-specific effects, could present as an enhanced genetic phenotype; thus, given the inability to identify a strong enhancer, I focused my efforts on the Su(*bam*) genes. Second, the unexpected identification of a Su(*bam*) provided the opportunity to study a protein, CSN4, that might be involved directly with Bam protein turnover or activity, as suggested by the dominant suppression result. At this point, I decided to forego analyses of the putative E(*bam*) genes from the stemness lists and focus my efforts on CSN4 and other related Su(*bam*) genes.

III. Characterization of CSN4 as a Su(*bam*) gene

To verify candidate modifier genes, I developed a quantitative secondary screen noting that the decreased fecundity of $bam^{Z3\text{-}2884}/bam^{\Delta 86}$ females could be scored by counting the number of nurse cell-positive cysts per ovariole (hereafter "cyst/ovariole ratio"). The number of ovarioles and nurse cell-positive cysts can be easily determined by staining fixed ovaries with Hoescht or DAPI dye. In a wild-type ovariole from 3 day old females, the cyst/ovariole ratio is 6.7 ±0.7; for the sensitized $bam^{Z3\text{-}2884}/bam^{\Delta 86}$ genotype, the ratio was 1.2 ±0.5 (Table 4.2).

XX; $bam^{Z3\text{-}2884}/bam^{\Delta 86}$	+/+	*bgcn*/+	*CSN4*/+
cyst/ovariole	1.2 ±0.5	0.1 ±0.05	4.7 ±0.4

Table 4.2: Quantitative assay for genetic modifiers of the *bam* phenotype. The 2nd chromosome genotype ("XX") noted in each column header. All animals carry the $bam^{Z3\text{-}2884}/bam^{\Delta 86}$ genotype on the 3rd chromosome.

Of particular interest was *CSN4*, a subunit of the COP9 signalosome (CSN), which was identified as a dominant Suppressor of *bam*, Su(*bam*). Using the cyst/ovariole ratio, I found that multiple alleles of CSN4 acted as Su(*bam*), confirming my previous findings in the original screen of stemness genes. Moreover, ovaries dissected from *CSN4*/+; $bam^{Z3\text{-}2884}/bam^{\Delta 86}$ females

resembled wild-type ovaries in overall morphology. These data suggest that *CSN4* acted as a dominant Suppressor of *bam*, allowing for near wild-type levels of Bam+ function.

To determine whether *CSN4* function as a Su(*bam*) was due to requirement in the germ cells, I decided to employ both clonal analyses as well as germ cell specific expression of CSN4 using an EP element. Null alleles of *CSN4* are lethal and result in lethality at the late larval or pupal stage, likely due to the pleiotropic requirements for CSN during various stages of development (Freilich et al., 1999; Oron et al., 2002). Clonal analysis using the $CSN4^{null}$ allele (obtained from S. Beckendorf) revealed a germ cell lethal phenotype, similar to that described in Doronkin *et al*. 2003. As these results did not allow for downstream characterization of germ cell differentiation in the absence of CSN4, further clonal analyses were not pursued due to the inability to generate viable germline clones. However, work from Ting Xie's lab suggests that CSN4 is required for GSC maintenance (T. Xie, personal communication).

Another approach to determine the germline requirement for *CSN4*'s Su(*bam*) activity is through EP-mediated cell-type specific expression, using the Gal4/UAS system (Bellen et al., 2004; St Johnston, 2002). Three alleles of *CSN4* all acted as Su(*bam*) genes giving a cyst/ovariole ratio of between 3.8 to 5.1 (Table 4.3). Since the Su(*bam*) phenotype was recapitulated by three different *CSN4* alleles, I was reasonably confident that the suppression activity was due to the reduced gene dosage of *CSN4*. More importantly, since the $CSN4^{EY08080}$ allele is an EP element, I combined it with a P{*nosP-Gal4:VP16*} transgene to drive germline expression of *CSN4* in the weak *bam* background (genotype $CSN4^{EY0808}$/+; $bam^{Z3\text{-}2884}/bam^{\Delta 86}$, P{*nosP-Gal4:VP16*}). This genotype suppressed the dominant Su(*bam*) activity of *CSN4*, with a cyst/ovariole ratio of 0.7 (Table 4.3). Therefore, since the Su(*bam*) activity corresponded with three different *CSN4* alleles and that the Su(*bam*) activity could be suppressed by EP-mediated

germline expression of CSN4, this suggests strongly that CSN4 acts in the germline to stabilize Bam function in a weak *bam* background. Taken together, these data suggest that CSN4 plays a direct role in the early germ cells to promote GSC maintenance by antagonizing Bam function.

Table 4.3: Quantification of *CSN4* and *cul1* as Su(*bam*) genes

Genotype	Cyst/Ovariole ratio
+/+ (wild-type)	6.7 ±0.7
+/+; $bam^{Z3\text{-}2884}/bam^{\Delta 86}$	1.1 ±0.2
$CSN4^{k08018}$/+; $bam^{Z3\text{-}2884}/bam^{\Delta 86}$	5.1 ±0.9
$CSN4^{null}$/+; $bam^{Z3\text{-}2884}/bam^{\Delta 86}$	3.8 ±0.8
$CSN4^{EY08080}$/+; $bam^{Z3\text{-}2884}/bam^{\Delta 86}$	4.4 ±0.8
+/+; $bam^{Z3\text{-}2884}$/ $bam^{\Delta 86}$ P{*nosP-Gal4:VP16*}	0.96 ±0.24
$CSN4^{EY08080}$/+; $bam^{Z3\text{-}2884}$/ $bam^{\Delta 86}$, P{*nosP-Gal4:VP16*}	0.68 ±0.37
$cul1^{k01207}$/+; $bam^{Z3\text{-}2884}/bam^{\Delta 86}$	3.5 ±1.1
$CSN5^{null}$/+; $bam^{Z3\text{-}2884}/bam^{\Delta 86}$	0.74 ±0.45
$CSN4^{k08018}$/ $cul1^{k01207}$; $bam^{Z3\text{-}2884}/bam^{\Delta 86}$	5.2 ±1.2

IV. CSN4-associated proteins also act as Su(*bam*)s

CSN4 is a component of the COP9 signalosome (CSN), which regulates the activity of SCF uniquitin ligases and, in turn, regulates the stability of various proteins, including Cyclin E, p27, c-Jun, and p53 (Cope and Deshaies, 2003; Doronkin et al., 2003; Wei and Deng, 2003). The CSN is a multiprotein complex that removes neddyl groups at the cullin-based SCF E3-ubiquitin ligases. Modification of the SCF by Nedd8, a small ubiquitin-like molecule, is required for proper SCF function. In addition, I have also found that inactivating alleles of *cullin-1* (*cul1*, also

known as *lin19*) also act as a Su(*bam*); *cul1*^{k01207}/+; *bam*$^{Z3\text{-}2884}$/*bam*$^{\Delta 86}$ females have a cyst/ovariole ratio of 3.5 (Table 4.3). I also examined whether double heterozygous *CSN4*/+ *cul1*/+ in a *bam*$^{Z3\text{-}2884}$/*bam*$^{\Delta 86}$ background would give a greater Su(*bam*) effect. However, I did not observe an additive effect in double heterozygous females (Table 4.3). This might be attributed to the strong Su(*bam*) phenotype seen in *CSN4*/+ heterozygotes, which have a comparable cyst/ovariole ratio to wild-type females. Nevertheless, these data suggest that the wild-type function of CSN4 and Cullin-1 (and by extension, the CSN and the SCF) acts to antagonize Bam activity, perhaps through the same mechanism.

V. Bam protein stability in Su(*bam*) heterozygous animals

Since the COP9 signalosome and SCF E3 ubiquitin ligases play an important role in the turnover and degradation of proteins, I hypothesized that Bam might also be targeted for degradation by these protein complexes. To test this possibility, I examined the levels of an epitope-tagged Bam protein in wild-type and heterozygous females for several Su(*bam*) candidate genes, *CSN4* and *cul1*. Ovarian extracts from these genetic backgrounds revealed that Bam protein was more abundant when the gene dosage was reduced for CSN4 and Cul1 (Figure 4.1). Importantly, a non-Su(*bam*) gene, *CSN5*, which is also part of the COP9 signalosome holocomplex, did not alter the levels of Bam protein. This finding supports the genetic evidence that *CSN5* does not act as a Su(*bam*) and suggests that Bam protein levels are uniquely sensitive to a select subset of genes that comprise the COP9 and SCF complexes. In particular, examination of the subunit interactions of the CSN complex suggests that the CSN4 subunit may serve a scaffolding function, as it has been reported to form contacts with all other CSN subunits (Wei and Deng, 2003). Similarly, the Cullin subunit forms the platform for the

assembly of the SCF E3 ubiquitin ligase (Wolf et al., 2003). Taken together, these data suggest that disrupting the CSN and SCF complexes through reducing the gene dosage of the core subunits results in the increase or stabilization of Bam protein.

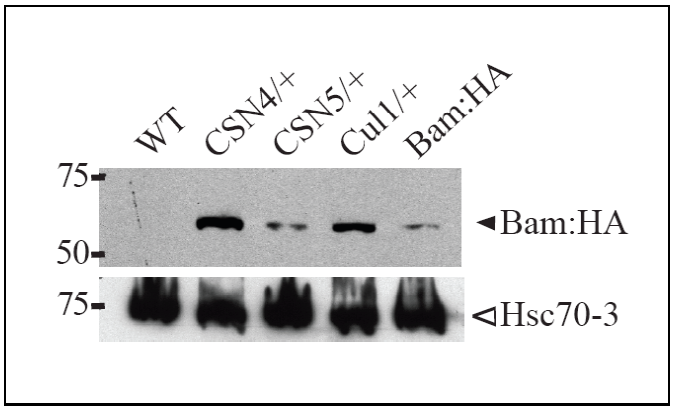

Figure 4.1: Levels of Bam protein in ovary lysates from wild-type and Su(*bam*) heterozygotes. Ovary extracts were generated from wild-type and Su(*bam*) heterozygous females carrying a P{*bam*P-Bam:HA} transgene. Western blots were probed with anti-HA antibody to detect Bam protein and anti-Bip to detect Hsc70-3 as a loading control.

Interestingly, other components of the COP9 signalosome complex (tested *CSN5* alleles and P-element insertions in *CSN7* and *CSN3*) also did not reveal a *bam* modifier phenotype. Similarly, other components of the SCF complex (Skp proteins, candidate F-box proteins, and Nedd8) did not act as *bam* modifiers. This suggests that (a) CSN4 is a core component of the COP9 signalosome and that it is dose-sensitive and/or (b) CSN4 affects Bam function in a COP9-independent fashion.

VI. Discussion

The data presented in this set of experiments studies the function of the CSN and SCF E3 ubiquitin ligases as dominant Suppressors of *bam*, Su(*bam*), suggesting that Bam protein turnover is critical to maintaining an undifferentiated state. I propose two hypotheses about this mechanism, either through direct turnover of Bam protein at the fusome or through a direct interaction between Bam and CSN through the CSN4 subunit.

VI.A. Stemness genes and the *Drosophila* GSC

In these experiments, I examined whether genes identified by expression profiling experiments in mammalian stem cell systems could be screened to identify factors that also affect *Drosophila* GSC biology (Ivanova et al., 2002; Ramalho-Santos et al., 2002). To test this hypothesis, I utilized a previously identified hypomorphic *bam* background to screen for factors that modulate the weak female fertile phenotype (Ohlstein et al., 2000). To provide quantitative rigor to a qualitative phenotype, I developed an assay measuring the index of maturing egg chambers per ovariole. Using this assay, I was able to identify a class of genes that act as dominant Suppressors of *bam*, Su(*bam*)s. Among these were the CSN4 subunit of the CSN signalosome holocomplex and the Cullin-1 subunit of the SCF E3 ubiquitin ligase.

Since many other stemness genes did not modify the weak *bam* phenotype, I would speculate that many of these genes might not modulate GSC fate. However, screening for factors that affect GSC fate using the hypomorphic *bam* phenotype might represent too narrow a criterion, as Bam represents a necessary and sufficient differentiation factor. As such, the hypomorphic *bam* background is uniquely tuned to identify factors that either promote Bam activity (e.g., Bgcn) or stabilize Bam protein (e.g., CSN4 and Cul1). Future experiments to identify factors influencing Bam activity could be identified through a P{*nosP-Gal4:VP16*} mediated, germline-specific EP screen in a $bam^{Z3\text{-}2884}/bam^{\Delta 86}$ genotype, screening for Su(*bam*) or E(*bam*) genes. This approach might uncover factors that act downstream of Bam function, whose overexpression would promote cyst development despite reduced Bam activity.

VI.B. Bam, Encore and the SCF ubiquitin ligases

Recent studies have provided insights into the possible connection between the SCF ubiquitin ligases and Bam turnover through the protein Encore (Enc). Mutations in *enc*, a novel protein, result in egg chambers that contain 32 cells instead of the normal complement of 16 cells (Hawkins et al., 1996; Van Buskirk et al., 2000). Previous studies have shown that *enc* mutations expand the region of *bam* expressing cells and that *bam* acts as a dominant suppressor of the extra-division *enc* phenotype (Hawkins et al., 1996). This suggests that Enc functions as a negative regulator of Bam.

Moreover, recent studies of Enc have shown that it associates with the proteasome and the cullin subunit of the SCF E3 ubiquitin ligase (Ohlmeyer and Schupbach, 2003). They found that reducing the gene dosage of *cul1* and *archipelago* (*ago*), the Cullin and F-box component of the SCF complex, dominantly enhanced the *enc* extra division phenotype. In *enc* mutant extracts, they found a slower rate of a slower rate of Cyclin E degradation as evidenced by the accumulation of ubiquitinated isoforms of CycE. The most intriguing finding of this study was the observation that Cul1 protein and a subunit of the 19S-regulatory particle in the germarium is enriched in the fusome (Ohlmeyer and Schupbach, 2003). This last finding is of most interest to the studies reported here, as our lab has previously shown that Bam protein is found both in the cytoplasm of differentiating germline cysts as well as the fusome of early germ cells, including the GSC (McKearin and Ohlstein, 1995). Thus, it is tempting to speculate that the fusome represents a docking site for the SCF ubiquitin ligase complex and the location of Bam degradation.

VI.C. A direct interaction between Bam and CSN4?

Independent studies conducted in the laboratory of Ting Xie identified CSN4 as a Bam-interacting protein by yeast-two-hybrid analyses (T. Xie, personal communication). Additionally, using germline mosaics, they also determined that CSN4 is required for GSC maintenance. Future collaborative studies between the McKearin and Xie labs will focus on the nature of Bam protein turnover with respect to CSN activity. With regards to the Bam-CSN4 interaction uncovered by yeast two-hybrid analysis, it will be important to map the protein-protein interaction domain, as this will yield important insights into their function. For example, does the CSN4 interaction overlap with the lesion associated with the *bam*$^{z3\text{-}2884}$ lesion (L255P)? If so, this might provide a direct explanation for the Su(*bam*) phenotype observed in *CSN4* heterozygotes.

Previous studies have suggested that subunits of the CSN may form subcomplexes that consist of a subset of CSN subunits (Karniol et al., 1999; Mundt et al., 2002; Oron et al., 2002; Tomoda et al., 2002; Wang et al., 2002). Thus, it is possible that the Bam-CSN4 complex may represent a bioactive complex that functions independently of the CSN holocomplex. However, although this is a viable hypothesis, it is unlikely as mutations in both *CSN4* and *cul1* produce a Su(*bam*) phenotype. This suggests that the mechanism of Su(*bam*) action is through protein turnover, with Bam as the likely target.

In future studies, it will be important to examine Bam protein levels in *CSN4* germline clones. Based upon the Su(*bam*) data, I predict that Bam protein will be elevated in *CSN4* clones relative to wild-type, stage-matched cysts. However, it will also be important to observe whether the *CSN4* clones display concomitant defects associated with inappropriate Bam turnover, including cell cycle defects, changes in fusome morphology, and extra rounds of mitotic division

(i.e., 32-cell cysts, similar to that observed in *enc* mutants). Ultimately, the studies of the CSN signalosome and SCF E3 ubiquitin ligases as dominant Su(*bam*) genes reveal the importance for protein turnover in promoting GSC-to-CB differentiation.

Chapter 5. Generation of new *loquacious* alleles and transgenic constructs

I. Summary

This set of experiments was designed to generate null alleles of *loqs*. Genetic and biochemical characterization revealed that the original piggyBac allele of *loqs* was a hypomorphic allele that proved insufficient for further analysis. Using two parallel approaches, both a deletion allele and a gene-targeted knockout allele of *loqs* was generated.

The original piggyBac allele provided the ability to generate a deletion of the *loqs* locus using a FLP/FRT-mediated deletion approach. Three deletions, $loqs^{del}$, were isolated and they were homozygous lethal. Complementation tests with the *loqs* hypomorphic allele recapitulated the GSC maintenance defects that were originally described.

Targeted *loqs* knockout alleles, $loqs^{KO}$, were generated by ends-out homologous recombination. The $loqs^{KO}$ alleles were protein null and homozygous lethal, with escaper females displaying severe defects in GSC maintenance. While most mutant animals died during the larval/pupal transition, depletion of maternally loaded Loqs protein resulted in embryonic lethality. All of these defects could be rescued by a *loqs* transgene driven by the endogenous *loqs* promoter. Interestingly, the Loqs-PB isoform is sufficient to rescue all defects associated with *loqs* mutant animals.

Germline mosaic analyses revealed that *loqs*+ function is required cell-autonomously for GSC maintenance. This finding is corroborated by cell-type specific expression of *loqs-PB* using the Gal4/UAS system. Taken together, these studies demonstrate that Loqs is an essential protein required for embryonic viability and GSC maintenance.

II. Characterization of hypomorphic *loqs* allele

Independent studies from the labs of Qinghua Liu and Phil Zamore identified a piggyBac element inserted in the 5' UTR of *loqs* (*loqs*^{f00791}) (Forstemann et al., 2005; Jiang et al., 2005). This transposon insertion behaved as a hypomorphic allele, with mutants displaying defects in miRNA processing as well as defects in female GSC maintenance and female sterility.

However, we felt it necessary to pursue our studies of *loqs* function with null alleles for the following reasons. First, *loqs*^{f00791} homozygotes produced a low but detectable level of *loqs* transcript (Forstemann et al., 2005; Jiang et al., 2005). Second, *loqs*^{f00791} homozygotes displayed defects in miRNA production that presented with an accumulation of the precursor pre-miRNA; curiously, mature miRNA production seemed unaffected (Jiang et al., 2005). Accordingly, we were unable to fully ascertain Loqs requirement during miRNA biogenesis, as we could not rule out the possibility that the reduced level of Loqs produced by the hypomorphic allele was affecting baseline miRNA processing. Third, while working with an outcrossed, isogenized *loqs*^{f00791} allele, I noticed that the female sterility phenotype was unlinked with the transposon insertion, whereas the GSC maintenance defects were still linked with the transposon. This suggested that a second-site mutation on the initial *loqs*^{f00791} chromosome was confounding our analysis of the *loqs* phenotype. Taken together, these findings indicated that the *loqs*^{f00791} allele alone would be insufficient for genetic and biochemical analyses.

III. Generation of *loqs* deletion allele by FLP/FRT recombination

To fully elucidate the requirement for Loqs in studying both miRNA biogenesis as well as germline stem cell maintenance, we felt it necessary to pursue our studies with *loqs* null

alleles. Standard *Drosophila* genetics often employs P-element mobilization to generate deletion alleles that generate chromosomal deletions during the excision process. However, the piggyBac transposon class does not allow for this method as excision of these elements results in "clean" removal of the transposon without deletions of the surrounding chromosomal locus. Thus, in order to generate *loqs* null alleles, we employed two methods simultaneously: FLP/FRT recombination mediated deletion and gene targeting by ends-out homologous recombination (Parks, et al. 2004; Gong and Golic, 2003). FLP/FRT mediated gene deletion utilized two FRT-bearing piggyBac transposons flanking *loqs* and CG9293, a downstream gene. Even though this strategy would delete two genes, we pursued this endeavor for two reasons: first, I planned to make this deletion and rescue the CG9293 deletion with a rescuing transgene and, second, there were no existing deficiencies that uncovered genes in this chromosomal locus.

In brief, the two transposons were placed in *trans* and heat-shocked to induce the expression of Flippase, mediating recombination between the FRT sites of the two transposons. Progeny bearing putative deletion events (n=75) were collected and used to establish stocks and screened for deletion by two-sided PCR (see Materials and Methods for details). Of the 75 progeny screened, three were identified (hereafter, $loqs^{del}$) that carried the deletion of both *loqs* and CG9293, representing a 4.9 kb deletion product. These three lines were homozygous lethal and each failed to complement the GSC maintenance defects of the original $loqs^{f00791}$ allele. Since this deletion removed both *loqs* and the downstream gene CG9293, the lethality of this allele could be attributed to loss of either gene. In order to use these deletions effectively as a *loqs* null allele, a rescuing allele for CG9293 should be constructed. However, since we were generating targeted *loqs* knockouts by ends-out homologous recombination (see next section), I

decided not to pursue generating a CG9293 rescuing transgene, focusing instead on generating other reagents (e.g., *loqs* rescuing transgenes).

Nonetheless, the *loqs*^{del} allele proved useful because I could corroborate and quantify GSC maintenance defects observed in the original *loqs*^{f00791} allele. Transallelic *loqs*^{del}/*loqs*^{f00791} females lost GSCs at rates similar to *loqs*^{f00791} homozygotes, indicating that the GSC maintenance defects are associated with lesions in the *loqs* gene (Table 5.1). Additionally, *loqs*^{del}/*loqs*^{f00791} females were weakly fertile, supporting the finding that a second-site mutation on the original *loqs*^{f00791} chromosome accounted for the previously described sterility phenotype (Forstemann et al., 2005). Rescuing transgenes for both the *loqs-PB* and *loqs-PA* isoforms driven by a ubiquitin promoter were able to rescue the GSC maintenance defects associated with the *loqs*^{del}/*loqs*^{f00791} genotype (see Table 5.2 for transgenic constructs).

Table 5.1: *loqs* mutant females display GSC maintenance defects

Genotype	***w*^{1118}**	***loqs*^{del}/*loqs*^{f00791}**			***loqs*^{del}/*loqs*^{f00791} +P{*ubi*P-*loqs-PB*}**	***loqs*^{del}/*loqs*^{f00791} +P{*ubi*P-*loqs-PB*}**
# days post eclosion	7	3	5	12	7	7
# GSC per germarium	2.6	0.45	0.17	0	2.4	2.1

Unlike the original *loqs*^{f00791} allele, the transallelic *loqs*^{del}/*loqs*^{f00791} females were weakly fertile. This suggested that a second site mutation on the *loqs*^{f00791} chromosome accounts for female sterility. In fact, backcrossing the original *loqs*^{f00791} allele to a *w*^{1118} wild-type stock and subsequent isogenization was also sufficient to separate the second site mutation from the

loqs^{f00791} transposon, resulting in homozygous mutant females displaying GSC maintenance defects and weak fertility.

IV. Generating a *loqs* knockout allele by ends-out homologous recombination

Targeted knockout alleles of *loqs* were generated by ends-out homologous recombination (Gong & Golic, 2003). In brief, a targeting vector was generated by cloning genomic sequences flanking the *loqs* gene locus and used to make transgenic lines (Figure 5.1). Subsequent heat-induced expression of FLP recombinase and *I-SceI* endonuclease excised the targeting construct from the genome and induced double-stranded breaks that mediate homologous recombination, respectively.

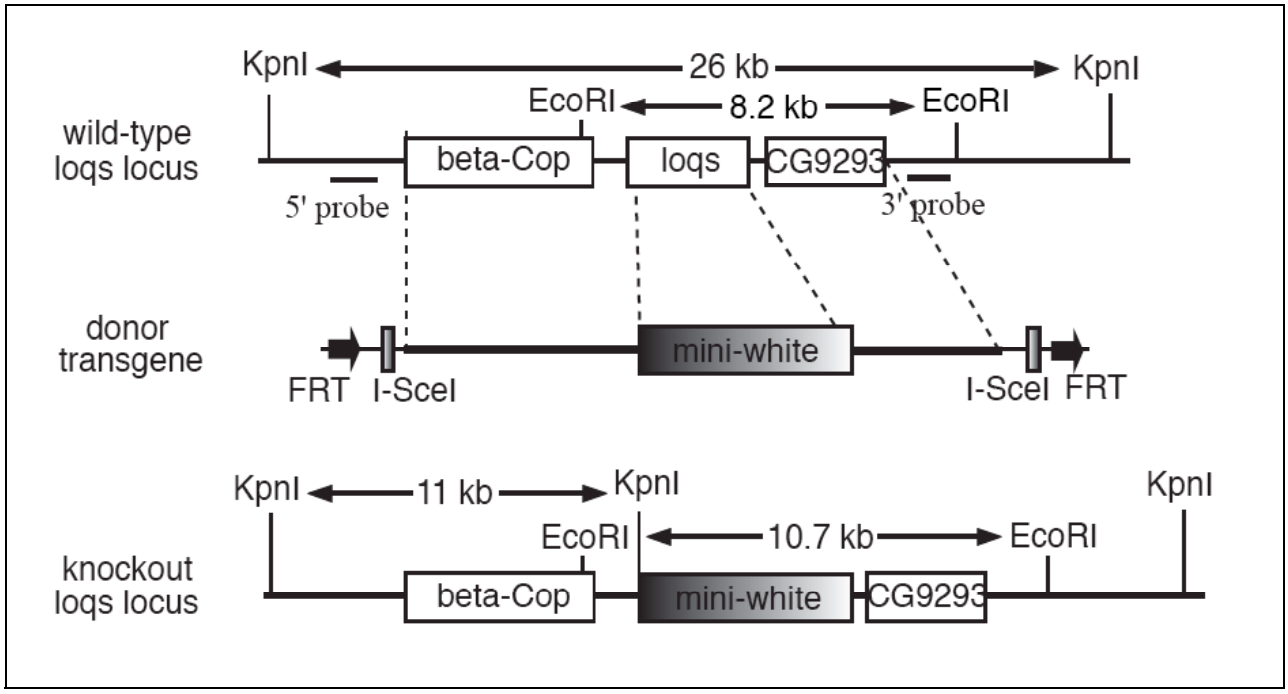

Figure 5.1: Generation of *loqs*^{KO} lines by ends-out homologous recombination. The donor targeting transgene was surrounded by genomic sequences 4.4 kb upstream and 2.3 kb downstream of the *loqs* locus. The entire targeting construct was flanked by I-SceI restriction sites and FRT sites. KpnI and EcoRI restriction sites are shown for wild-type and knockout *loqs* loci. The 5′ and 3′ probes used for Southern blot analyses are represented as short bars external to the recombination locus.

We observed candidate targeting events, screened on the basis of full w^+ eye color, in approximately 1:450 progeny. A total of 192 candidate targeted lines were screened initially by PCR analysis and subsequently confirmed by Southern blotting (Figure 5.2); a total of 34 independent *loqs*^{KO} alleles were identified (~18% of candidate targeted lines). Two independent lines (*loqs*$^{KO1\text{-}53}$, *loqs*$^{KO2\text{-}49}$) were selected for subsequent genetic analyses.

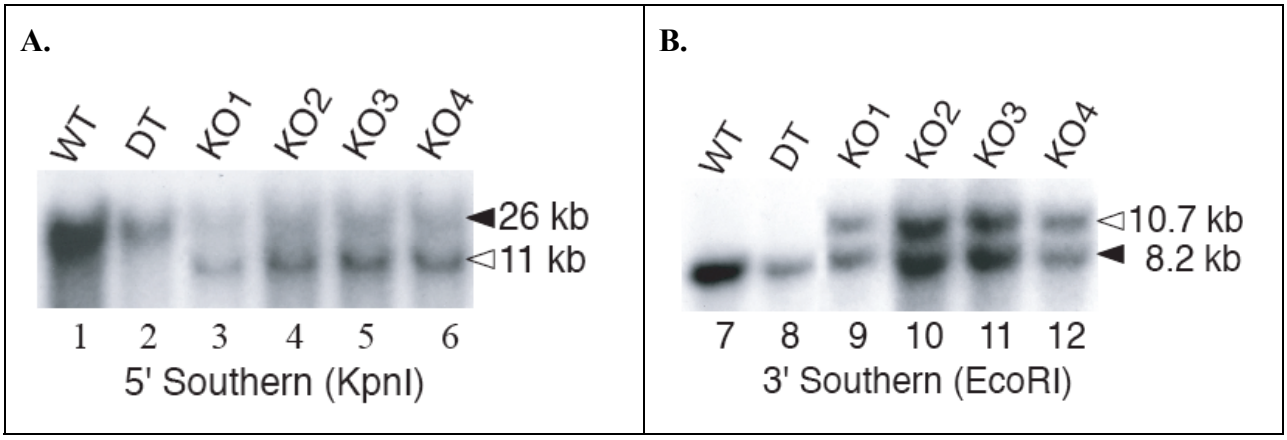

Figure 5.2: Southern blots using KpnI or EcoRI-digested genomic DNA of whole flies. Probes were designed to both the (A) 5′- and (B) 3′-regions of the targeted locus. WT = wild type; DT = donor transgenic; KO = heterozygous *loqs*^{KO} lines. **(Southern blots performed by Xiang Liu).**

V. Characterization of the *loqs* knockout lines

All of the 34 independently derived *loqs*^{KO} alleles were homozygous lethal. I selected 10 different lines for a genetic complementation test against both the *loqs*^{f00791} allele and the *loqs*^{del} allele. As expected, the *loqs*^{del} allele failed to complement each of the *loqs*^{KO} alleles; this indicated that the lethality observed in the *loqs*^{KO} lines was due to the absence of wild-type *loqs* function. Similarly, as observed in the *loqs*^{del}/*loqs*^{f00791} females, the *loqs*^{KO}/*loqs*^{f00791} females displayed GSC maintenance defects (Figure 5.3).

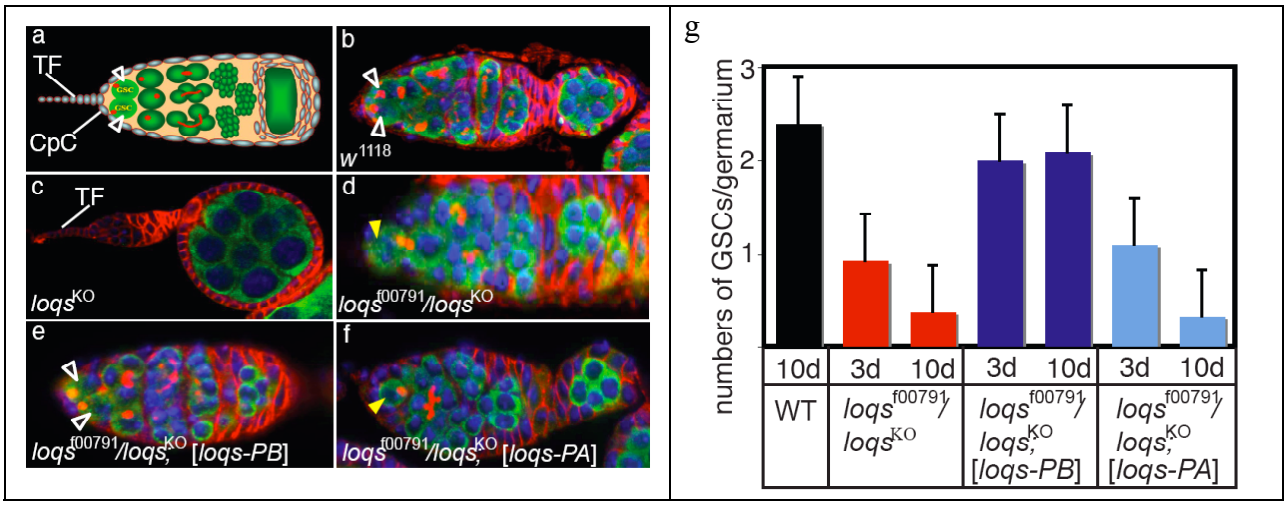

Figure 5.3: GSC maintenance requires Loqs-PB. (a) Schematic diagram of a wild-type germarium with germ cell (green), terminal filament (TF) and cap cells (CpC) (blue), and fusomes (red). Ovaries were dissected from (b) wild-type, (c) *loqs*^{KO}, (d) *loqs*^{KO}/*loqs*^{f00791}, (e) *loqs*^{KO}/*loqs*^{f00791}; P{*loqs-PB*}, and (f) *loqs*^{KO}/*loqs*^{f00791}; P{*loqs-PA*} females and stained for anti-Vasa (green, germ cells), anti-Hts (red, fusomes), DAPI (blue, nuclei). GSCs (open arrowheads) were identified as Vasa-positive germ cells in close apposition to the CpCs with anteriorly-positioned fusomes. Yellow arrowheads denote differentiated cysts at the anterior of the germarium, indicative of GSC loss. (g) The number of GSCs per germarium (Y-axis) was quantified at 3- and 10-days post-eclosion. Error bars represent standard deviation.

To determine the requirement for *loqs* function during development, we collected wild-type and *loqs*^{KO} and *dcr-1*^{Q1147X} homozygous embryos on standard apple juice/agar plates and monitored over the next 10-12 days during development. As shown in Figure 5.4, both wild-type and *loqs*^{KO} embryos hatched and developed at rates. However, viability dropped precipitously during the pupal/adult transition, with most *loqs*^{KO} animals dying during eclosion.

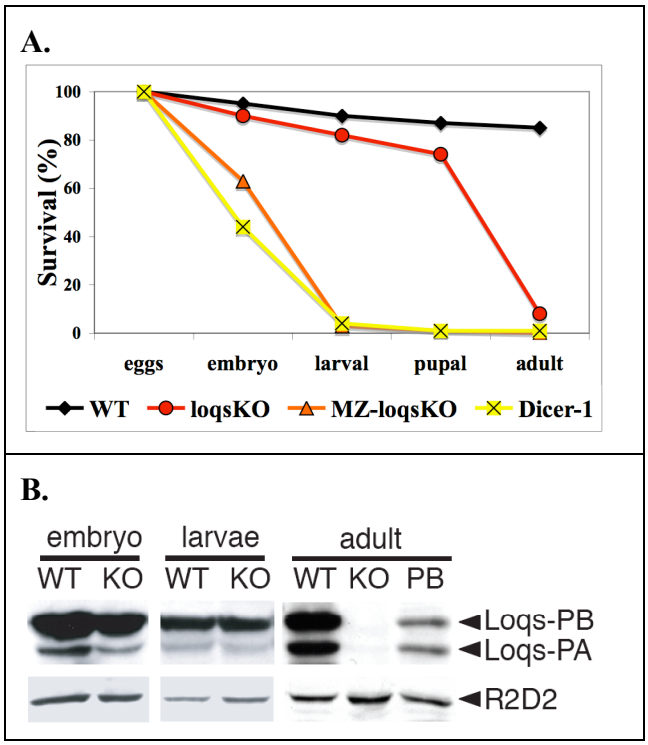

Figure 5.4: *loqs* mutant animals are lethal and lack Loqs protein.

(A) Lethal phase analysis of wild-type, *loqs*^{KO}, MZ-*loqs*^{KO} and *dcr-1*^{Q1147X} mutant animals. GFP-marked balancers were used to sort homozygous mutant embryos by the absence of GFP expression.

(B) Loqs and R2D2 protein levels measured by Western blots. Lysates from wild-type (WT) and zygotic *loqs*^{KO} (KO) null animals were isolated at various stages during development.

Interestingly, although Loqs-PA and Loqs-PB isoforms were not detected in *loqs*^{KO} adults, we noticed that both isoforms could be detected in mutant embryos and larvae. This suggested that Loqs proteins were maternally loaded and were exhausted at the pupal/adult transition in the zygotic *loqs*^{KO} null animals. Using the FLP-ovo^{D} system (Chou et al., 1993), I could eliminate maternal contribution of Loqs and observed that the maternal and zygotic (MZ)-*loqs*^{KO} null embryos could not develop past the first instar larval stage. This was similar to the lethal phase of *dcr-1* null embryos.

VI. Generating *loqs* rescuing transgenes

Loqs rescuing constructs were generated with two specific parameters in mind. First, I needed to ascertain the different requirements for the long and short *loqs* isoforms, *loqs-PB* and

loqs-PA, respectively. Secondly, I needed to determine the temporal and spatial requirements for *loqs* expression. Thus, for both *loqs* isoforms, we generated rescuing transgenes driven by the endogenous *loqs* promoter (i.e., genomic sequences 2.5 kb upstream of *loqs*), a ubiquitin promoter and an inducible UASp promoter. Each of these constructs also included an N-terminal myc tag. In addition, a GFP-tagged construct driven by as UASp promoter was also generated. (see Table 2.2 for full information on *loqs* transgenes).

Each of the *loqs* transgenes was tested for rescue of $loqs^{KO}$ associated lethality and GSC maintenance defects. Both the ubiquitin- and loqs-promoter driving expression of *loqs-PB* were able to rescue *loqs*-associated lethality (Figure 5.5). In addition, the expression of *loqs-PB* from a UASp promoter by *P*{*tub*-Gal4} and P{*nos*P-Gal4:VP16} was sufficient to rescue lethality and GSC maintenance, respectively. Interestingly, the P{*ubi*P-*loqs-PA*} was also able to rescue $loqs^{KO}$ null animals, suggesting that overexpression of the *loqs-PA* isoform could rescue *loqs*-associated developmental defects.

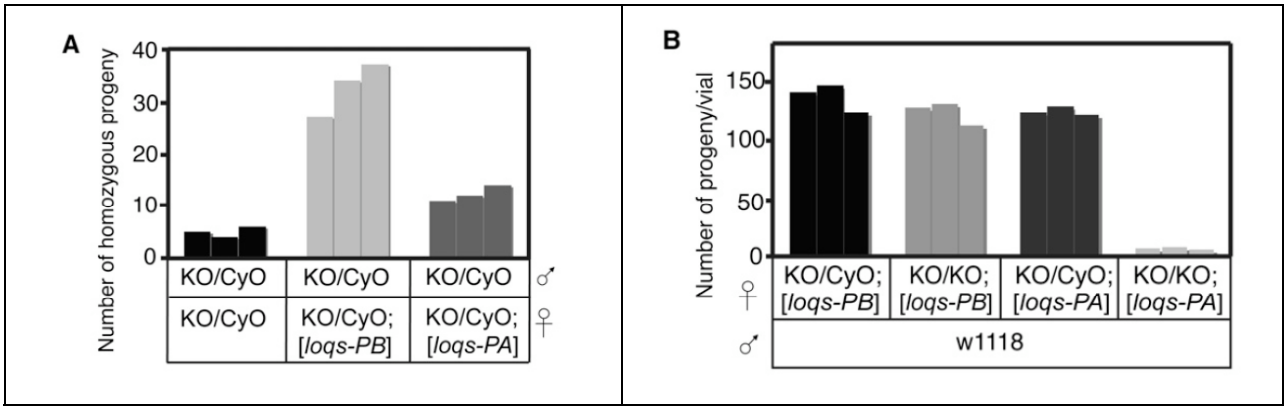

Figure 5.5: Loqs-PB, but not Loqs-PA, is sufficient for *Drosophila* development. All crosses were performed in triplicate. (A) Each cross contained three heterozygous males and five heterozygous females with or without a P{*loqs*P-*loqs-PB*} or P{*loqs*P-*loqs-PA*} transgene. The Y-axis is the number of homozygous $loqs^{KO}$ progeny per cross. (B) Five heterozygous or homozygous females carrying either the P{*loqs*P-*loqs-PB*} or P{*loqs*P-*loqs-PA*} transgene were mated with three wild-type males. The Y-axis measured the total number of progeny per cross.

VII. Discussion

The initial phenotypic characterization of the hypomorphic *loqs* allele pointed to a role for *loqs* in GSC maintenance and/or germ cell development. However the lack of additional *loqs* alleles made it difficult to further our understanding of *loqs*+ function. Additionally, the fortuitous discovery of a second-site mutation on the original $loqs^{f00791}$ chromosome revealed the necessity of generating new *loqs* mutant alleles.

Taking two parallel approaches, we developed two useful *loqs* null alleles: a *loqs* deficiency and a *loqs* knockout allele. Genetic complementation studies revealed that both alleles were deficient for *loqs*+ function. Molecular examination of both alleles showed that both the deficiency allele and knockout allele produced deletions of the *loqs* gene locus. Western blot analyses of the *loqs* knockout allele demonstrated that it was a protein null, allowing for subseqeuent genetic and biochemical analyses.

Construction of transgenic *loqs* rescuing constructs allowed for a detailed analysis of the two major *loqs* isoforms, *loqs-PB* and *loqs-PA*. I found that the longer *loqs-PB* isoform is sufficient to rescue the lethality and GSC maintenance defects associated with strong *loqs* genotypes. Intriguingly, transgenic constructs that overexpress *loqs-PA* showed a low but significant ability to rescue *loqs*-associated lethality but not GSC maintenance defects. This suggests that *loqs-PA* could partially substitute for *loqs-PB* function in vivo, though limited in its redundancy.

These isoforms both share the three putative dsRNA-binding domains, but alternative splicing removes exon 4 and results in a protein differeing by 46 amino acids that contain no obvious sequence motif. Biochemical studies have demonstrated that Dcr-1 forms a stable complex with Loqs-PB, but not with Loqs-PA, and that this association greatly enhances Dcr-1-

mediated miRNA processing (Jiang et al., 2005). I speculate that the 46 residues that are present in Loqs-PB are responsible for its higher affinity for Dcr-1. Alternatively, it is possible that Loqs-PA may play a role as a negative regulator of the miRNA pathway by interfering miRNA biogenesis. Taken together, these set of experiments reveal that Loqs is required in a cell-autonomous manner for GSC maintenance. Cell-type specific expression using isoform-specific *loqs* transgenes revealed that Loqs-PB is sufficient to rescue biological and biochemical defects associated with *loqs* mutants. In subsequent immunohistochemical studies with respect to Loqs protein, my studies deal with the Loqs-PB isoform, as it is likely the major active isoform during oogenesis.

Chapter 6. Cell-autonomous requirement for Loqs in GSC maintenance

I. Summary

Previous studies described a single, hypomorphic *loqs*^{f00791} allele caused by the insertion of a piggyBac transposon that caused GSC loss and female sterility (Forstemann et al., 2005; Jiang et al., 2005). These studies suggested that the microRNA pathway might play a key role in the regulation of GSC maintenance.

Using a *loqs*^{KO} null allele, I fully characterized the nature of the *loqs* GSC maintenance defects by examining the time-course and mechanisms of GSC loss. Genetic epistasis experiments with *bam* suggested that *loqs* mutant GSCs are lost by a *bam*-dependent mechanism. In addition, premature activation of *bam* transcription or Bam protein levels was not observed in *loqs* mutant GSCs. These experiments suggest that Loqs plays a role in controlling GSC maintenance by repressing the function of CB-promoting genes that function downstream or in parallel to Bam function.

Using both germline clone induction and tissue-specific expression, I determined that *loqs* is required in a cell-autonomous fashion for GSC maintenance. *loqs* mutant germline clones are rapidly lost from the GSC niche and progress through cyst formation and egg chamber development. In addition, germline-specific expression, but not niche cell expression, of *loqs* was sufficient to restore GSC maintenance in *loqs* mutant females. Taken together, this series of experiments convincingly demonstrates that *loqs* and the miRNA pathway are required intrinsically for GSC maintenance. Abrogating this pathway, through mutations in *loqs*, *dicer-1* and *ago1* result in GSC loss.

II. *loqs* mutant females lose GSCs

Preliminary studies of *loqs* alleles demonstrated that Loqs is required for embryonic development and female GSC maintenance. In the following series of experiments, I examine the nature of Loqs-dependent GSC maintenance. Using genetic epistasis experiments, I determine that *bam* is epistatic to *loqs* function and that *loqs* mutant GSCs are lost in a Bam-dependent differentiation pathway. In addition, I also show that $loqs^{+}$ function is required in a cell-autonomous fashion.

III. *loqs* mutant GSCs lost via *bam*-dependent differentiation

One possible mechanisms of GSC loss in *loqs* mutant females is through premature activation of *bam*. Mutations in *bam* mutant blocks CB differentiation whereas the ectopic expression of *bam* forces GSC loss. Genetic epistasis experiments have shown that *pum*, a protein involved in translational control, is required for GSC self-renewal by repressing *bam*-independent differentiation pathways (Chen and McKearin, 2005; Szakmary et al., 2005). GSCs that are mutant for both *pum* and *bam* are not maintained and differentiate into maturing cysts with branched fusomes. This suggests that *pum* plays a role in controlling GSC maintenance by antagonizing the function of differentiation-promoting genes that function downstream or independent to *bam* function.

To determine whether *loqs* controls GSC self-renewal by repressing *bam*-independent pathways, I generated *loqs bam* double mutant animals to determine whether these *loqs bam* double mutant germ cells behave like *bam* mutants or *loqs* mutants. Since $loqs^{KO}$ mutant animals are lethal, I first performed epistasis experiments in $loqs^{f00791}/loqs^{KO}$; $bam^{\Delta 86}$ double mutant

animals. Similar to *bam*$^{\Delta 86}$ single mutants, *loqs bam* double mutant germ cells arrested in the pre-CB stage and did not differentiate into cysts (Figure 6.1). Whereas *pum bam* double mutant ovaries displayed signs of differentiation, including branched fusomes connecting germline cysts or polyploid cells reminiscent of nurse cells (Chen and McKearin, 2005; Szakmary et al., 2005), *loqs bam* double mutant ovaries were filled with single pre-CB cells with round unbranched fusomes. In addition, the anteriormost germ cell in a *loqs bam* double mutant ovary does not prematurely activate the P{*bam*P-GFP} transcriptional reporter, suggesting that *loqs*-mediated maintenance of GSCs does not act through depression of *bam* transcription (Figure 6.1).

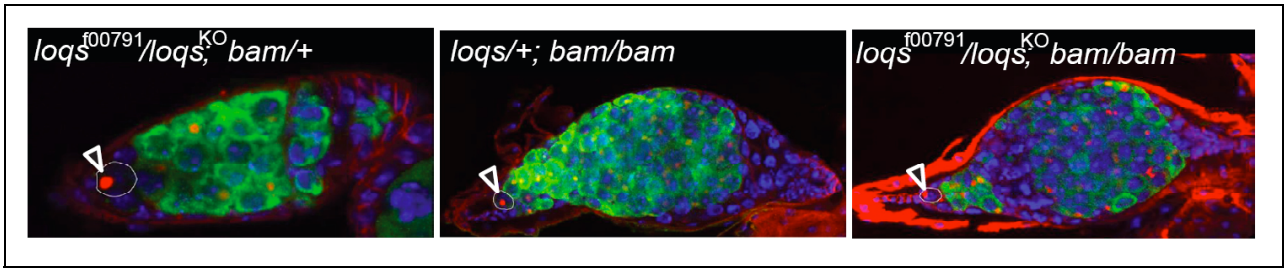

Figure 6.1: *bam* epistatic to *loqs* GSC phenotype. (Image taken from Park et al., 2007). Ovaries of *loqs*, *bam* or *loqs bam* double mutant females carrying a P{*bam*P-GFP} transcriptional reporter were immunostained with anti-Hts (red), anti-GFP (green), and DAPI (blue). Arrowheads represent GSCs lacking expression of P{*bam*P-GFP} reporter.

Although the *loqs*^{f00791}/*loqs*^{KO} genotype faithfully recapitulates the *loqs*-associated GSC loss phenotype, this background produces low but detectable levels of both *loqs* mRNA and Loqs protein (Jiang et al., 2005). Accordingly, I also performed the *loqs bam* epistasis experiments by generating *loqs*^{KO} germline clones in a *bam* mutant background. Again, similar to the *loqs*^{f00791}/*loqs*^{KO}; *bam*$^{\Delta 86}$ double mutant analysis, *loqs*^{KO} germline clones in a *bam* mutant background did not display signs of differentiation (Figure 6.2). Instead, within the *loqs*^{KO} germline clones, the double mutant cells were unable to produce cysts and arrested as pre-CB

cells with round unbranched fusomes. These data indicate that *loqs* mutant GSCs are lost via *bam*-dependent mechanism, requiring *bam*+ function in order to differentiate to CBs.

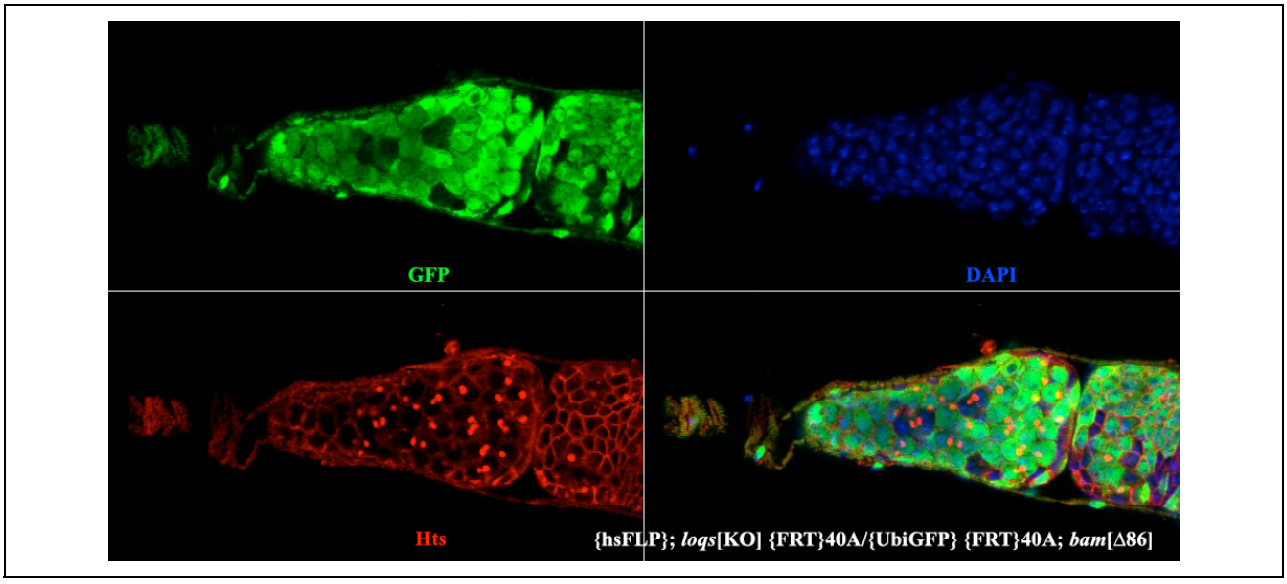

Figure 6.2: *loqs* does not act as a bypass suppressor of *bam*. $loqs^{KO}$ germline clones induced in *bam* mutant females. Clones were induced in females of the genotype {hsFLP}; $loqs^{KO}$ {FRT}40A/{UbiGFP} {FRT}40A; $bam^{\Delta 86}/bam^{\Delta 86}$. Negatively-marked *loqs* clones can be identified by the absence of GFP (green). Fusomes stained with anti-Hts (red) and nuclei stained with DAPI (blue).

IV. *bam* transcriptional control maintained in *loqs* mutant GSCs

Transcriptional quiescence of *bam* in the GSC is required for proper GSC maintenance; ectopic expression of *bam* in the GSC results in premature GSC differentiation. *bam* transcription is repressed by the Dpp/BMP signaling pathway in the GSC. Using a P{*bam*P-GFP} transgene, I can faithfully trace the germline cells in which *bam* transcription is active. In $loqs^{f00791}/loqs^{KO}$; bam^{+} mutant ovaries, I observed that the P{*bam*P-GFP} transgene is properly silenced in the anteriormost germ cells of each germarium (Figure 6.1, Table 6.1). In addition, I also noted that Bam protein does not accumulate prematurely in *loqs* mutant GSCs.

Taken together, these data suggest that *loqs* mutant GSCs are lost in a bam-dependent manner but not through premature activation or accumulation of Bam.

Table 6.1: P{*bam*P-GFP} in *bam* and *loqs bam* mutant ovaries

Genotype* with P{*bam*P-GFP}	# germaria	# GSC	*bam*GFP-	*bam*GFP+
$loqs^{+/+}$; $bam^{\Delta 86}/bam^{\Delta 86}$	N = 30	38	33	5
$loqs^{f00791}$/CyO; $bam^{\Delta 86/}bam^{\Delta 86}$	N = 30	37	32	5
$loqs^{f00791}/loqs^{KO}$; $bam^{\Delta 86}/bam^{\Delta 86}$	N = 30	39	35	4

* All genotypes listed also carry a P{*bam*P-GFP} transcriptional reporter. GSCs were scored based upon their close apposition to the anterior somatic niche cells of the germarium. Activation of the *bam* transcriptional reporter was scored in the GSCs. GFP+ GSCs likely represent CB cells near the GSC niche.

V. Cell-autonomous requirement for *loqs* function in GSC self-renewal

GSC self-renewal requires both intrinsic and extrinsic factors (Chen and McKearin, 2005; Szakmary et al., 2005). Accordingly, Loqs could function intrinsically within GSCs or extrinsically in somatic niche cells to control GSC maintenance. To distinguish between these possibilities, I generated mosaic germline clones using FLP/FRT-mediated mitotic recombination (Xu and Rubin, 1993). This method allows for the examination of the lethal $loqs^{KO}$ null allele and study Loqs requirement in the GSC.

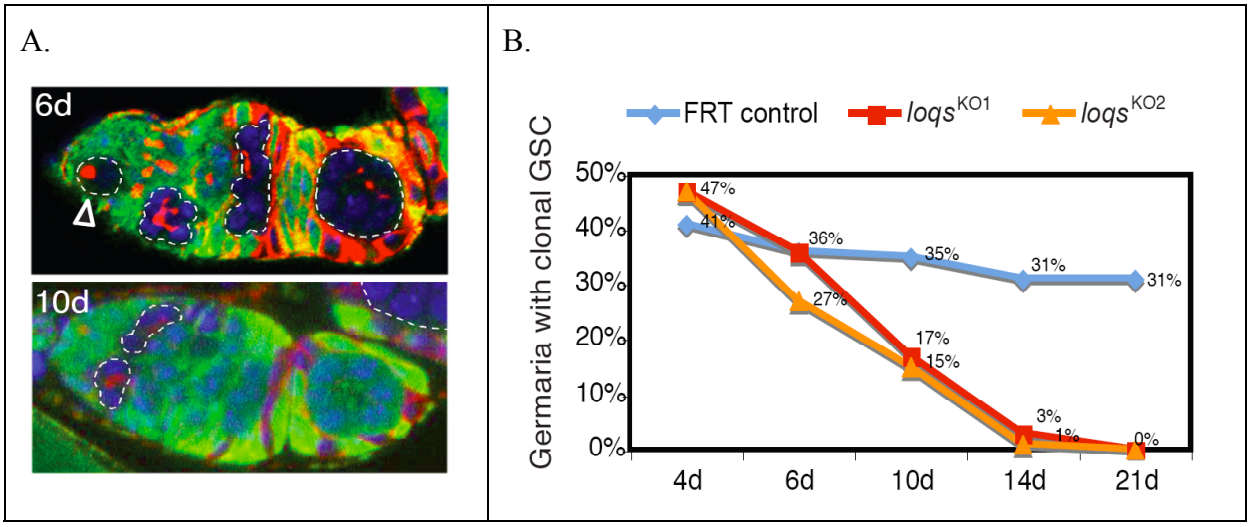

Figure 6.3: Germline mosaic analysis of *loqs* mutant GSC maintenance. (Images taken from Park et al., 2007). (A) Images of heat-shock induced mosaic germaria at 6- and 10-days after clonal induction. Negatively marked clones are marked by dotted lines. Arrowhead indicates a *loqs*-mutant GSC. (B) Time course analysis to measure half-life of wild-type (FRT; blue) or *loqs* (*loqs*^{KO1}, *loqs*^{KO2}; red, orange) mutant GSCs. Percentages indicate the germaria containing GSC clones (n > 100 germaria per genotype per time point).

GSC clones lacking Loqs in *loqs*^{KO} heterozygous females could be readily identified by the lack of GFP expression (Figure 6.3). This approach allowed us to bypass the lethality of *loqs*^{KO} homozygotes and to examine the cell-specific requirements for Loqs in GSC maintenance. Negatively-marked wild-type and *loqs* mutant GSC clones were followed for three weeks after clonal induction. The percentage of wild-type clones per germaria over the 21 day time course of the experiment declined from 41% to 31%. This represents a half-life of 42 days and reflects the wild-type GSC turnover rate (Lin and Spradling, 1993; Xie and Spradling, 1998). However, the percentage of germaria containing *loqs*^{KO} GSC clones declined from 47% to 0 over the 21 day experimental time course (Figure 6.3), representing a half-life of 6 days. The half-life of *loqs*^{KO} mutant GSCs is similar to those of other genes required for GSC maintenance,

including *mad* (Xie and Spradling, 1998). These data suggest that *loqs* is required cell-autonomously for GSC maintenance.

VI. Cell division rate of *loqs* mutant GSCs is not affected

One possible interpretation of the *loqs* GSC clonal analysis is that *loqs* mutant GSCs have faster rates of GSC division than wild-type GSCs. This would lead to a quicker rate of elimination of *loqs* mutant GSCs from the niche relative to wild-type GSCs. To determine whether the rates of GSC cell division was affected in *loqs* mutant clones, I examined the number of negatively-marked cysts that were produced at a point after clonal induction when both wild-type and *loqs* mutant GSCs could be identified at similar levels. Prior to the GSC loss phenotype of *loqs* mutant clones, I observed that the initial rates of cyst produced by negatively marked *loqs* mutant GSCs was similar to the rates of cyst produced by wild-type GSC clones.

Table 6.2: Initial rates of cyst production from wild-type and *loqs*^{KO} GSC clones.

6d post clonal induction	**FRT control**	***loqs*^{f00791}**	***loqs*^{KO1}**	***loqs*^{KO2}**
% germaria with clonal GSC	41%	34%	47%	47%
cysts per clonal GSC	1.28	1.06	0.86	1.34

Since *loqs*^{KO} GSC clones are lost from the niche, they stop producing a continuous lineage of *loqs* mutant cysts unlike wild-type cysts. Thus, at later time point after clonal induction, I observe that wild-type germline clones evenly distributed throughout all stages of oogenesis whereas *loqs* mutant germline clones, like *loqs* mutant GSCs, become depleted over time. Since *loqs* mutant egg chambers develop normally and do not display signs of cell death,

these data suggest that *loqs* mutant GSCs and their daughter germline cysts are lost through differentiation.

VII. Germline expression of Loqs-PB rescues GSC maintenance in *loqs* mutant females

Although germline mosaic analysis strongly suggested a cell-autonomous role for Loqs in controlling GSC maintenance, it did not rule out a requirement for Loqs in somatic niche cells. To examine this question, I used the Gal4/UAS system to drive tissue-specific expression of Loqs in both germline cells and somatic niche cells (Figure 6.4). I used the P{*nos*P-Gal4:VP16} transgene to drive expression in germline cells; P{*bab*-Gal4} and P{*c587*-Gal4} transgenes were used to drive expression in terminal filament and cap cells of the niche, respectively (Cabrera et al., 2002; Manseau et al., 1997; Van Doren et al., 1998).

I found that an endogenous *loqs* promoter driving the expression of *loqs-PB*, but not *loqs-PA*, was able to rescue the *loqs* mutant GSC loss phenotype. As such, I used the P{UASp-*loqs-PB*} transgene alone for the tissue-specific rescue experiments. At two weeks post-eclosion, $loqs^{f00791}/loqs^{KO}$ mutant females had on average 0.5 GSC per germarium, whereas wild-type females had on average 2.2 GSCs per germarium. Germline-specific expression of *loqs-PB* mediated by the P{*nos*P-Gal4:VP16} was able to restore GSC maintenance in *loqs* mutant females, supporting the germ-cell autonomous requirement observed by mosaic analysis (Figure 6.4). Alternatively stated, wild-type GSCs can be maintained in a *loqs* mutant somatic niche. However, niche cell-specific expression of *loqs*, either by P{*bab*-Gal4} and P{*c587*-Gal4} transgenes, was not able to maintain GSCs, suggesting that the germline-intrinsic function of Loqs is critical for GSC maintenance.

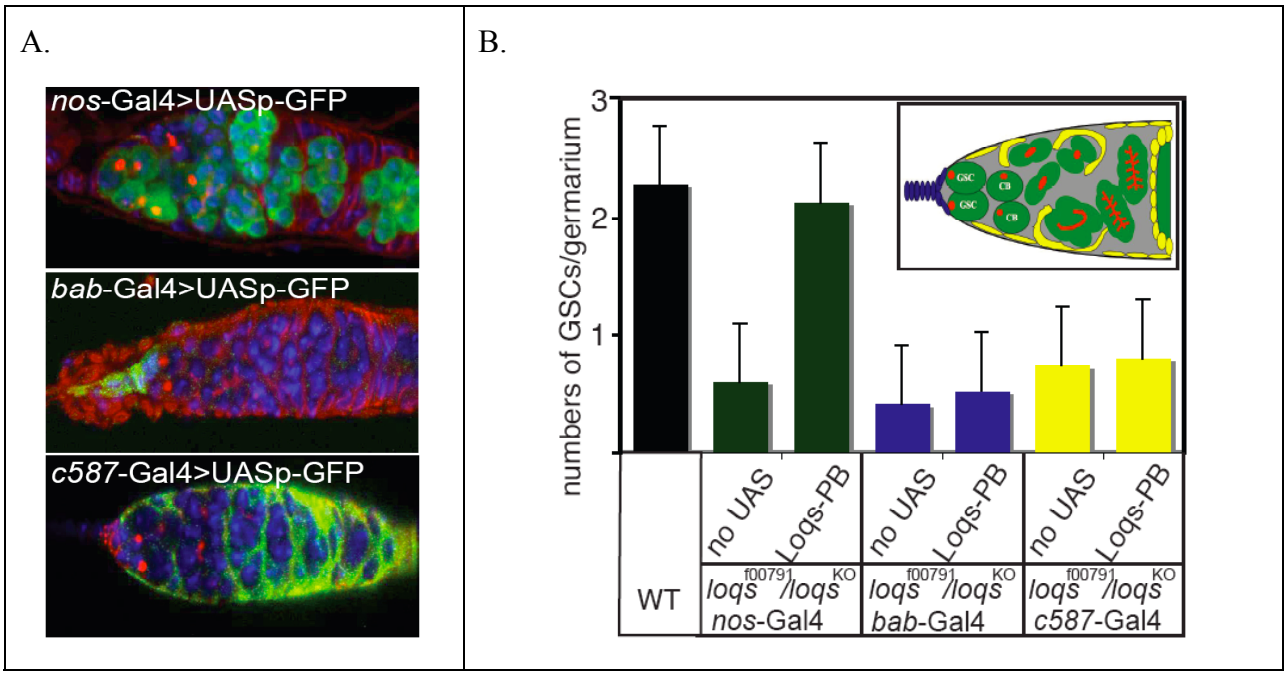

Figure 6.4: Germline expression of Loqs-PB restores GSC maintenance in *loqs* mutant females. (Images taken from Park et al., 2007). Different Gal4 drivers were used for cell lineage-specific expression of P{UASp-*loqs-PB*} in $loqs^{f00791}/loqs^{KO}$ mutant females. (A) Gal4 drivers included P{*nos*-Gal4:VP16} (germline; green); P{*bab*-Gal4} (terminal filament; blue); P{*c587*-Gal4} (escort cells; yellow) and were used to drive the expression of P{UASp-GFP} to demonstrate each expression pattern. (B) Inset shows a schematic diagram of a germarium, color-coded to indicate patterns of Gal4-driven expression. The number of GSCs per germarium (Y-axis) was determined at 13 days post-eclosion (>50 germaria per genotype; error bars represent standard deviation).

VIII. Differential requirement for Loqs in miRNA processing

Similar to our studies with *loqs*, other groups have demonstrated that *dcr-1* and *ago1* are also required cell-autonomously for GSC maintenance (Jin and Xie, 2007; Yang et al., 2007). Since Loqs enhances Dicer-1's ability to process pre-miRNA hairpin moieties to mature miRNAs and Ago1 forms a core component of the miRISC complex, these studies strongly implicate an intrinsic requirement for the miRNA pathway in controlling GSC maintenance. Toward this end, we focused on the biochemical requirement for Loqs in processing of all miRNAs.

To determine if Loqs is required for the efficient processing of all miRNAs, the Liu lab performed Northern blots to systematically examine the levels of 32 of the 78 known *Drosophila* miRNAs in both wild-type and *loqs*^{KO} mutant embryo lysates (Figure 6.5; X. Liu, Q. Liu, unpublished). Of these 32 miRNAs, only 16 Northern blots produced a detectable signal with clean background. Among these, a significant accumulation of pre-miRNAs was observed in lysates from *loqs*^{KO} mutant lysates indicating a general requirement for Loqs in efficient Dcr-1-mediated pre-miRNA processing.

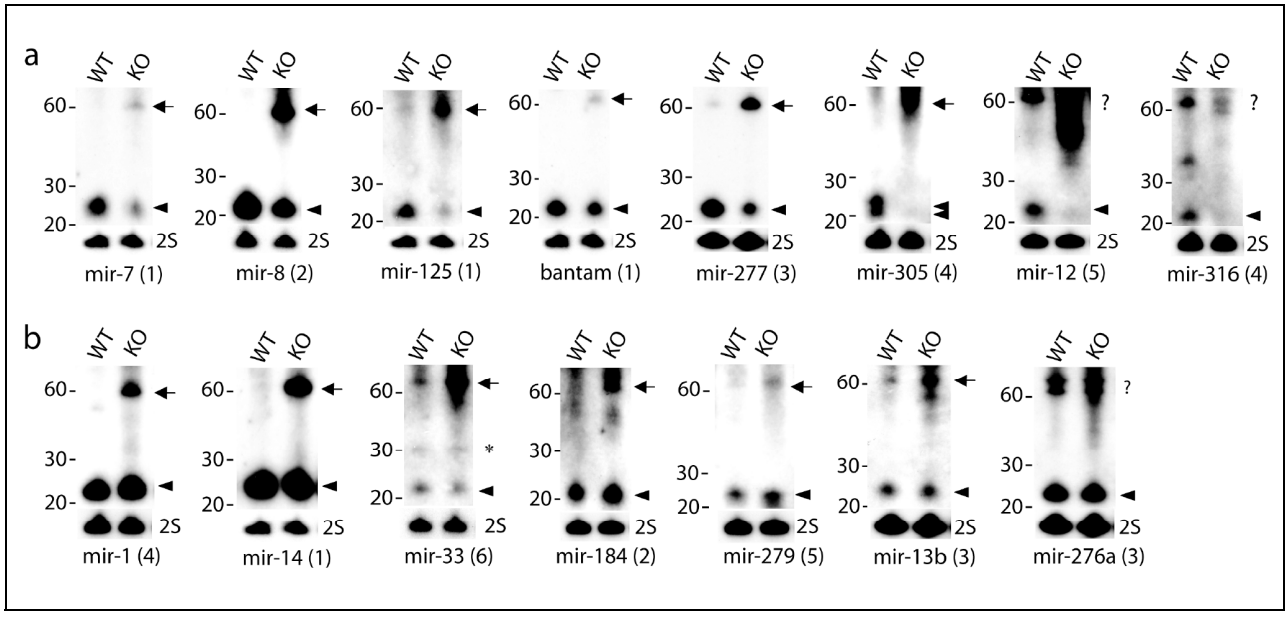

Figure 6.5: Differential requirement for Loqs in controlling levels of mature miRNAs. Lysates were collected from wild-type (WT) and *loqs*^{KO} (KO) embryos and used for Northern blot analyses. (a) A subset of miRNAs show diminished levels of mature miRNAs in *loqs*^{KO} null lysates relative to wild-type. (b) Northern blots showing equivalent levels of seven miRNAs between wild type and *loqs*^{KO} lysates. For each Northern blot, size markers are shown on the left and 2S rRNA was probed as loading control. Arrows and arrowheads mark pre-miRNAs and miRNAs, respectively. The numbers in parentheses correspond to the same blots used for multiple Northerns. The question marks refer to the inability to clearly determine the ~60-nt pre-miRNA. **(Analyses performed by Xiang Liu, Qinghua Liu, unpublished)**

However, examination of the mature miRNA levels revealed a differential requirement for Loqs+ function. For example, the levels of eight miRNAs, including mir-7 and mir-8, were eliminated or markedly reduced in *loqs*^{KO} flies (Figure 6.5, panel a). Alternatively, seven miRNAs, such as mir-1 and mir-14, were detected at equivalent levels between wild-type and *loqs*^{KO} flies (Figure 6.5, panel b). The efficient excision of some miRNA from pre-miRNA in the absence of Loqs suggests that some aspects of miRNA biogenesis may not require Loqs+ function. Taken together, these results indicate a differential requirement for Loqs during the biogenesis of mature *Drosophila* miRNAs.

IX. Discussion

The results from this set of experiments support the conclusion that Loqs plays a cell-autonomous role for GSC maintenance. *loqs* mutant GSCs are lost from the GSC niche via a *bam*-dependent pathway, but not through precocious activation of Bam. Germline *loqs* null clones are rapidly eliminated from the GSC niche. Additionally, cell-type specific expression of *loqs* revealed that germline expression of *loqs* is sufficient to rescue GSC maintenance defects in *loqs* mutant females. Taken together, these data indicate that Loqs and, by extension, the miRNA pathway play a critical cell-autonomous role for GSC maintenance.

Studies from other groups have also examined the requirement for other miRNA pathway components in GSC maintenance. Examination of *dcr-1* GSC clones revealed defects in cell-cycle progression (Hatfield et al., 2005) as well as a cell-autonomous requirement for GSC maintenance (Jin and Xie, 2007). In addition, dFMR1, a regulatory component of the miRISC complex, is also required for both GSC maintenance as well as pole cell formation (Ishizuka et al., 2002; Jin et al., 2004; Megosh et al., 2006; Yang et al., 2007). Taken together with my

analysis of Loqs requirement in the GSC, these data indicate that the miRNA biogenesis pathway is intrinsically required for GSC maintenance.

In order to determine the mechanism of miRNA-mediated control of GSC maintenance, we began a preliminary examination of miRNA biogenesis of all miRNAs (Figure 6.5). Surprisingly, we found a differential requirement for Dcr-1 and Loqs in the efficient excision of mature miRNA duplexes from pre-miRNA moieties. While recombinant Dcr-1 alone is sufficient to produce mature miRNA duplexes, Loqs greatly enhances Dcr-1's activity by increasing its affinity for pre-miRNA (Jiang 2005). However, for a subset of miRNAs, wild-type levels of mature miRNAs are observed even in the absence of Loqs (Figure 6.5b). I speculate that these "Loqs-independent" miRNAs are not likely to be critical for controlling GSC maintenance. Instead, I hypothesize that the "Loqs-dependent" miRNAs (Figure 6.5a) will play a pivotal role in controlling GSC differentiation. In a *loqs* mutant background, these Loqs-dependent miRNAs do not accumulate to mature wild-type levels; presumably, the decrease in abundance of this subset of miRNAs promotes GSC loss. Taken together, these data suggest that Loqs and Dicer-1 are required for likely results in the inefficient translational inhibition of factors that promote GSC maintenance, and that the subset of Dicer-1-dependent/Loqs-dependent miRNAs is critical for controlling GSC fate.

The data about the miRNA biogenesis pathway components corroborate previous studies highlighting the importance of translational repressors in GSC maintenance. In particular, studies of *pum* and *nos* function demonstrated that they play a key role in GSC maintenance (Chen and McKearin, 2005; Forbes and Lehmann, 1998; Szakmary et al., 2005) Future studies related to Loqs and Dcr-1 function in the GSC will focus on the identification of the miRNAs that presumably control the translational repression of key CB differentiation factors.

Chapter 7. Loqs protein localizes to cytoplasmic, perinuclear RNP-like granules

I. Summary

Antibodies against Loqs were generated to determine its distribution in the ovary as well as to identify additional Loqs-interacting proteins. A full-length, His-tagged Loqs fusion protein was used to immunize two rabbits. Both produced antisera that recognized Loqs protein isoforms on Western blots from *Drosophila* and S2 cell extracts and failed to recognize a band in *loqs* protein null extracts.

Immunolocalization experiments revealed that Loqs is a cytoplasmic protein enriched in the gonads of adult flies. In *Drosophila* females, Loqs is abundantly expressed in the ovarian germ cells and, to a lesser extent, in the somatic cells of the ovary. Loqs protein is detected as perinuclear foci in the GSCs, CBs and cysts of the germarium. This expression pattern increases during the pre-vitellogenic stages 2 through 8 of oogenesis, with Loqs protein dotting the cytoplasmic face of the 15 nurse cell nuclei. During the vitellogenic stages of oogenesis, stages 8 through 10, Loqs protein localizes to the posterior pole of the oocyte cytoplasm, in a specialized region termed the pole plasm.

Loqs localization was examined in relationship to proteins previously identified in RNP complexes during oogenesis using a series of antibodies and GFP-fusion proteins. Initially, the localization patterns of Vasa, Me31B, Aubergine and Exuperantia appeared similar to Loqs expression; however, closer examination revealed that most of the Loqs+ particles were not positively-marked with these RNP proteins. This suggested that Loqs is not a component of these previously defined protein complexes and that these RNP complexes, sometimes referred to as P-granule and nuage components, may be heterogenous in both their composition and distribution

throughout oogenesis. However, AGO1 protein also localized to cytoplasmic puncta and approximately 50% of AGO1+ particles were also Loqs+. Since AGO1 forms the core of the miRISC, this suggests that Loqs and AGO1 may associate with one another, either transiently through RNA-mediated interactions or directly through an involvement in miRNA loading or miRISC targeting to translationally-repressed mRNAs.

II. Generation of Loquacious antibodies

I initially obtained a rabbit polyclonal serum (hereafter α-R3) against Loquacious from Qinghua Liu's lab. This reagent ultimately proved to be an inadequate reagent, primarily due to relatively low titer and cross-reactivity with non-specific bands on Western blot analyses, despite previous attempts to purify the sample. As such, we deemed it necessary to generate new antibodies to Loqs. Xuecheng Ye (Liu lab) had generated a full-length His-tagged Loqs fusion protein (concentration = 20 mg/mL), which he generously provided for antibody production. Loqs antisera were produced at the Immunological Resource Center at the University of Illinois, under the guidance of Dr. Liping Wang. Rabbits (n=2) were chosen as the host species.

After the initial boost, I received bleeds from two rabbits (rabbit UY1 and UY2) and examined their immunoreactivity by Western blot analysis on whole fly lysates. Both sera were tested at 1:2,500 and displayed robust immunoreactivity against two major bands of approximately 55 kD and 45 kD, corresponding to the two major isoforms of *loqs*. Based on the relatively high titer and specificity of the immunoreactivity, we sacrified both animals after a subsequent boost and received the sera from the exsanguinated animals. Both sera were again tested by Western blot on whole fly extracts from wild-type and *loqs* null adults (Figure 7.1). The UY1 serum shows no activity in $loqs^{KO}$ extracts, whereas the UY2 serum shows a non-specific cross-reacting band at 70 kD. Importantly, in $loqs^{KO}$ extracts, neither sera detected a Loqs-specific bands at the predicted sizes for Loqs, 55 kD, 45 kD and, possibly 40 kD (Forstemann et al., 2005; Jiang et al., 2005). In wild-type extracts, both sera are able to identify bands corresponding to the two predominant isoforms of Loqs: Loqs-PB at 55 kD and Loqs-PA at 45 kD. Both sera, especially the UY1 serum, were able to identify a weak 40 kD band that corresponds to the predicted Loqs-PC isoform. This isoform was previously detected only in S2

cell extracts and not in fly lysates. These data indicate that the sera have specific reactivity to Loqs protein, especially to the two predominant Loqs-PB and Loqs-PA isoforms.

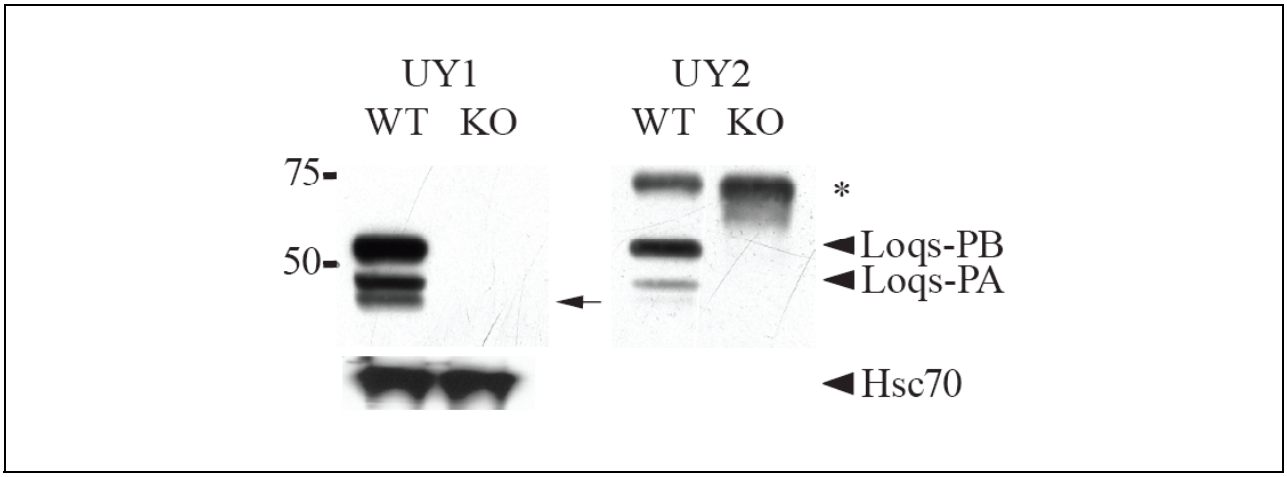

Figure 7.1: Loqs protein in extracts from wild-type and *loqs*^{KO} flies. Lysates were generated by collecting wild-type or *loqs*^{KO} mutant adults. Blots were probed with two anti-Loqs rabbit polyclonal antibodies, UY1 and UY2. Closed arrowheads correspond to the Loqs-PB and Loqs-PA isoforms. Arrow indicates a 40 kD band that corresponds to the minor Loqs-PC isoform. Asterisk indicates a non-specific 70 kD band. Equivalent aliquots from both WT and KO lysates were probed with Hsc70 as a protein loading control (left-hand side).

III. Immunolocalization of Loqs protein in ovaries

Immunofluorescence (IHC) analysis with sera UY1 and UY2 recapitulated the staining pattern seen with α-R3 serum. Prior to use as an immunostaining reagent, both sera need to be pre-incubated against fixed ovaries at a ten-fold higher dilution (1:750) than that for final analysis (1:7,500). I examined the expression of both Loqs sera in standard formaldehyde-fixed ovaries. Loqs protein appears exclusively cytoplasmic and concentrated to discrete perinuclear cytoplasmic foci. This pattern can be seen in all germ cells of the germarium and is most prominent in the nurse cells of stage 2 to stage 8 egg chambers. We noted that Loqs is identified in discrete puncta, concentrated at the perinuclear region of nurse cells (Figure 7.2). During these stages of oogenesis, the large polyploid nurse cells undergo endoreduplication to produce mRNA

stores that are deposited in the pole plasm of the developing oocyte at the posterior end of each egg chamber.

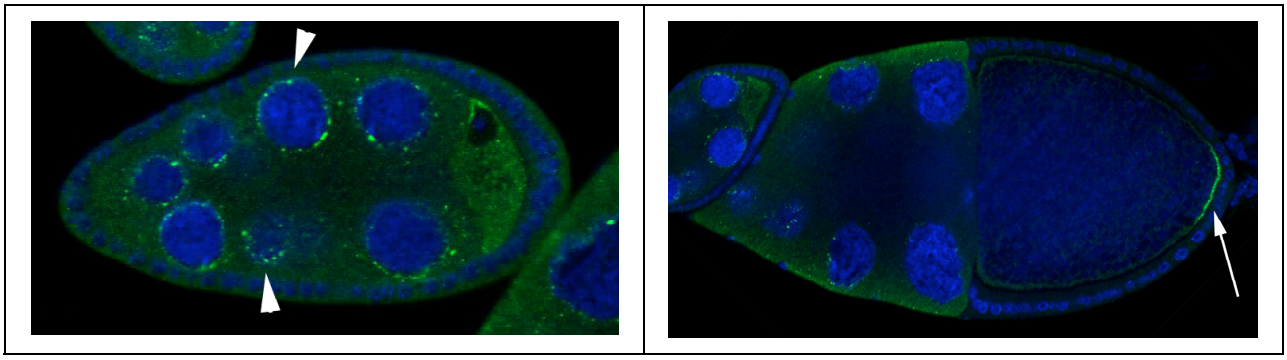

Figure 7.2: Immunolocalization of Loqs protein during oogenesis. (LEFT) Image of stage 8 egg chamber stained for Loqs (green) and DAPI (blue). Arrowheads indicate foci of Loqs localization adjacent to nuirse cell nuclei. (RIGHT) Stage 10 egg chamber stained as above. Arrow indicates pole plasm at the oocyte posterior.

To determine whether Loqs+ particles are identified in the cytoplasmic or nuclear compartments of germ cells during oogenesis, ovaries were fixed and double labeled with Loqs and Lamin antibodies (Figure 7.3). Loqs particles were excluded from the nucleus and most of the Loqs+ particles during the pre-vitellogenic stages of oogenesis were closely apposed to the cytoplasmic face of the nuclear membrane. This staining pattern was very similar to those observed for polar granule or nuage components, suggesting that Loqs+ particles may comprise a class of RNP complexes (Breitwieser et al., 1996; Nakamura et al., 2001; Snee and Macdonald, 2004; Wilhelm et al., 2000; Wilsch-Brauninger et al., 1997).

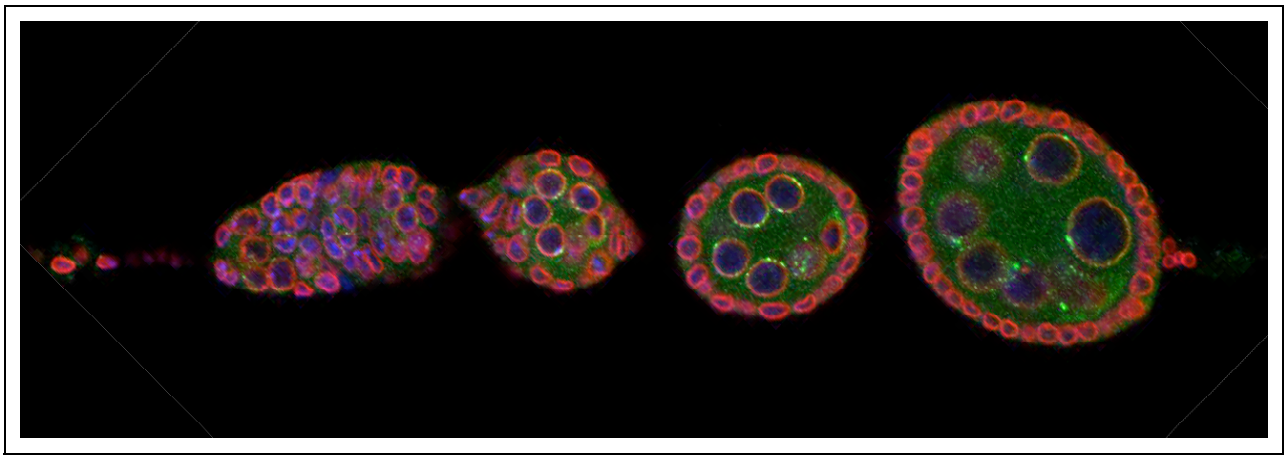

Figure 7.3: Loqs localization to perinuclear face of germ cells. Ovaries from wild-type ovaries were immunostained for anti-Loqs (green), anti-Lamin (red) and DAPI (blue). Loqs+ puncta can be observed on the cytoplasmic face of the nuclear envelope in germ cells.

To test the specificity of the anti-Loqs sera, I generated *loqs*^{KO} germline clones by FLP/FRT-mediated recombination and tested immunoreactivity on formaldehyde-fixed ovaries. In mosaic animals, *loqs*$^{-/-}$ clones are negatively marked and readily identified by the absence of GFP; as expected, the GFP$^{-/-}$ clones were also Loqs-negative (Figure 7.4). These data, together with the previous examination of wild-type and Loqs-null extracts, suggest that the Loqs sera are specific for the identification of Loqs isoforms on Western blot analysis and recognize Loqs as a cytoplasmic protein enriched in perinuclear puncta and the oocyte pole plasm.

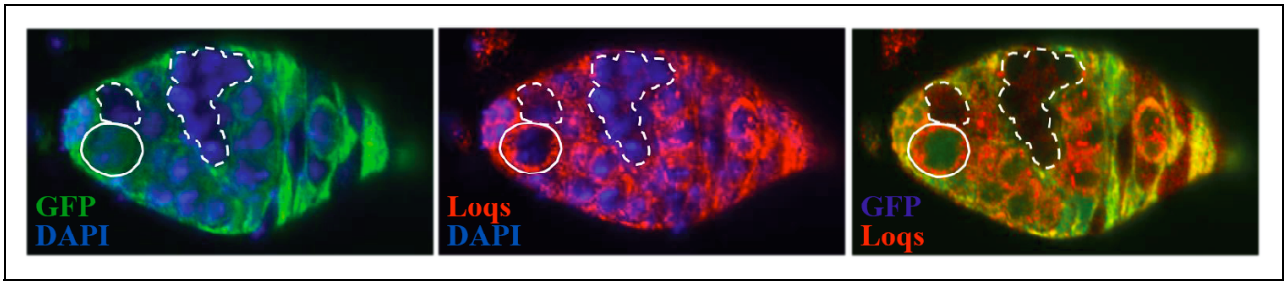

Figure 7.4: Immunostaining of endogenous Loqs protein in mosaic animals. Loqs null GSC clones were induced by heat-shock in adult animals and distinguished from wild-type cells (solid lines) by the absence of a ubiquitin-GFP marker (dotted lines). Ovaries were labeled with anti-GFP (green), anti-Loqs (red) and DAPI (blue).

Importantly, the antibody staining for Loqs was more robust using the UY1 and UY2 sera as compared with the α-R3 serum. One example of this was the pole plasm staining observed with both sera. Pole plasm assembly occurs during mid-oogenesis, during the onset of vitellogenesis, with the localization of factors to the posterior pole of the developing oocyte (Williamson and Lehmann, 1996). These data indicated that Loqs was broadly expressed during oogenesis, localized to discrete perinuclear punctae in pre-vitellogenic egg chambers and subsequently localized to the pole plasm during later vitellogenic stages.

IV. Perinuclear localization of Loqs

During stages 2-8 of oogenesis, Loqs protein is identified in the nurse cells localized to discrete perinuclear puncta. These Loqs+ puncta are reminiscent of RNP particles, such as nuage or polar granules, which are germline-specific, electron-dense granules. In the following experiments, I examine the co-localization of Loqs with nuage and other RNP proteins by immunohistochemistry.

IV.A. Loqs does not co-localize with nuage components

Previous studies have identified three proteins that localize to the nuage: Vasa, Aubergine (Aub) and Tudor (Breitwieser et al., 1996; Harris and Macdonald, 2001). Based upon previous analyses of these proteins and their associated functions, it has been proposed that nuage plays a function in post-translational RNA-associated regulation. During *Drosophila* oogenesis, these proteins are found in two distinct components: the nuage particles and the pole plasm. Pole

plasm contains polar granules, a determinant that is essential to induce formation of germ lineage in early embryogenesis (Williamson and Lehmann, 1996).

To determine whether Loqs protein is a nuage component, I took two separate approaches; immunofluorescence analysis and co-immunoprecipitation (co-IP). I examined Loqs localization in wild-type fixed ovaries and examined its localization relative to other known nuage components. Ovaries were co-stained with a polyclonal Loqs antibody and various antibodies to nuage components, either directly to the protein or a GFP-tagged form of the protein. For each co-labeling experiment, multiple ovarioles were examined.

Double labeling of Loqs and Vasa showed a marginal overlap of germline granules through stage 10 of oogenesis (Table 7.1). In addition, double labeling of Loqs and Aub (GFP-tagged Aub) showed a minimal overlap of germline granules (Table 7.1). Based upon data from IHC analysis, Loqs+ particles are not components of the Vasa+ Aub+ nuage particles. Indeed, co-IP experiments with Loqs failed to identify these nuage-associated proteins as an interacting protein. These data, taken together with the IHC data that showed little co-localization of Loqs+ particles with Vasa+ or Aub+ particles, likely suggest that Loqs+ particles are not components of classically defined nuage particles.

Table 7.1: Percent colocalization of Loqs-containing particles with P-granule, nuage or RNP components

Genotype	**wild-type**			**GFP-*aub***	**GFP-*me31B***	***exu*-GFP**
Antibody*	**Cup**	**dFMR1**	**Vasa**	**GFP**	**GFP**	**GFP**
Percent colocalization with anti-Loqs	11% (16/144)	16% (25/157)	12% (18/148)	19% (29/151)	8% (10/127)	5% (8/149)
Pole plasm overlap with anti-Loqs	Yes	No**	Yes	Yes	Yes	Yes

*Each antibody tested was used with Loqs polyclonal antibodies. Parentheses represent number of double-positive/total number of Loqs-positive granules counted.

**Megosh 2006 demonstrated that dFMR1 mutant embryos have fewer pole cells. Indicates that dFMR1 is a likely component of pole plasm, even though immunological reagents were unable to detect pole plasm localization.

IV.B. Loqs does not co-localize with other defined RNP proteins

In addition to nuage, other ribonuclear protein (RNP) particles have been identified in studies of *Drosophila* oogenesis, which include proteins such as Exuperantia (Exu) and Me31B. Exu is involved in the proper localization of *bcd* mRNA, presumably through the organization and transport of large RNP complexes (Wilhelm et al., 2000; Wilsch-Brauninger et al., 1997). Similar to the data observed for nuage particles, I found that few Loqs+ particles were also positive for other RNP proteins (Table 7.1). Taken together, these data suggest that Loqs+ particles may represent a new class of RNP particles or that Loqs+ particles interact dynamically or perhaps stochastically with other RNP particles.

IV.C. Loqs and AGO1 share similar punctate staining patterns during oogenesis

Based upon previous data, Loqs has been demonstrated to interact with both Dicer-1 and AGO1 in vitro (Jiang et al., 2005; Saito et al., 2005). To determine the distribution of Dicer-1 and AGO1 during oogenesis, I examined the expression pattern of these proteins using IHC. Although several Dicer-1 antibodies were generated in Dr. Qinghua Liu's lab (Xuecheng Ye, personal communication), none of them proved to be useful IHC reagents. However, anti-AGO1 antibodies were successful IHC reagents. Immunostaining of ovaries with AGO1 revealed an expression pattern similar to that of Loqs. AGO1-positive staining was observed in punctate particles during the early stages of oogenesis. Unexpectedly, I found that approximately 50% of AGO1+ particles overlapped with Loqs+ particles based upon IHC analysis. The presence of both single- and double-positive Loqs+, AGO1+ particles suggest that there might exist multiple different miRNP complexes. The double-positive particles may represent miRNA processing centers whereas the Loqs-negative/AGO1-positive particles represent miRNA loading centers or sites of mRNA degradation (Meister et al., 2004; Mourelatos et al., 2002). This is consistent with the data that Loqs is not required for miRNA loading onto miRISC complexes (Q. Liu, X. Ye, X. Liu, unpublished data).

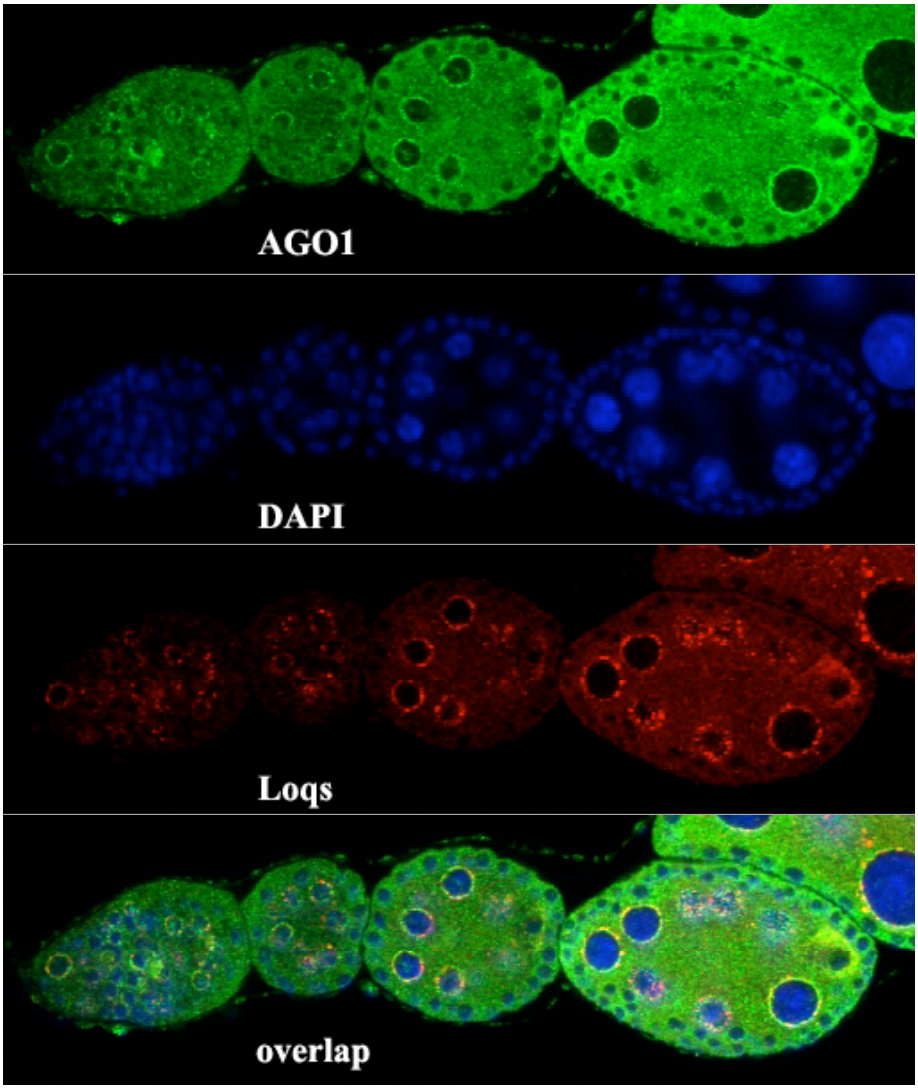

Figure 7.5: Immunolocalization of Loqs and AGO1 during oogenesis. Ovaries from wild-type ovaries were immunostained for anti-Loqs (green), anti-AGO1 (red) and DAPI (blue). Loqs+ puncta can be observed on the cytoplasmic face of the nuclear envelope in germ cells.

V. Pole plasm localization of Loqs

A dramatic accumulation of Loqs is observed during vitellogenic stages of oogenesis, stages 8 to 10. Although Loqs+ puncta are still observed in the nurse cell cytoplasm, a secondary accumulation of Loqs is also observed at the posterior pole of the developing oocyte (Figure 7.5). This region, termed the pole plasm, has been extensively studied for its requirement

in the localization of posterior determinant genes, such as *oskar*, as well as its later role as the precursor to the cytoplasm of the pole cells, the zygotic progenitor cells that are required for the establishment of the future germ cells (Ephrussi et al., 1991; Ephrussi and Lehmann, 1992). Further examination of Loqs localization to the pole plasm will be detailed in Chapter 8.

VI. Discussion

We successfully generated new Loqs antisera that are useful tools both from IHC as well as Western blotting and co-IP analyses. The sera were specific for Loqs protein based upon negative controls using both *loqs* null germline clones and Western blots on Loqs protein null extracts.

Loqs is a cytoplasmic protein that displays a dynamic pattern of expression during oogenesis. In the pre-vitellogenic stages, including the germarium through stage 8 of oogenesis, Loqs is largely localized to discrete perinuclear puncta. During the vitellogenic stages of oogenesis, from stage 8 through 10, Loqs becomes enriched in the developing oocyte and is enriched in a specialized region of the oocyte cytoplasm termed the pole plasm. The pole plasm is a critical determinant of germ cell fate in the developing embryo. Seminal work on pole plasm transplantation studies demonstrated that it was sufficient to induce primordial germ cell formation at sites of transplantation (Illmensee and Mahowald, 1974). Additionally, mutations of genes that affect posterior embryonic development, including the disruption of the pole plasm, prevent the formation of posterior pole cells (Ephrussi et al., 1991; Kim-Ha et al., 1991; St Johnston et al., 1991). In subsequent studies, I have examined the requirement for Loqs and other miRNA pathway components in the establishment and maintenance of the pole plasm and pole cells (Chapter 8).

The perinuclear punctate staining pattern of Loqs is reminiscent of a class of RNP-associated proteins that are loosely referred to as either nuage, polar granules or RNP proteins (Breitwieser et al., 1996; Harris and Macdonald, 2001; Nakamura et al., 2001; Wilhelm et al., 2000; Wilsch-Brauninger et al., 1997). Co-labeling experiments were performed to determine whether Loqs is associated with these factors. Surprisingly, Loqs showed surprisingly low overlap with these proteins, suggesting that Loqs+ particles are either peripherally associated with or not critical for the function of these RNP proteins. In fact, subsequent analyses of *loqs* mutant embryos showed that it did not share the patterning defects and pole cell formation defects observed in pole plasm mutants (Ephrussi and Lehmann, 1992; Hazelrigg et al., 1990; Lehmann and Nusslein-Volhard, 1991; Wilson et al., 1996). These data suggest that the RNP complexes are heterogenous in their composition. This is an important observation, as it suggests that different RNP complexes may target different mRNAs for translational repression of targeted localization.

Chapter 8. Pole plasm localization of miRNA components suggests heterogeneity of pole plasm associated proteins

I. Summary

The experiments presented in Chapter 7 analyzed the expression pattern of Loqs, focusing primarily on the cytoplasmic perinuclear foci. My analyses showed that these Loqs+ foci did not significantly overlap with previously described nuage or RNP components. However, AGO1 also demonstrated a staining pattern similar to Loqs and many of the Loqs+ puncta were also AGO1+. In addition, during the early stages of vitellogenesis, both AGO1 and Loqs proteins are enriched in the pole plasm. This suggested that components of the miRNA processing pathway form protein complexes during oogenesis and are discrete from previously described RNP complexes.

In addition to its use as an IHC reagent, Loqs polyclonal antibodies were also used to immunoprecipitate endogenous Loqs protein from ovarian extracts to identify associated protein partners. In particular, Loqs can immunoprecipitate Cup, and eIF4E-binding protein, from ovarian extracts and the Loqs-Cup complexes are RNase insensitive. By IHC analyses, approximately 10% of Loqs+ puncta were also Cup positive; however, both Cup and Loqs were also enriched in the oocyte and pole plasm. To determine whether both Loqs and Cup were authentic pole plasm proteins, we examined their distribution in wild-type ovaries and mutant ovaries with aberrant pole plasm. Two mutant alleles, osk^{6} and $stau^{D3}$ indicated that both Loqs and Cup are associated with *osk* mRNA. In addition, studies of P{*osk*-*bcd*-3′UTR} demonstrated that both Loqs and Cup associate with ectopically-induced pole plasm. Taken together, these studies indicate that Loqs is a true pole plasm factor and that its association with Cup and *osk* mRNA may indicate a role with mRNA cap-mediated translational repression.

Mutant genes for pole plasm associated proteins also result in defects of abdominal segmentation of germ cell formation, including mutations in *osk* and *nos*. However, *loqs* null embryos developed without evidence of abdominal segmentation defects and Loqs was dispensable for pole cell formation. Additionally, *loqs* mutant alleles did not suppress the bicaudal phenotype associated with the P{*osk-bcd*3′UTR} transgene, though they did reduce the number of anteriorly-localized pole cells. Therefore, despite its specific localization to the pole plasm, Loqs is largely dispensable for pole cell formation. Additionally, similar to the heterogeneity of nuage components in earlier stages of oogenesis, the pole plasm may also represent a heterogenous mélange of different RNP complexes.

Examination of AGO1, a core component of the miRISC, also reveals an expression pattern reminiscent of Loqs staining. AGO1 localized to punctate perinuclear particles in mid-oogenesis and became localized to the pole plasm as the egg chambers entered vitellogenesis. However, unlike Loqs and Cup, AGO1 protein was undetectable by stage 10 of oogenesis. This dynamic pattern of AGO1 expression in the pole plasm suggests that miRNAs may play a critical function in pole plasm maturation. Subsequent examination of *dcr-1* germline clones revealed that pole plasm protein distribution was no longer tightly localized to the posterior cortex of the oocyte. However, in *loqs* germline clones, the pole plasm remained tightly localized to the posterior of the oocyte. These data indicate that a subset of miRNAs that do not require $Loqs^{+}$ function for full activity are important for proper sequestration of the pole plasm to the oocyte posterior.

In order to determine the functions of Loqs protein during oogenesis, Qinghua Liu's lab performed IP and subsequent mass spectroscopy analysis of Loqs-associated proteins (see Appendix). This analysis revealed a suite of proteins, many of which were previously implicated

in both RNA-binding and translational control. One of these proteins, dFMR1, was validated by co-IP experiments with Loqs. dFMR1 is a component of the miRISC and suggests that Loqs might associate directly with the miRISC. Additional IP-MS candidate proteins solidify the potential roles for Loqs in RNA binding, translational repression, and RNA localization. Taken together, the data presented in this chapter focus on studying Loqs function through its interacting partners and their associated phenotypes.

II. Loqs and Cup co-localization during oogenesis

Both Loqs and Cup show a similar dynamic expression pattern during oogenesis. During the pre-vitellogenic stages of oogenesis, both Loqs and Cup are identified in perinuclear foci with slight enrichment in the oocyte (Figure 8.1A). However, the Cup+ foci overlapped with only ~10% of Loqs+ foci. At the pole plasm of stage 10 egg chambers, both Loqs and Cup proteins are enriched in the pole plasm (Figure 8.1B). Therefore, based upon immunohistochemical studies of fixed ovaries, I determined that Loqs and Cup might form active complexes. In addition, detection of Loqs and Cup both in the perinuclear foci as well as the pole plasm suggest that both proteins are subject to the dynamic intracellular transport that has been studied extensively for Cup (Wilhelm et al., 2003).

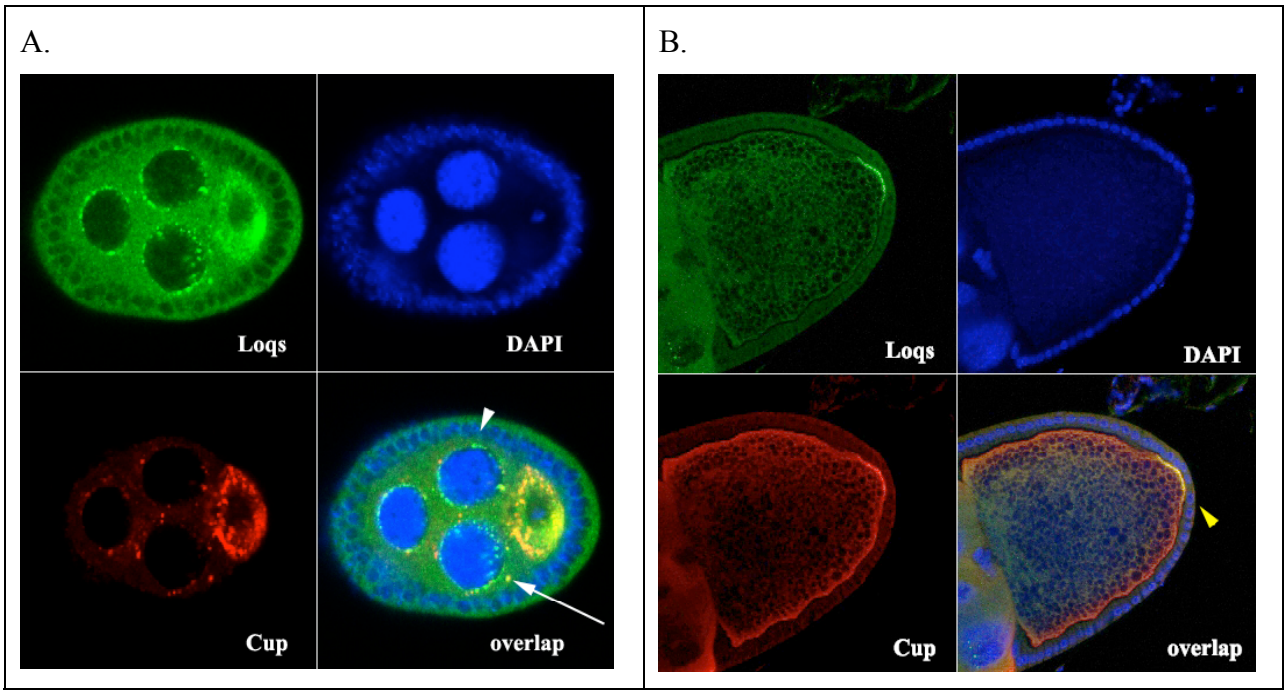

Figure 8.1: Colocalization of Loqs and Cup proteins. Ovaries were dissected from wild-type ovaries and immunostained for Loqs (green), Cup (red) and DAPI (blue). (A) Image of stage 6 egg chamber. Arrow indicates Loqs+ Cup+ staining focus. Arrowhead indicates a Loqs+ Cup- focus. (B) Image of posterior half of stage 10 egg chamber. Yellow arrowhead indicates Loqs+ Cup+ pole plasm.

III. Loqs co-immunoprecipitation with Cup

Cup, an eIF4E-binding protein that inhibits translation by preventing the recruitment of eIF4G, has been characterized previously as a pole plasm associated protein (Nelson et al., 2004; Wilhelm et al., 2003; Zappavigna et al., 2004). Cup was identified as a protein that associates with *osk* mRNA, which is restricted to the posterior pole of the developing oocyte during oogenesis (Ephrussi et al., 1991; Ephrussi and Lehmann, 1992; Wilhelm et al., 2003). To determine whether Loqs interacts directly with Cup, we performed co-IPs from ovarian extracts with anti-Loqs polyclonal antibodies. IPs were performed in ovarian extracts with anti-Loqs polyclonal antibodies and Western blotting performed with an anti-Cup antibody. This experiment revealed that anti-Loqs antibody brought down two, and perhaps three, Cup protein isoforms (Figure 8.2). Previous studies have shown that multiple isoforms of Cup, including 110 kD, 150 kD and 180 kD isoforms, could be identified in *Drosophila* extracts (Keyes and Spradling, 1997). These data suggest that endogenous Loqs associates with Cup in ovarian extracts, suggesting that both proteins may play a role in regulating pole plasm activity.

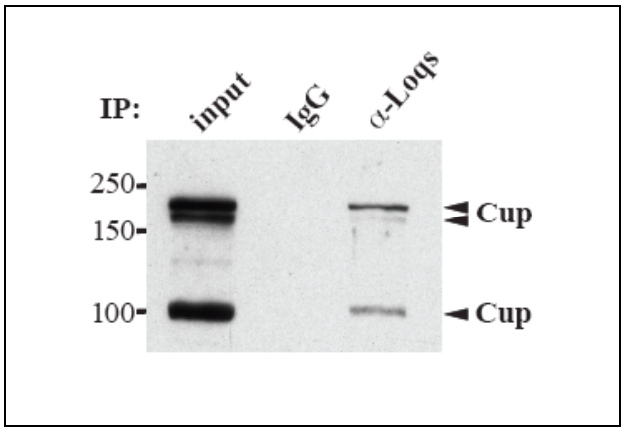

Figure 8.2: Loqs immunoprecipitates with Cup. Immunoprecipitations were performed in ovarian extracts from wild-type females with anti-Loqs or pre-immune serum (IgG). Input lane represents 10% of extract used for IP reactions.

One of the principal functions of pole plasm proteins is to aggregate the specialized mRNA transcripts that are important for germ cell formation. To determine whether the endogenous Loqs-Cup complexes require RNA for efficient interaction, ovarian extracts were treated with RNase A prior to immunoprecipitation. RNase treatment of ovarian extracts did not affect the ability of anti-Loqs antibody to efficiently pulldown Loqs protein (Figure 8.3A). Co-IP experiments in RNase-treated and untreated extracts demonstrated that treatment did not affect the ability of Loqs to co-IP with Cup, suggesting that the Loqs-Cup complexes do not contain RNA or are not dependent upon RNA for efficient interaction (Figure 8.3B). However, the overall abundance of Cup protein in RNase A-treated extracts was slightly reduced, suggesting that Cup protein stability is affected by RNase A treatment.

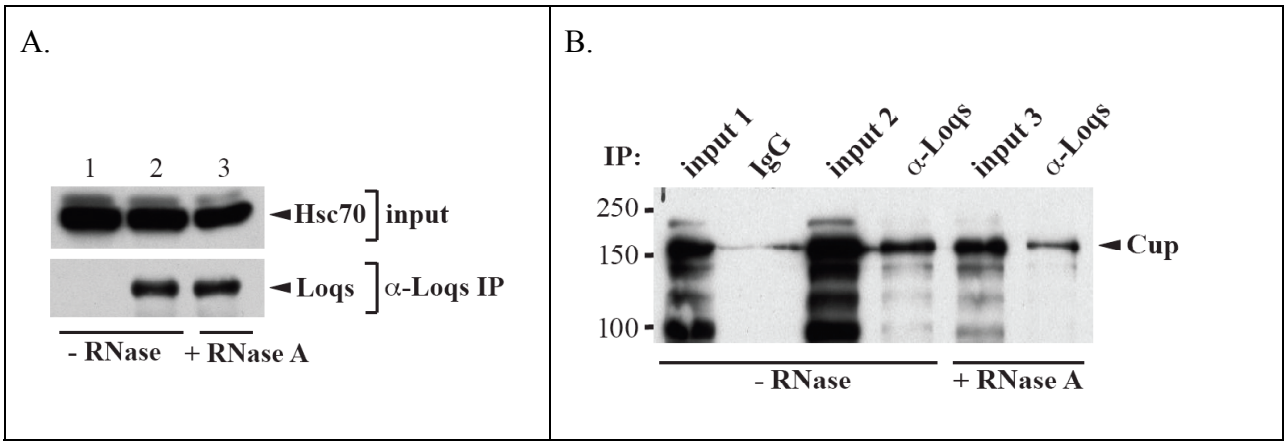

Figure 8.3: Loqs and Cup co-immunoprecipitation not dependent upon RNA. Ovary extracts were treated with an RNase Inhibitor (- RNase) or RNase A (+ RNase A) prior to IP with anti-Loqs sera. (Left) RNase treated and untreated extracts were probed for Hsc70 as a loading control and α-Loqs as an IP control. Lane 1 corresponds to a mock IP sample (IgG). Lane 2 corresponds to a sample immunoprecipitated with anti-Loqs sera - RNase. Lane 3 corresponds a sample immunoprecipitated with anti-Loqs sera + RNase A. (Right) IPs performed on RNase treated and untreated lysates with anti-Loqs sera or pre-immune sera. Western blot performed with anti-Cup antibody.

IV. Cup, but not Loqs, is a mRNA cap-associated protein

The 5′ ends of mRNAs are modified by the addition of a 7-methyl guanosine cap (hereafter, 7me-GTP). mRNA translation requires the binding of eIF4E to the 7me-GTP cap, reviewed in (Richter and Sonenberg, 2005). Through its association with eIF4E, Cup inhibits translation by preventing the recruitment of eIF4G (Zappavigna et al., 2004). To test whether Loqs-Cup complexes associate with the 7me-GTP cap, I tested ovarian extracts for ability to bind to 7me-GTP-conjugated sepharose beads (Figure 8.4). As demonstrated previously, I used an anti-Loqs serum to co-immunoprecipitate Cup from ovarian extracts (Figure 8.4, lane 2). I also found that Cup interacted with the 7meGTP sepharose (lane 4) while incubation with non-reactive beads did not associate with Cup (lane 3). Importantly, I also found that the cap-analog resin bound most of the Cup protein from the ovarian extracts, as observed by the depletion of Cup in the supernatant (lane 5). These data suggest that the 7meGTP-conjugated sepharose beads were able to pulldown cap-associated Cup protein from ovarian extracts. This also suggests that the majority of Cup protein is likely found in a complex with eIF4E and bound to mRNAs that are poised in an inhibited translational state.

Since Cup and Loqs can be co-immunoprecipitated from wild-type ovarian extracts, I also tested whether Loqs protein could be pulled down using the cap-analog resin. Whereas Cup readily associated with the 7meGTP sepharose beads, Loqs proteins were largely detected in the supernatant after resin incubation (Figure 8.4, compare lanes 4 and 5). These data suggest that the cap-associated Cup protein does not interact with Loqs or that the 7meGTP sepharose reagent is not sufficient to quantitatively pulldown proteins that are not in direct proximity to cap-associated proteins. Alternatively, the Loqs-Cup interaction may represent a protein complex that is either RNA-independent (Figure 8.3) or required for mRNA degradation and not cap-

dependent translational inhibition (Coller and Parker, 2004). Based upon the function of Cup (eIF4E-binding protein) and the proposed function for Loqs (dsRNA binding protein involved in miRNA-mediated translational repression through the 3′ UTR of cognate mRNAs), I propose that Loqs may be too far removed from the mRNA cap to be efficiently pulled down with 7me-GTP cap-analog resin.

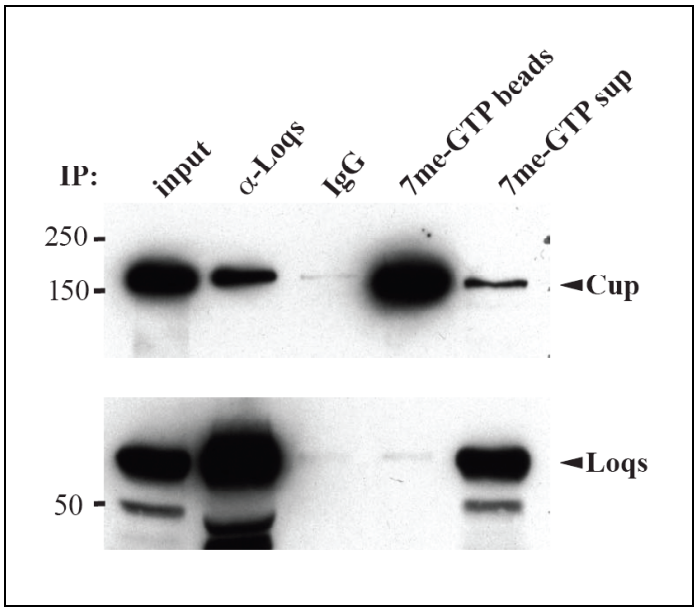

Figure 8.4: Cup, but not Loqs, is an mRNA cap associated protein. Wild-type ovarian extracts were incubated with anti-Loqs (lane 2), pre-immune serum (IgG; lane 3), or 7-methyl-GTP-Sepharose beads (lane 4). Both input (lane 1) and supernatant (lane 5) from the 7-methyl GTP pulldown experiment represent ~5% of total lysate. Membranes were probed for Cup (top) and Loqs (bottom).

V. Loqs and Cup associated with pole plasm

Since only ~ 10% of Loqs+ puncta are also Cup+, this suggests that the Loqs-Cup protein complexes detected by IP are present mainly in the pole plasm. To determine whether Loqs-Cup interaction requires an intact pole plasm, we examined Loqs and Cup distribution in wild-type and pole plasm mutant ovaries. In wild-type ovaries, both Loqs and Cup are enriched in the pole plasm. In an *osk*^{6} mutant ovary, *osk* mRNA is present and properly localized to the posterior pole of the developing oocyte, but unable to form pole plasm due to a point mutation in *osk* (Kim-Ha et al., 1991). In an *osk*^{6} mutant ovary, both Loqs and Cup expression patterns are nearly

indistinguishable from wild-type, suggesting that their localization is not dependent directly on an intact pole plasm but rather upon *osk* mRNA (Figure 8.5 A-F). Additionally, in a *stau*^{D3} mutant ovary, in which the pole plasm formation is completely abolished, neither Loqs nor Cup can be detected in the pole plasm (Figure 8.5 G-I).

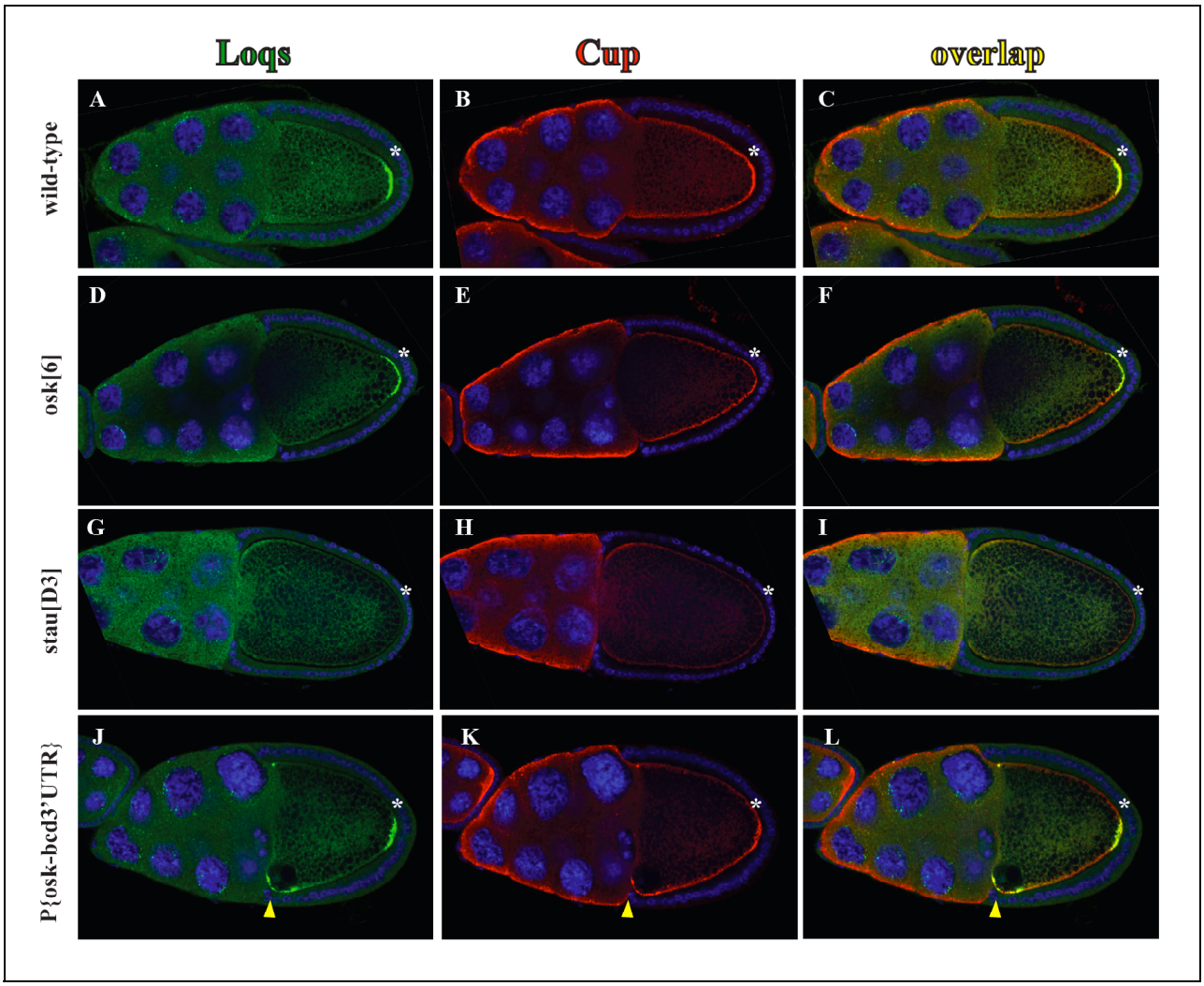

Figure 8.5: Pole plasm localization of Loqs and Cup dependent on *osk* mRNA. Ovaries were dissected from wild-type (A-C), *osk*^{6} (D-F), *stau*^{D3} (G-I) and P{*osk-bcd*-3′UTR} (J-L) females and immunostained with anti-Loqs (green), anti-Cup (red) and DAPI (blue). Asterisk indicates location of pole plasm at posterior pole of developing oocyte. Yellow arrowhead indicates anterior-localized, ectopic pole plasm induced by P{*osk-bcd*-3′-UTR} transgene. All images are oriented with anterior end pointed toward left.

Most importantly, both Loqs and Cup co-localize to sites of ectopic pole plasm generated by a P{*osk*-*bcd*-3′UTR} transgene (Ephrussi and Lehmann, 1992). Females carrying this transgene are dominant sterile because their progeny have a bicaudal phenotype. Ovaries from these females were immunostained with Loqs and Cup antibodies, showing that both proteins were localized to the anterior border of the developing oocyte (Figure 8.5 J-L). Taken together, the examination of Loqs distribution in these mutant ovaries demonstrate it is a true pole plasm protein and that its association with Cup and *osk* mRNA suggest a role for Loqs in mRNA cap-dependent translational repression.

VI. Loqs does not have associated segmentation defects

Mutations in the maternal posterior-group genes, including *osk*, *nos*, and *vasa*, display a defect in abdominal segmentation in addition to a defect in germ cell formation (Ephrussi et al., 1991; Hay et al., 1990; Lehmann and Nusslein-Volhard, 1991). This is likely due to the inappropriate localization of posterior germ cell determinants that are required for the formation of the nascent germ plasm. To determine whether *loqs* mutant embryos also display similar phenotypes, we examined both zygotic and maternal-zygotic (MZ) *loqs* null embryos for segmentation defects. Zygotic *loqs* null embryos hatched at rates similar to wild-type embryos and most mutant larvae underwent pupariation (Figure 5.4). When these *loqs* null progeny were examined for segmentation defects by larval cuticle preparations, I observed that they were indistinguishable from wild-type controls in their gross morphological features, such as the number of body segments and denticle belt patterning. In fact, the zygotic null *loqs* animals were morphologically similar to wild-type controls, aside from the fact that they became progressively sluggish and unable to eclose from their pupal case.

The viability of zygotic *loqs* null animals dropped off at the pupal/adult transition, suggesting that Loqs proteins were maternally loaded. Therefore, we examined whether MZ-*loqs* null embryos displayed segmentation or patterning defects. In these animals, embryogenesis, body axis formation and grastrulation appeared indistinguishable from wild-type. In fact, immunostaining of the embryonic nervous system with anti-Elav antibodies and gonads with anti-Vasa demonstrated that both systems were comparable to wild-type controls. A detailed examination of early germ cell formation is addressed in the following section. Taken together, these data indicate that although Loqs is a pole plasm-associated protein that is maternally contributed gene product, *loqs* null embryos do not display overt defects in body patterning or organization.

VII. Loqs dispensable for pole cell formation

To determine whether Loqs is required for pole cell formation, I counted the number of Vasa+ pole cells in blastoderm embryos at cycle 13 or 14. I found that the number of pole cells was unchanged in wild-type or maternal- and zygotic-null (MZ)-$loqs^{KO}$ embryos (Table 8.1). This indicated that Loqs, a pole plasm associated protein, was dispensable for proper pole cell establishment and formation.

In addition to Loqs, the dsRNA-binding protein R2D2 has been studied for its role in interacting with Dicer-2 to facilitate the role of Dicer-2-mediated loading of siRNAs onto the siRISC (Liu et al., 2003; Tomari et al., 2004). Since both Loqs and R2D2 are dsRBPs, it is possible that *r2d2*-redundancy can substitute for *loqs*+ function in *loqs* mutant animals. To test this possibility, we generated *r2d2 loqs* double mutant MZ-null embryos and examined the number of pole cells in both single and double mutant backgrounds (Table 8.1). Again, we found

that the number of pole cells was largely unchanged, suggesting that neither *loqs* nor *r2d2* plays a critical role in pole cell formation. However, mutations in two miRNA-associated proteins, Dcr-1 and dFMR1, produce embryos with reduced number of pole cells. This suggests that the miRNA pathway is critical for pole cell formation but that Loqs+ function is largely dispensable for this function.

Table 8.1: Number of pole cells in cycle 13-14 embryos from wild-type, *loqs* and *r2d2* embryos. (n = 25 embryos per genotype)

Genotype	**wild-type**	***loqs*^{KO}**	***r2d2*^{1}**	***loqs*^{KO} *r2d2*^{1}**
# of Vasa+ pole cells	23.9 ± 2.1	22.7 ± 2.4	22.4 ± 2.1	22.6 ± 1.8

The P{*osk-bcd*-3′UTR} transgene produces embryos with a bicaudal phenotype, due to the ectopic anterior localization of *osk* mRNA by the *bcd* 3′UTR (Ephrussi and Lehmann, 1992). Previous studies have used this transgenic construct to screen for factors that dominantly suppress the bicaudal phenotype (Wilson et al., 1996). One of the factors identified in this manner was Aubergine (Aub), a protein required for pole cell formation and *osk* translation (Harris and Macdonald, 2001). Genetic screens isolated *aub* as a dominant suppressor of the bicaudal phenotype produced by the P{*osk-bcd*-3′UTR} transgene, suggesting that *aub* plays a role in promoting *osk* translation. To determine whether *loqs* acted on modulate the translation of *osk* mRNA, we examined the number of pole cells in wild-type females, females carrying a P{*osk-bcd*-3′UTR} transgene, and females with the P{*osk-bcd*-3′UTR} transgene and heterozygous for a *loqs* null allele (Table 8.2). The number of posteriorly-positioned pole cells were similar in these three genotypes, which was consistent with our studies showing that MZ-*loqs*^{KO} null embryos do not display a change in the number of pole cells (Table 8.1). However, the number of ectopic anteriorly-positioned Vasa+ cells appeared to be mildly

suppressed in *loqs*^{KO} heterozygotes carrying a copy of the P{*osk-bcd*-3′UTR} transgene (Table 8.2). This mild suppression of the ectopic anteriorly-localized pole plasm, though highly reproducible, is not sufficient to suppress the bicaudal phenotype as seen with *aub* mutants (Wilson et al., 1996). Taken together with the data that *loqs* mutants do not display defects in pole cell formation, these data suggest that Loqs plays a minor but largely dispensable role in pole cell formation.

Table 8.2: Suppression of anteriorly-localized Vasa+ cells induced by P{*osk-bcd*-3′UTR} (n = 50 embryos per genotype)

Genotype	**# anterior Vasa+ cells**	**# posterior Vasa+ cells**
wild-type	0	23.5 ± 1.3
P{*osk-bcd*-3′UTR}/+	17.0 ± 1.2	23.8 ± 1.5
P{*osk-bcd*-3′UTR}/*loqs*^{KO}	12.6 ± 2.0	23.9 ± 1.5

VIII. Pole plasm localization of AGO1

To determine whether other miRNA-associated proteins might play a role in pole cell formation, we examined the expression pattern of AGO1 during oogenesis. In wild-type ovaries, I noted that AGO1 protein distribution was remarkably similar to that of Loqs (Figure 7.5) and that ~50% of Loqs+ puncta were also positive for AGO1. This suggested that Loqs and AGO1 might have both shared and discrete functions as components of different RNP complexes during oogenesis.

To determine whether the staining pattern of Loqs and AGO1 were consistent throughout oogenesis, I focused on the distribution of each protein during later stages of oogenesis, especially on their localization to the pole plasm. We observed that in stage 8 and 9 of oogenesis,

both Loqs and AGO1 localized to the nascent pole plasm (Figure 8.6A). Intriguingly, by stage 10 of oogenesis, AGO1 protein was no longer detectable at the pole plasm, while Loqs was still present (Figure 8.6B). The dynamic nature of AGO1 suggested a possible role for the relationship between AGO1 turnover and derepression of mRNA transcripts.

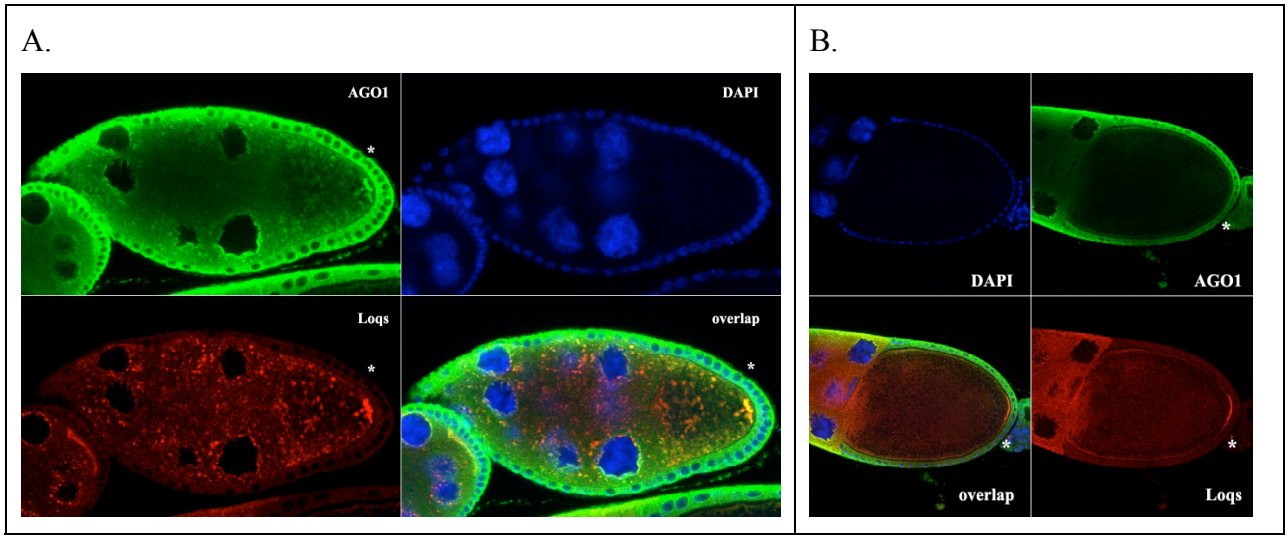

Figure 8.6: Loqs and AGO1 staining in stage 9 egg chambers. Wild-type ovaries were stained with anti-AGO1 (green), anti-Loqs (red), and DAPI (blue). Asterisk indicates pole plasm at posterior pole of oocyte. (A) Stage 9 egg chamber. (B) Posterior half of a wild-type stage 10 egg chamber.

To investigate the process of pole plasm formation and maintenance with respect to miRNA-associated proteins, I began by examining the dynamic distribution of AGO1 with respect to Osk protein. Previous in situ hybridization experiments have shown that *osk* mRNA is localized to the oocyte and enriched at the posterior pole of the developing oocyte (Ephrussi et al., 1991; Kim-Ha et al., 1991). However, subsequent studies revealed that the two *osk* isoforms, Long Osk and Short Osk, have different roles in pole plasm formation. In ovaries that specifically express only one *osk* mRNA isoform, Vanzo and Ephrussi noted that the *osk* mRNA in ovaries expressing Long Osk accumulate at the posterior pole similar to wild-type distribution

(Vanzo and Ephrussi, 2002). However, in ovaries expressing only Short Osk, the *osk* mRNA becomes separated from the posterior cortex of the oocyte and is delocalized to the middle of the oocyte cytoplasm. These data suggested that the translation of Long Osk is required to properly anchor *osk* mRNA and, by extension, the pole plasm to the posterior pole of the oocyte.

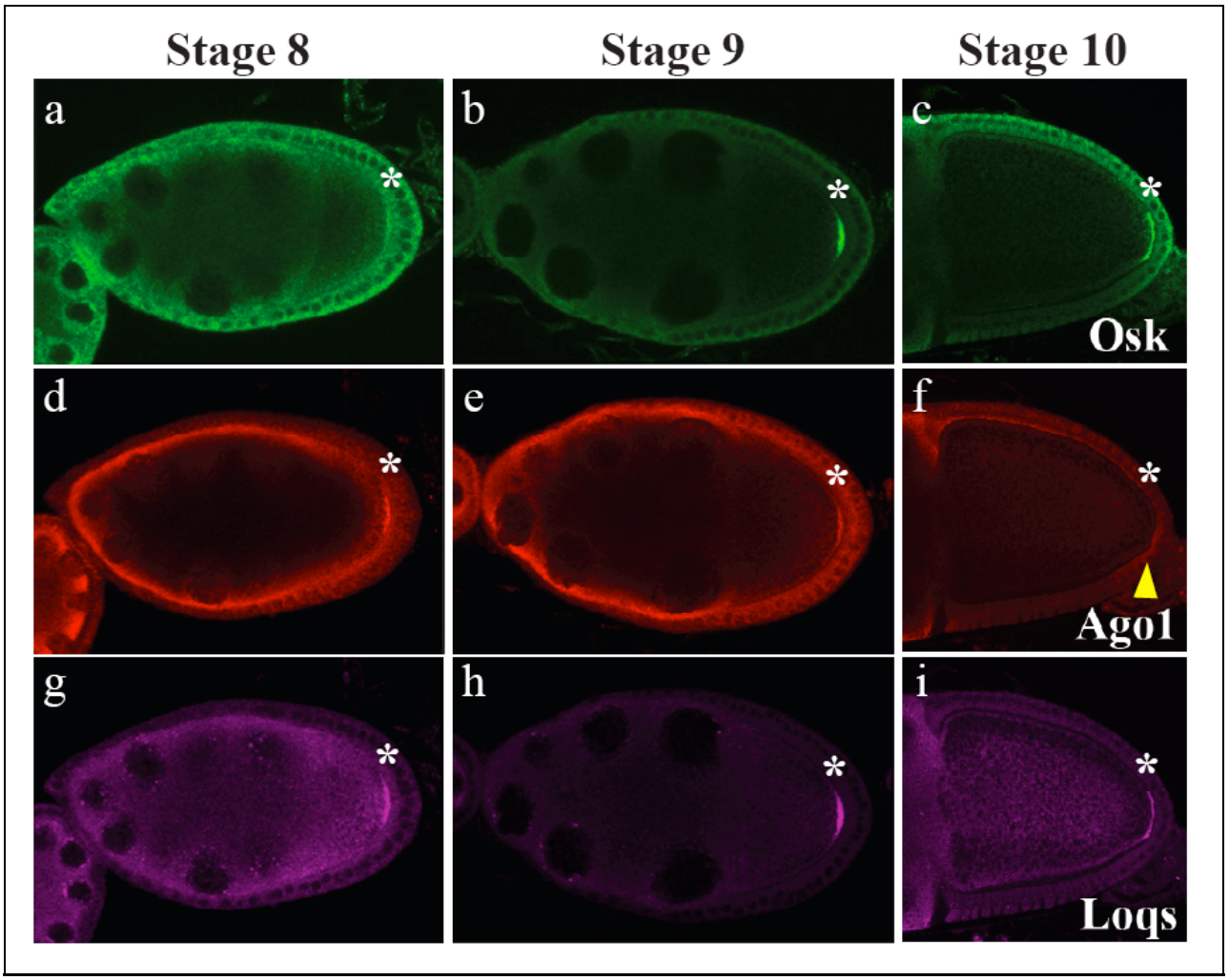

Figure 8.7: Dynamic expression of AGO1 and Osk at pole plasm. Ovaries dissected from wild-type females and examined at stage 8 (left column); stage 9 (middle column); and stage 10 (right column) of oogenesis. Ovaries were immunostained with (a-c) Osk (green); (d-f) AGO1 (red); (g-i) Loqs (purple). Asterisks indicate location of pole plasm. Yellow arrowhead indicates absence of AGO1 staining in stage 10 egg chambers.

I decided to examine the expression of AGO1 and Osk proteins through the vitellogenic stages of oogenesis, during which pole plasm formation occurs. As previously described, *osk* mRNA is translated from stage 8 to stage 10 and Osk protein gradually accumulates at the pole plasm (Figure 8.7, a-c) (Vanzo and Ephrussi, 2002). Intriguingly, just as Osk protein levels rise, AGO1 protein appears to decline through stages 8 to 10 of oogenesis (Figure 8.7, d-f). This inverse correlation between the decline of AGO1 staining and Osk protein accumulation suggests that AGO1-containing complexes (i.e., the miRISC) may be involved in the repression of *osk* mRNA. It is important to note that Loqs protein levels are unchanged during the assembly of pole plasm (Figure 8.7, g-i). Thus, it is tempting to speculate that the turnover of the AGO1 complexes allow for the translation and accumulation of Osk protein, which is required for proper pole plasm establishment. Taken together, this suggests again that the miRISC, but not Loqs, is required at the posterior for proper pole plasm attachment.

IX. Pole plasm architecture maintained by subset of miRNAs independent of Loqs+ function

The dynamic expression of AGO1 during the vitellogenic stages of oogenesis suggests that the miRNA pathway may play a critical role in pole plasm establishment or maintenance. To examine the requirement for miRNAs in pole cell formation, we examined the distribution of two pole plasm proteins, Osk and Cup, in stage 10 egg chambers from wild-type and *dicer-1* or *loqs* germline clones (GLCs). In wild-type stage 10 egg chambers, we observed that Osk, Cup, and Loqs were all tightly restricted to the posterior cortex of the oocyte (Figure 8.8, A-C). In *loqs* null GLCs, we also noted that Osk and Cup were localized to the pole plasm (Figure 8.8, D-F). Therefore, despite the absence of Loqs protein, the pole plasm appears to establish normally,

which is consistent with our previous findings that the number of embryonic pole cells is unchanged in *loqs* null embryos.

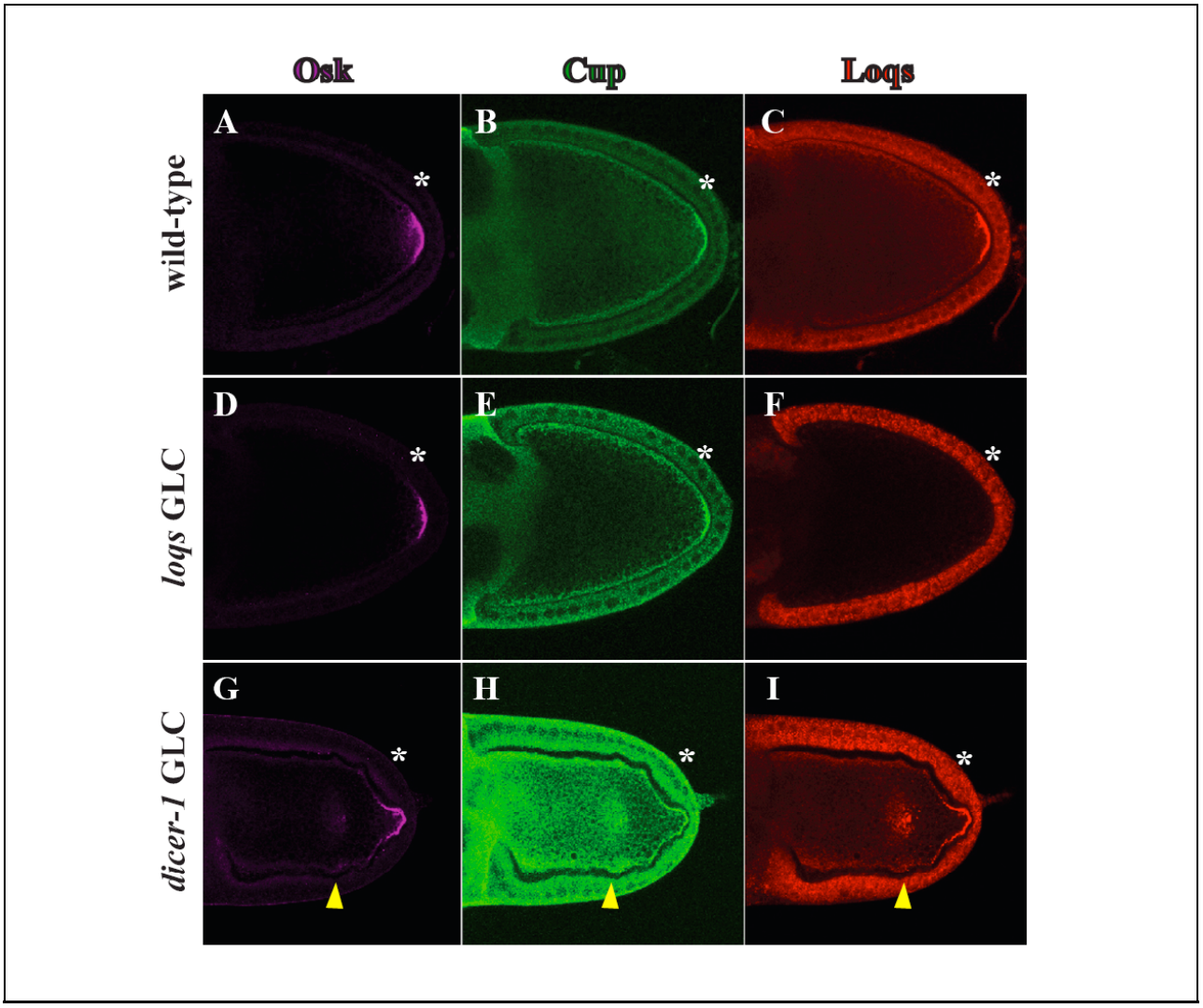

Figure 8.8: Disrupting the Loqs-independent branch of the miRNA pathway destabilizes pole plasm. Ovaries were dissected from wild-type (A-C), and germline clones (GLC) for *loqs* (D-F) and *dicer-1* (G-I). IHC were performed using anti-Osk (purple), anti-Cup (green) and anti-Loqs (red). Asterisks indicate the location of the pole plasm. Yellow arrowheads reflect location of pole plasm-positive staining positioned anterior to the pole plasm.

However, in *dicer-1* null GLCs, we observed a dramatic mislocalization of Osk, Cup and Loqs from the posterior oocyte cortex (Figure 8.8, G-I). Instead of the proteins being tightly

localized the posterior pole, we often noted a mislocalized aggregation of pole plasm proteins in the center of the oocyte cytoplasm (Figure 8.8, G-I, yellow arrowhead). Since Dicer-1 is required for the production of all miRNAs, we speculate that mature miRNAs play a critical role in proper pole plasm tethering to the posterior pole of the oocyte. In addition, since *loqs* null GLCs do not display these same defects, we can also conclude that the miRNAs that control pole plasm formation are dependent upon Dicer-1 for full activity but do not require Loqs, that is Dicer-1-dependent/Loqs-independent.

X. Mass-spectroscopy of Loqs-associated proteins

In order to understand the function of Loqs in oogenesis, Qinghua Liu's lab performed an immunoprecipitation/mass spectroscopy (IP-MS) analysis of Loqs-associated proteins from S2 cells (Q. Liu, unpublished data). Among the 51 unique proteins that were identified (see Appendix), hits to both Dicer-1 and Loqs were identified, serving as an internal control for the quality of the IP-MS data, as Loqs/Dicer-1 complexes have been identified in previous studies (Jiang et al., 2005; Saito et al., 2005). Intriguingly, several known RNA-associated proteins were also identified in this study, including Trailer-Hitch (Tral), poly-A binding protein (PABP), Hrb27C, dFMR1, IGF-II mRNA binding protein (Imp) and Ataxin-2 (Goodrich et al., 2004; Ishizuka et al., 2002; Nielsen et al., 2002; Roy et al., 2004; Satterfield and Pallanck, 2006; Wilhelm et al., 2005). We decided to validate the IP-MS data by examining the subcellular distribution and protein association of dFMR1, a putative component of the RISC complex (Ishizuka et al., 2002; Jin et al., 2004; Megosh et al., 2006).

Previous studies have demonstrated a role for dFMR1 in the formation of pole cells, suggesting that it may also represent a pole plasm associated factor (Megosh et al., 2006). To

determine whether Loqs and dFMR1 form a complex in vivo, I generated ovarian extracts from wild-type females and used anti-Loqs polyclonal antibodies as an IP reagent. Western blots against dFMR1 protein revealed that Loqs and dFMR1 co-IP from ovaries (Figure 8.9). This, in addition to previous data showing the interaction of Loqs and AGO1, suggest that Loqs might be associated with the miRISC complex, though it may not play a direct role in miRNA loading onto the miRISC (Jiang et al., 2005; Saito et al., 2005); and (X. Liu and Q. Liu, unpublished).

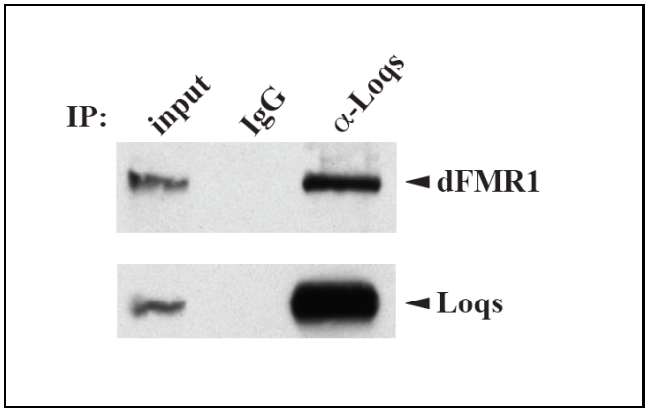

Figure 8.9: Loqs and dFMR1 co-immunoprecipitate from ovarian extracts. Extracts were preprared from wild-type ovaries and either pre-immune serum (IgG) or anti-Loqs were used as IP reagents. Input represents ~20% of total lysate. Membranes were probed for dFMR1. Anti-Loqs antibodies were used as an IP control.

The IP-MS analysis also revealed that Tral is a Loqs-associated protein. Previous studies have demonstrated that Tral exists as a part of a large protein-RNA complex that includes other proteins such as Me31B and Cup (Wilhelm et al., 2005). Both Cup and Me31B have been described as playing various roles in translational control, mRNA stabilization and localization (Nakamura et al., 2001; Wilhelm et al., 2000). Conversely, analysis of *tral* mutants suggest that it is involved in efficient membrane trafficking, as Tral associates with ER exit sites in nurse cells and is required for the secretion of Grk and Yl (Wilhelm et al., 2005). Although I have been unable to validate the association of Loqs and Tral by co-IP or IHC analyses, the IP-MS results suggest that Loqs may play a role in the sequestration of secreted mRNAs through a miRISC-associated mechanism.

XI. Discussion

The initial observations that Loqs is localized both to RNP-like perinuclear particles and the pole plasm, a specialized posterior region of the oocyte cytoplasm, suggest that Loqs is involved in the binding and sequestration of localized mRNAs. Another pole plasm and RNP-associated protein, Cup, is involved in translational inhibition through binding to eIF4E and preventing eIF4G recruitment (Nakamura et al., 2004; Wilhelm et al., 2003; Zappavigna et al., 2004). My data show that Loqs and Cup overlap in their pattern of expression and interact with each other through co-immunoprecipitation studies.

XI.A. Loqs dispensable for pole plasm and pole cell formation

Loqs is a genuine pole plasm factor, as disrupting pole plasm formation or ectopic pole plasm localization changes the pattern of Loqs distribution. Mutations in *stau* ablate pole plasm formation, presumably though the inability to localize *osk* mRNA to the posterior pole of the developing oocyte (Micklem et al., 2000; St Johnston et al., 1991). Conversely, ectopic localization of *osk* mRNA to the anterior pole of the developing oocyte result a bicaudal phenotype, with the formation of "pole plasm" at the oocyte's anterior cortex (Ephrussi and Lehmann, 1992). As Loqs is closely associated with the pole plasm, I expected that strong *loqs* loss-of-function alleles would present with defects in pole plasm formation or posterior patterning defects. Surprisingly, I found that mutations in *loqs* affected neither pole plasm nor pole cell formation. Additionally, embryonic patterning was grossly unaffected by loss of Loqs^{+} function. These data suggest that while Loqs is a component of the pole plasm, it is not required for the formation or integrity of pole plasm function.

XI.B. Dicer-1and Loqs have differential requirements for pole plasm assembly

However, Loqs pole plasm localization suggested that the miRNA pathway plays a role in pole plasm biology. Studies of pole cell formation in *dicer-1* mutant embryos showed that 70% of Dicer-1 depleted embryos completely lacked pole cells and the remaining 30% of embryos contained on average 16 pole cells, significantly fewer than the 24 pole cells observed in wild-type embryos (Megosh et al., 2006). Since the pole plasm is a critical determinant of germ cell fate in the developing embryo, the decreased pole cell formation in *dcr-1* mutant embryos indicates that the miRNA pathway plays a critical role (Illmensee and Mahowald, 1974; Megosh et al., 2006). However, as *loqs* null embryos do not display a concomitant decrease in the average number of pole cells (Table 8.1), this suggests a miRNA-dependent yet Loqs-independent role for the miRNA pathway in primordial germ cell formation.

One possible explanation for the different pole cell formation phenotypes observed in *dcr-1*$^{-}$ versus *loqs*$^{-}$ embryos could be attributed to the differential requirement for Dicer-1 and Loqs proteins in miRNA biogenesis (Figure 6.5). While recombinant Dcr-1 is capable of producing mature miRNA duplexes, Loqs greatly enhances Dcr-1's activity by increasing its affinity for pre-miRNA (Jiang et al., 2005). Interestingly, we found that some miRNAs can be efficiently excised from pre-miRNA hairpin moieties by Dcr-1 even in the absence of Loqs (Figure 6.5). Therefore, this differential requirement for the excision of some miRNAs might serve to explain the different pole plasm phenotypes observed in *loqs* and *dcr-1* mutant embryos. In a *dcr-1* mutant ovary, all mature miRNAs would be absent due to the lack of Dcr-1 function. Since *dcr-1* mutant embryos have fewer pole cells (Table 8.1), presumably due to the loss of pole plasm integrity (Figure 8.8), I conclude that miRNAs are required for proper pole plasm/pole cell formation. However, in a *loqs* mutant embryo, pole plasm and pole cell formation are grossly

unaffected. Since a subset of miRNAs can be efficiently generated by Dcr-1 alone, even in the absence of Loqs, I propose that the Dcr-1-dependent but Loqs-independent miRNAs (Figure 6.5b) define the set that are critical for pole plasm formation.

XI.C. Reciprocal expression of AGO1 and Osk reveal role for miRISC and pole plasm tethering

Another important observation of pole plasm biology centers on the dynamic expression of AGO1 protein. During early stages of vitellogenesis (stage 8), AGO1 is localized to the pole plasm along with Loqs and Cup. However, as the egg chambers continue through vitellogenesis, the levels of AGO1 protein begin to decrease until they are nearly undetectable in stage 10 oocytes (Figure 8.7). Coincidentally, the decrease in AGO1 expression corresponds with the increased detection of Osk protein at the pole plasm. Previous studies have shown that the cortical anchoring of Osk protein to the posterior pole of the oocyte is required for proper pole plasm tethering (Vanzo and Ephrussi, 2002). Ovaries lacking Osk protein are unable to retain *osk* mRNA at the posterior pole and embryos have corresponding defects in pole cell formation, reminiscent of the phenotypes observed in *dcr-1* mutant animals (Megosh et al., 2006) and (this study Figure 8.8). Therefore, since AGO1 forms the catalytic core of the miRISC complex and since Dcr-1^{+} function is required for restriction of pole plasm to the posterior pole (Jiang et al., 2005; Liu et al., 2004; Meister et al., 2004), I hypothesize that miRNAs dependent on Dcr-1 for full processing are required to repress premature translation of pole plasm promoting factors via the miRISC. Additionally, I speculate that the turnover of AGO1/miRISC allows for the translational activation of *osk* mRNA, thereby promoting proper pole plasm tethering.

Chapter 9. Conclusions and Future Directions

I. GSC maintenance promoted by multiple mechanisms of transcriptional, translational and epigenetic repression

My studies support the hypothesis that GSC maintenance is controlled by a series of repressive mechanisms, including transcriptional repression of *bam*, translational repression mediated by the Nos-Pum and miRNA pathways, and epigenetic repression mediated by Stwl function. Genome-wide expression profiling experiments underscored the lack of transcriptional differences between the GSC and the CB. Instead, the GSC to CB differentiation pathway is likely controlled by the actions of Nos-Pum complexes, acting as translational repressors (Chen and McKearin, 2005; Szakmary et al., 2005). Indeed, the key transcriptional difference between the GSC and the CB is likely the transcriptional derepression of *bam* in the CB (Chen and McKearin, 2003b). However, my experiments examining the expression profiles of germ cells blocked from differentiation by a *bam* mutation against ectopically induced GSCs by germline-specific expression of a constitutively-active Dpp receptor, Tkv^{CA}, revealed that a small subset of genes may be differentially expressed between these two cell populations.

In order to establish parameters that would better highlight the transcriptional differences between the GSC and its differentiated daughter cells, we examined the expression profile of *bam* mutant germ cells against *stwl bam* double mutant cells. Stwl, a transcription factor that likely interacts with histone-modifying proteins, is required cell-autonomously for GSC maintenance (Maines et al., 2007). While *bam* mutant GSCs are unable to undergo CB differentiation, *stwl bam* double mutants are able to undergo limited differentiation in a *bam*-independent fashion. Therefore, comparison of *bam* mutant germ cells against *stwl bam* germ

cells would reveal Stwl target genes whose transcriptional silencing is required for GSC maintenance. We uncovered a small number of genes that were differentially expressed two-fold or more in *stwl bam* mutants relative to *bam* mutant ovaries. Future examination of these genes will likely reveal a greater understanding of the molecular triggers that promote GSC-to-CB differentiation.

As a parallel exercise, I examined whether we could utilize previously defined stemness genes from mammalian systems to identify factors that also regulate *Drosophila* GSC fate (Ivanova et al., 2002; Ramalho-Santos et al., 2002). I used a hypomorphic *bam* background for this genetic screen and used fertility as an indicator of *bam* modification. Surprisingly, CSN4, a subunit of the COP9 signalosome complex, CSN, was identified as a Suppressor of *bam*, Su(*bam*). This suggested that the CSN holo-complex normally acts as a negative regulator of *bam*, either by destabilizing Bam function or directly affecting Bam protein turnover. Toward the latter hypothesis, I also found that the Cullin-1 component of the SCF E3 ubiquitin ligase complex also acted as a Su(*bam*) gene, further supporting the requirement for Bam degradation in GSC maintenance.

Finally, I conducted studies examining the requirement of a double-stranded RNA-binding protein, Loqs, in GSC maintenance, oogenesis, and miRNA biogenesis. Germline mosaic analyses demonstrated that Loqs is required cell-autonomously for GSC maintenance (Park et al., 2007). Loqs antibodies revealed that it localizes to two sites commonly associated with protein-RNA complexes during oogenesis: the nuage and the oocyte pole plasm. I found that Loqs does not overlap in its distribution with previously described nuage proteins, suggesting that the RNPs identified in oogenesis are heterogenous in their composition. Additionally, I observed that the miRNA pathway, independent of Loqs function, maintains the

pole plasm assembly and architecture. In *dcr-1* mutant egg chambers, the pole plasm is not tightly localized to the posterior pole of the developing oocyte. This suggests that *dcr-1*-dependent miRNAs, independent of Loqs+ function are required for the proper sequestration of pole plasm components.

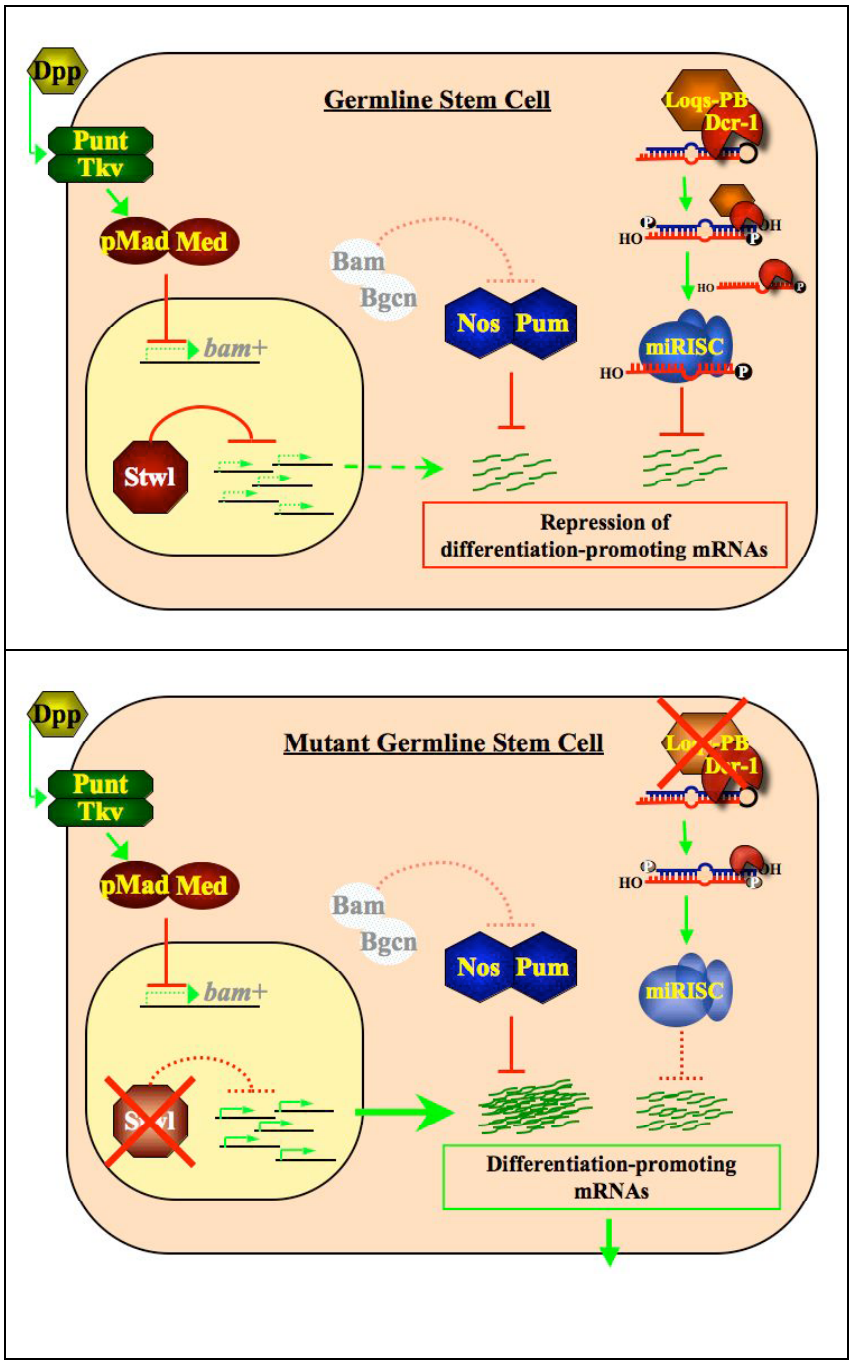

Figure 9.1: A model for the Stwl- and Loqs-mediated maintenance of GSC fate through transcriptional and translational repression.

(Top) In a wild-type germline stem cell, the Dpp signaling pathway represses the *bam* transcription. The absence of Bam-Bgcn complexes promotes the activity of Nos-Pum complexes, allowing for the translational inhibition of CB-promoting mRNAs. Stwl activity in the GSC represses the transcription of these mRNAs. Loqs-Dcr-1 complexes produce miRNAs that function through the miRISC to repress translation of a pool of CB-promoting mRNAs.

(Bottom) In a mutant GSC, lacking Stwl, transcription of differentiation-promoting mRNAs increases the mRNA pool and allows for differentiation despite full Nos-Pum activity. In a Loqs mutant GSC, miRNA biogenesis is altered and the lack of mature miRNAs impairs the ability of the miRISC to repress translation of CB-promoting mRNAs.

II. Future Aims

In the following section, I will detail some future experiments that will further our understanding of *Drosophila* GSC biology and the role of translational repression in controlling GSC differentiation and pole plasm formation.

II.A. Protein profiling of GSCs, CBs and differentiated cysts

Previous studies have shown that the GSC is largely prevented from differentiation by translational repression, mediated by Nos-Pum and miRISC complexes. Genome-wide expression profiling experiments revealed that the transcriptional differences between the GSC and CB are largely indistinguishable. Instead, the action of Bam-Bgcn serves to antagonize the function of Nos-Pum as translational repressors, allowing for the translation of CB-promoting differentiation factors. If this hypothesis is true, this predicts that there will be key proteins that will be abent in the translationally-repressed GSC and present in the translationally-active CB.

Toward the identification of these proteins, we can utilize a two-dimensional gel electrophoresis with subsequent mass spectrometry (2D/MS; methods reviewed in (Delahunty and Yates, 2005). Ovarian extracts from $bam^{\Delta 86}$ mutant females and P{hs-*bam*}; $bam^{\Delta 86}/bam^{\Delta 86}$ females will be compared to one another, with both genotypes exposed to heat-shock induction immediately prior to dissection. In the *bam* mutant females carrying the P{hs-*bam*} transgene, heat-shock induction will force each of the undifferentiated *bam* mutant germ cells to simultaneously initiate the CB-differentiation pathway (Ohlstein and McKearin, 1997). Extracts from these two genotypes can be collected and separated first by isoelectric focusing and subsequently by molecular weight. A protein gel stain will be used to identify protein spots on

each gel and image analysis will be performed with available gel analysis algorithms. The differentially expressed sports will be excised from the gels and trypsinized to extract proteins. Subsequently, each extracted protein mixture will be examined by mass spectrometry to identify each peptide identity. Common Western blotting and immunohistochemical techniques can be used to validate 2D/MS analyses.

Another similar approach would use a technique termed 2D Differential In-gel Electrophoresis (2D-DIGE). This approach is similar to the one detailed above, except that the two protein samples will be differentially labeled with fluorescent dyes prior to 2D electrophoresis (Zhou et al., 2002). This should allow for a simpler, quantitative identification of differentially expressed spots, as the samples will not experience the variability associated with running separate gels for each extract.

Using these or similar approaches should uncover proteins that are differentially expressed between the undifferentiated *bam* mutant germ cells and the *bam* mutant germ cells forced to differentiate by induction of the P{hs-*bam*} transgene. Bam protein will serve as an internal control, which should be highly abundant in the P{hs-*bam*} induced extracts. This methodology should allow for identification of the pool of CB-promoting mRNAs that are actively translated to promote GSC differentiation.

II.B. Differential requirement of Loqs- and Dcr-1-mediated miRNA processing during oogenesis

Loqs binds to and enhances Dcr-1-mediated excision of mature miRNA duplexes from the pre-miRNA hairpin moiety. In the absence of Dcr-1, miRNA processing is completely abolished. However, studies of Loqs from Qinghua Liu's lab have shown that some miRNAs are efficiently excised from pre-miRNA hairpin structures in the absence of Loqs. This differential

requirement has allowed for a greater understanding of miRNA requirements during oogenesis. Since both Dcr-1 and Loqs are required for GSC maintenance, the set of miRNAs that regulate GSC maintenance will be defined by the subset that requires both Dcr-1+ and Loqs+ function for efficient miRNA excision (i.e., miRNAs produced by Loqs-dependent miRNA excision). However, pole plasm assembly and integrity require Dcr-1+ function but not Loqs+ function. This suggests that the subset of miRNAs that control pole plasm architecture are defined by the subset that do not absolutely require Loqs+ function (i.e., miRNAs produced by Dcr-1-dependent but Loqs-independent miRNA excision).

In order to determine the subsets of miRNAs that play roles in the GSC or the pole plasm, it will be important to determine the complete set of miRNAs that are efficiently excised from pre-miRNA precursors in the presence or absence of Loqs. Currently, we only have a collection of 16 out of 78 *Drosophila* miRNAs that have been examined in wild-type and *loqs* mutant extracts (Figure 6.5). However, this may provide a starting point for the examination of variables, such as the secondary pre-miRNA stem-loop structure, to determine the requirement for Loqs in Dcr-1-mediated miRNA excision. This approach, taken together with efforts to identify ovary-enriched miRNAs, will provide key insights into the multiple requirements for the miRNA pathway in GSC maintenance and pole plasm assembly.

II.C. Identification of Loqs-associated RNAs

Based upon the double-stranded RNA binding domains of Loqs and its localization to both nuage-like particles and pole plasm, a reasonable prediction follows that Loqs protein will be found in protein-RNA complexes with miRNAs and/or translationally-repressed mRNAs. To identify the mRNAs and miRNAs associated with Loqs RNP complexes, future experiments will

focus on the immunoprecipitation of Loqs followed by nucleic acid recovery and probing oligonucleotide microarrays; protocol reviewed in (Keene et al., 2006).

Using this approach, we should be able to identify the RNAs that are associated with Loqs. Based upon pole plasm studies of Loqs, I am confident that some pole plasm associated RNAs will be found in Loqs immunoprecipitates. For example, both *osk* and *nos* RNAs are found in the pole plasm. Based upon studies in osk^{6}, $stau^{D3}$, and P{*osk-bcd*3′UTR} ovaries, there is a high probability that Loqs might be associated with *osk* RNA. In addition, studies of Loqs in a weak *nos* background suggest that *loqs* mutations act as dominant suppressors of *nos* (Verrotti and Wharton, 2000). These data suggest that Loqs acts as a negative regulator of *nos*, presumably through translational repression, and indicate that Loqs and *nos* mRNA might be found in Loqs RNP complexes.

APPENDIX

Summary of Loqs Immunoprecipitation-Mass Spectrometry data

Gene identifier	Gene name/identify	Peptide hits	Notes
CG11148		37 of 93	
CG18102	shibire	23 of 116	
	poly A binding protein	34 of 102	
RE19210p		37 of 111	two genes found within cDNA: CG32781 and CG32782 (tlk)
AT27578p	**rasputin (rin)**	34 of 103	RNA binding
CG4857		12 of 79	
AT05170	**Atx2**	12 of 27	
GA18066		17 of 104	D.pse; BLAST Hsc70
CG8715-PA	lingerer	5 of 26	copulation defect
GH08269	**trailer hitch**	7 of 15	RNA binding protein
LP14942	CG18811	5 of 36	
CG17271		8 of 43	
GA18704	**Atx2**	7 of 32	D.pse; BLAST Atx2
GA10795		12 of 82	D.pse; ?
GA10287	**Hrb27C**	6 of 22	D.pse; BLAST Hrb27C
GA15090		10 of 44	D.pse;
CG7177		5 of 31	kinase activity
RE18252	CG5953	6 of 12	
Hrb27C	**Hrb27C**	4 of 6	hnRNP
CG4792	**Dicer-1**	2 of 33	Known interaction
CG6866	**Loqs (R3D1L)**	5 of 13	Positive control
CG17255		4 of 36	
RH35990	CG14648	3 of 14	
Hsp70	Hsp70	2 of 21	
GA19915	**Loqs**	5 of 9	D.pse; BLAST Loqs
CG8937	Hsc70-1	2 of 34	
CG10543		1 of 10	RNA pol II fxn; nucleic acid metabolism?
GA21277		2 of 16	D.pse; lingerer
LD21622	shibire	5 of 9	

Gene identifier	Gene name/identify	Peptide hits	Notes
CG6143	Protein on ecdysone puffs	1 of 11	Pep; mRNA splicing?
CG18740	moira	2 of 24	
AT22221	**Atx2**	3 of 7	
CG11505		3 of 28	
	dFMR1	3 of 48	
LD05893	CG15735	2 of 3	
RE72930	**IGF-II mRNA binding protein (Imp)**	1 of 7	mRNA binding; translational reg
CG2017		2 of 8	
LD02061	legless (lgs)	1 of 30	Wnt sig; beta-cat binding
LD02225	CG5640	1 of 37	transcr. repressor?
GH10652	CG10077	2 of 24	helicase fxn?
	Hsp70Bb	2 of 11	
GA19640		4 of 52	D.pse; BLAST CG6498
CG6944	Lamin	1 of 27	
RE48592	Hsp68	1 of 14	
GA10457	Numb-associated kinase	1 of 22	D.pse; BLAST Nak
anon2A12	pavarotti	2 of 62	cytokinesis
SD01621	**Dicer-1**	1 of 13	
CG13280		5 of 41	
GA13081		1 of 20	D.pse; BLAST CG14562
GA12985		1 of 58	D.pse; BLAST CG14438
GA10551		---	D.pse; BLAST CG10761

* genes in bold indicate those that have been previously identified as having a role in RNA binding or RNA-associated function

BIBLIOGRAPHY

Ahmad, K. and Henikoff, S. (2002). The histone variant H3.3 marks active chromatin by replication-independent nucleosome assembly. *Mol Cell* **9**, 1191-200.

Akiyama, T. (2002). Mutations of stonewall disrupt the maintenance of female germline stem cells in Drosophila melanogaster. *Dev Growth Differ* **44**, 97-102.

Bellen, H. J., Levis, R. W., Liao, G., He, Y., Carlson, J. W., Tsang, G., Evans-Holm, M., Hiesinger, P. R., Schulze, K. L., Rubin, G. M. et al. (2004). The BDGP gene disruption project: single transposon insertions associated with 40% of Drosophila genes. *Genetics* **167**, 761-81.

Bhaskar, V. and Courey, A. J. (2002). The MADF-BESS domain factor Dip3 potentiates synergistic activation by Dorsal and Twist. *Gene* **299**, 173-84.

Boyer, L. A., Langer, M. R., Crowley, K. A., Tan, S., Denu, J. M. and Peterson, C. L. (2002). Essential role for the SANT domain in the functioning of multiple chromatin remodeling enzymes. *Mol Cell* **10**, 935-42.

Breitwieser, W., Markussen, F. H., Horstmann, H. and Ephrussi, A. (1996). Oskar protein interaction with Vasa represents an essential step in polar granule assembly. *Genes Dev* **10**, 2179-88.

Cabrera, G. R., Godt, D., Fang, P.-Y., Couderc, J.-L. and Laski, F. A. (2002). Expression pattern of Gal4 enhancer trap insertions into the bric ‡ brac locus generated by P element replacement. *Genesis* **34**, 62.

Casanueva, M. O. and Ferguson, E. L. (2004). Germline stem cell number in the Drosophila ovary is regulated by redundant mechanisms that control Dpp signaling. *Development* **131**, 1881-90.

Chen, D. and McKearin, D. (2003a). Dpp signaling silences bam transcription directly to establish asymmetric divisions of germline stem cells. *Curr Biol* **13**, 1786-91.

Chen, D. and McKearin, D. (2005). Gene circuitry controlling a stem cell niche. *Curr Biol* **15**, 179-84.

Chen, D. and McKearin, D. M. (2003b). A discrete transcriptional silencer in the bam gene determines asymmetric division of the Drosophila germline stem cell. *Development* **130**, 1159-70.

Cho, P. F., Poulin, F., Cho-Park, Y. A., Cho-Park, I. B., Chicoine, J. D., Lasko, P. and Sonenberg, N. (2005). A new paradigm for translational control: inhibition via 5'-3' mRNA tethering by Bicoid and the eIF4E cognate 4EHP. *Cell* **121**, 411-23.

Chou, T. B., Noll, E. and Perrimon, N. (1993). Autosomal P[ovoD1] dominant female-sterile insertions in Drosophila and their use in generating germ-line chimeras. *Development* **119**, 1359.

Christerson, L. B. and McKearin, D. M. (1994). orb is required for anteroposterior and dorsoventral patterning during Drosophila oogenesis. *Genes Dev* **8**, 614-28.

Clark, K. A. and McKearin, D. M. (1996). The Drosophila stonewall gene encodes a putative transcription factor essential for germ cell development. *Development* **122**, 937-50.

Coller, J. and Parker, R. (2004). Eukaryotic mRNA decapping. *Annu Rev Biochem* **73**, 861-90.

Cope, G. A. and Deshaies, R. J. (2003). COP9 signalosome: a multifunctional regulator of SCF and other cullin-based ubiquitin ligases. *Cell* **114**, 663-71.

Cope, G. A., Suh, G. S., Aravind, L., Schwarz, S. E., Zipursky, S. L., Koonin, E. V. and Deshaies, R. J. (2002). Role of predicted metalloprotease motif of Jab1/Csn5 in cleavage of Nedd8 from Cul1. *Science* **298**, 608-11.

Cutler, G., Perry, K. M. and Tjian, R. (1998). Adf-1 is a nonmodular transcription factor that contains a TAF-binding Myb-like motif. *Mol Cell Biol* **18**, 2252-61.

Delahunty, C. and Yates, J. R., 3rd. (2005). Protein identification using 2D-LC-MS/MS. *Methods* **35**, 248-55.

Denli, A. M., Tops, B. B., Plasterk, R. H., Ketting, R. F. and Hannon, G. J. (2004). Processing of primary microRNAs by the Microprocessor complex. *Nature* **432**, 231-5.

Diatchenko, L., Lau, Y. F., Campbell, A. P., Chenchik, A., Moqadam, F., Huang, B., Lukyanov, S., Lukyanov, K., Gurskaya, N., Sverdlov, E. D. et al. (1996). Suppression subtractive hybridization: a method for generating differentially regulated or tissue-specific cDNA probes and libraries. *Proc Natl Acad Sci U S A* **93**, 6025-30.

Doronkin, S., Djagaeva, I. and Beckendorf, S. K. (2002). CSN5/Jab1 mutations affect axis formation in the Drosophila oocyte by activating a meiotic checkpoint. *Development* **129**, 5053-64.

Doronkin, S., Djagaeva, I. and Beckendorf, S. K. (2003). The COP9 signalosome promotes degradation of Cyclin E during early Drosophila oogenesis. *Dev Cell* **4**, 699-710.

Dubnau, J., Chiang, A. S., Grady, L., Barditch, J., Gossweiler, S., McNeil, J., Smith, P., Buldoc, F., Scott, R., Certa, U. et al. (2003). The staufen/pumilio pathway is involved in Drosophila long-term memory. *Curr Biol* **13**, 286-96.

Ephrussi, A., Dickinson, L. K. and Lehmann, R. (1991). Oskar organizes the germ plasm and directs localization of the posterior determinant nanos. *Cell* **66**, 37-50.

Ephrussi, A. and Lehmann, R. (1992). Induction of germ cell formation by oskar. *Nature* **358**, 387-92.

Findley, S. D., Tamanaha, M., Clegg, N. J. and Ruohola-Baker, H. (2003). Maelstrom, a Drosophila spindle-class gene, encodes a protein that colocalizes with Vasa and RDE1/AGO1 homolog, Aubergine, in nuage. *Development* **130**, 859-71.

Forbes, A. and Lehmann, R. (1998). Nanos and Pumilio have critical roles in the development and function of Drosophila germline stem cells. *Development* **125**, 679-90.

Forstemann, K., Tomari, Y., Du, T., Vagin, V. V., Denli, A. M., Bratu, D. P., Klattenhoff, C., Theurkauf, W. E. and Zamore, P. D. (2005). Normal microRNA maturation and germ-line stem cell maintenance requires Loquacious, a double-stranded RNA-binding domain protein. *PLoS Biol* **3**, e236.

Freilich, S., Oron, E., Kapp, Y., Nevo-Caspi, Y., Orgad, S., Segal, D. and Chamovitz, D. A. (1999). The COP9 signalosome is essential for development of Drosophila melanogaster. *Curr Biol* **9**, 1187-90.

Furukawa, M., Zhang, Y., McCarville, J., Ohta, T. and Xiong, Y. (2000). The CUL1 C-terminal sequence and ROC1 are required for efficient nuclear accumulation, NEDD8 modification, and ubiquitin ligase activity of CUL1. *Mol Cell Biol* **20**, 8185-97.

Gilboa, L. and Lehmann, R. (2004). How different is Venus from Mars? The genetics of germ-line stem cells in Drosophila females and males. *Development* **131**, 4895-905.

Glickman, M. H., Rubin, D. M., Coux, O., Wefes, I., Pfeifer, G., Cjeka, Z., Baumeister, W., Fried, V. A. and Finley, D. (1998). A subcomplex of the proteasome regulatory particle required for ubiquitin-conjugate degradation and related to the COP9-signalosome and eIF3. *Cell* **94**, 615-23.

Gloor, G. B., Preston, C. R., Johnson-Schlitz, D. M., Nassif, N. A., Phillis, R. W., Benz, W. K., Robertson, H. M. and Engels, W. R. (1993). Type I repressors of P element mobility. *Genetics* **135**, 81-95.

Gong, W. J. and Golic, K. G. (2003). Ends-out, or replacement, gene targeting in Drosophila. *Proc Natl Acad Sci U S A* **100**, 2556-61.

Goodrich, J. S., Clouse, K. N. and Schupbach, T. (2004). Hrb27C, Sqd and Otu cooperatively regulate gurken RNA localization and mediate nurse cell chromosome dispersion in Drosophila oogenesis. *Development* **131**, 1949-58.

Gregory, R. I., Yan, K. P., Amuthan, G., Chendrimada, T., Doratotaj, B., Cooch, N. and Shiekhattar, R. (2004). The Microprocessor complex mediates the genesis of microRNAs. *Nature* **432**, 235-40.

Han, J., Lee, Y., Yeom, K. H., Kim, Y. K., Jin, H. and Kim, V. N. (2004). The Drosha-DGCR8 complex in primary microRNA processing. *Genes Dev* **18**, 3016-27.

Harris, A. N. and Macdonald, P. M. (2001). Aubergine encodes a Drosophila polar granule component required for pole cell formation and related to eIF2C. *Development* **128**, 2823-32.

Hatfield, S. D., Shcherbata, H. R., Fischer, K. A., Nakahara, K., Carthew, R. W. and Ruohola-Baker, H. (2005). Stem cell division is regulated by the microRNA pathway. *Nature* **435**, 974-8.

Hawkins, N. C., Thorpe, J. and Schupbach, T. (1996). Encore, a gene required for the regulation of germ line mitosis and oocyte differentiation during Drosophila oogenesis. *Development* **122**, 281-90.

Hay, B., Jan, L. Y. and Jan, Y. N. (1990). Localization of vasa, a component of Drosophila polar granules, in maternal-effect mutants that alter embryonic anteroposterior polarity. *Development* **109**, 425-33.

Hazelrigg, T., Watkins, W. S., Marcey, D., Tu, C., Karow, M. and Lin, X. R. (1990). The exuperantia gene is required for Drosophila spermatogenesis as well as anteroposterior polarity of the developing oocyte, and encodes overlapping sex-specific transcripts. *Genetics* **126**, 607-17.

Hofmann, K. and Bucher, P. (1998). The PCI domain: a common theme in three multiprotein complexes. *Trends Biochem Sci* **23**, 204-5.

Hutvagner, G., McLachlan, J., Pasquinelli, A. E., Balint, E., Tuschl, T. and Zamore, P. D. (2001). A cellular function for the RNA-interference enzyme Dicer in the maturation of the let-7 small temporal RNA. *Science* **293**, 834-8.

Illmensee, K. and Mahowald, A. P. (1974). Transplantation of posterior polar plasm in Drosophila. Induction of germ cells at the anterior pole of the egg. *Proc Natl Acad Sci U S A* **71**, 1016-20.

Ishizuka, A., Siomi, M. C. and Siomi, H. (2002). A Drosophila fragile X protein interacts with components of RNAi and ribosomal proteins. *Genes Dev* **16**, 2497-508.

Ivanova, N. B., Dimos, J. T., Schaniel, C., Hackney, J. A., Moore, K. A. and Lemischka, I. R. (2002). A stem cell molecular signature. *Science* **298**, 601-4.

Jiang, F., Ye, X., Liu, X., Fincher, L., McKearin, D. and Liu, Q. (2005). Dicer-1 and R3D1-L catalyze microRNA maturation in Drosophila. *Genes Dev* **19**, 1674-9.

Jin, P., Zarnescu, D. C., Ceman, S., Nakamoto, M., Mowrey, J., Jongens, T. A., Nelson, D. L., Moses, K. and Warren, S. T. (2004). Biochemical and genetic interaction between the fragile X mental retardation protein and the microRNA pathway. *Nat Neurosci* **7**, 113-7.

Jin, Z. and Xie, T. (2007). Dcr-1 maintains Drosophila ovarian stem cells. *Curr Biol* **17**, 539-44.

Kai, T. and Spradling, A. (2003). An empty Drosophila stem cell niche reactivates the proliferation of ectopic cells. *Proc Natl Acad Sci U S A* **100**, 4633-8.

Kai, T., Williams, D. and Spradling, A. C. (2005). The expression profile of purified Drosophila germline stem cells. *Dev Biol* **283**, 486-502.

Karniol, B., Malec, P. and Chamovitz, D. A. (1999). Arabidopsis FUSCA5 encodes a novel phosphoprotein that is a component of the COP9 complex. *Plant Cell* **11**, 839-48.

Keene, J. D., Komisarow, J. M. and Friedersdorf, M. B. (2006). RIP-Chip: the isolation and identification of mRNAs, microRNAs and protein components of ribonucleoprotein complexes from cell extracts. *Nat Protoc* **1**, 302-7.

Ketting, R. F., Fischer, S. E., Bernstein, E., Sijen, T., Hannon, G. J. and Plasterk, R. H. (2001). Dicer functions in RNA interference and in synthesis of small RNA involved in developmental timing in C. elegans. *Genes Dev* **15**, 2654-9.

Keyes, L. N. and Spradling, A. C. (1997). The Drosophila gene fs(2)cup interacts with otu to define a cytoplasmic pathway required for the structure and function of germ-line chromosomes. *Development* **124**, 1419-31.

Kim-Ha, J., Smith, J. L. and Macdonald, P. M. (1991). oskar mRNA is localized to the posterior pole of the Drosophila oocyte. *Cell* **66**, 23-35.

Landthaler, M., Yalcin, A. and Tuschl, T. (2004). The human DiGeorge syndrome critical region gene 8 and Its D. melanogaster homolog are required for miRNA biogenesis. *Curr Biol* **14**, 2162-7.

Lasko, P. F. and Ashburner, M. (1990). Posterior localization of vasa protein correlates with, but is not sufficient for, pole cell development. *Genes Dev* **4**, 905-21.

Lavoie, C. A., Ohlstein, B. and McKearin, D. M. (1999). Localization and function of Bam protein require the benign gonial cell neoplasm gene product. *Dev Biol* **212**, 405-13.

Lee, Y., Ahn, C., Han, J., Choi, H., Kim, J., Yim, J., Lee, J., Provost, P., Radmark, O., Kim, S. et al. (2003). The nuclear RNase III Drosha initiates microRNA processing. *Nature* **425**, 415-9.

Lee, Y. S., Nakahara, K., Pham, J. W., Kim, K., He, Z., Sontheimer, E. J. and Carthew, R. W. (2004). Distinct roles for Drosophila Dicer-1 and Dicer-2 in the siRNA/miRNA silencing pathways. *Cell* **117**, 69-81.

Lehmann, R. and Nusslein-Volhard, C. (1991). The maternal gene nanos has a central role in posterior pattern formation of the Drosophila embryo. *Development* **112**, 679-91.

Li, L. and Xie, T. (2005). Stem cell niche: structure and function. *Annu Rev Cell Dev Biol* **21**, 605-31.

Lin, H. and Spradling, A. C. (1993). Germline stem cell division and egg chamber development in transplanted Drosophila germaria. *Dev Biol* **159**, 140-52.

Lin, H. and Spradling, A. C. (1997). A novel group of pumilio mutations affects the asymmetric division of germline stem cells in the Drosophila ovary. *Development* **124**, 2463-76.

Liu, J., Carmell, M. A., Rivas, F. V., Marsden, C. G., Thomson, J. M., Song, J. J., Hammond, S. M., Joshua-Tor, L. and Hannon, G. J. (2004). Argonaute2 is the catalytic engine of mammalian RNAi. *Science* **305**, 1437-41.

Liu, Q., Rand, T. A., Kalidas, S., Du, F., Kim, H. E., Smith, D. P. and Wang, X. (2003). R2D2, a Bridge Between the Initiation and Effector Steps of the Drosophila RNAi Pathway. *Science* **301**, 1921-5.

Lund, E., Guttinger, S., Calado, A., Dahlberg, J. E. and Kutay, U. (2004). Nuclear export of microRNA precursors. *Science* **303**, 95-8.

Lyapina, S., Cope, G., Shevchenko, A., Serino, G., Tsuge, T., Zhou, C., Wolf, D. A., Wei, N., Shevchenko, A. and Deshaies, R. J. (2001). Promotion of NEDD-CUL1 conjugate cleavage by COP9 signalosome. *Science* **292**, 1382-5.

Mahowald, A. P. and Kambysellis, M. P. (1980). Oogenesis. In *The Genetics and Biology of Drosophila*, (ed. M. Ashburner and T. R. F. Wright), pp. 141-224. New York: Academic Press.

Maines, J. Z., Park, J. K., Williams, M. and McKearin, D. M. (2007). Stonewalling Drosophila stem cell differentiation by epigenetic controls. *Development* **134**, 1471-9.

Manseau, L., Baradaran, A., Brower, D., Budhu, A., Elefant, F., Phan, H., Philp, A. V., Yang, M., Glover, D., Kaiser, K. et al. (1997). GAL4 enhancer traps expressed in the embryo, larval brain, imaginal discs, and ovary of Drosophila. *Dev Dyn* **209**, 310.

McKearin, D. and Ohlstein, B. (1995). A role for the Drosophila bag-of-marbles protein in the differentiation of cystoblasts from germline stem cells. *Development* **121**, 2937-47.

McKearin, D. M. and Spradling, A. C. (1990). bag-of-marbles: a Drosophila gene required to initiate both male and female gametogenesis. *Genes Dev* **4**, 2242-51.

Megosh, H. B., Cox, D. N., Campbell, C. and Lin, H. (2006). The role of PIWI and the miRNA machinery in Drosophila germline determination. *Curr Biol* **16**, 1884-94.

Meister, G., Landthaler, M., Patkaniowska, A., Dorsett, Y., Teng, G. and Tuschl, T. (2004). Human Argonaute2 mediates RNA cleavage targeted by miRNAs and siRNAs. *Mol Cell* **15**, 185-97.

Micklem, D. R., Adams, J., Grunert, S. and St Johnston, D. (2000). Distinct roles of two conserved Staufen domains in oskar mRNA localization and translation. *Embo J* **19**, 1366-77.

Morimoto, M., Nishida, T., Honda, R. and Yasuda, H. (2000). Modification of cullin-1 by ubiquitin-like protein Nedd8 enhances the activity of SCF(skp2) toward p27(kip1). *Biochem Biophys Res Commun* **270**, 1093-6.

Mourelatos, Z., Dostie, J., Paushkin, S., Sharma, A., Charroux, B., Abel, L., Rappsilber, J., Mann, M. and Dreyfuss, G. (2002). miRNPs: a novel class of ribonucleoproteins containing numerous microRNAs. *Genes Dev* **16**, 720-8.

Mundt, K. E., Liu, C. and Carr, A. M. (2002). Deletion mutants in COP9/signalosome subunits in fission yeast Schizosaccharomyces pombe display distinct phenotypes. *Mol Biol Cell* **13**, 493-502.

Murata, Y. and Wharton, R. P. (1995). Binding of pumilio to maternal hunchback mRNA is required for posterior patterning in Drosophila embryos. *Cell* **80**, 747-56.

Nakamura, A., Amikura, R., Hanyu, K. and Kobayashi, S. (2001). Me31B silences translation of oocyte-localizing RNAs through the formation of cytoplasmic RNP complex during Drosophila oogenesis. *Development* **128**, 3233-42.

Nakamura, A., Sato, K. and Hanyu-Nakamura, K. (2004). Drosophila cup is an eIF4E binding protein that associates with Bruno and regulates oskar mRNA translation in oogenesis. *Dev Cell* **6**, 69-78.

Nelson, M. R., Leidal, A. M. and Smibert, C. A. (2004). Drosophila Cup is an eIF4E-binding protein that functions in Smaug-mediated translational repression. *Embo J* **23**, 150-9.

Nielsen, F. C., Nielsen, J., Kristensen, M. A., Koch, G. and Christiansen, J. (2002). Cytoplasmic trafficking of IGF-II mRNA-binding protein by conserved KH domains. *J Cell Sci* **115**, 2087-97.

Ohlmeyer, J. T. and Schupbach, T. (2003). Encore facilitates SCF-Ubiquitin-proteasome-dependent proteolysis during Drosophila oogenesis. *Development* **130**, 6339-49.

Ohlstein, B., Lavoie, C. A., Vef, O., Gateff, E. and McKearin, D. M. (2000). The Drosophila cystoblast differentiation factor, benign gonial cell neoplasm, is related to DExH-box proteins and interacts genetically with bag-of-marbles. *Genetics* **155**, 1809-19.

Ohlstein, B. and McKearin, D. (1997). Ectopic expression of the Drosophila Bam protein eliminates oogenic germline stem cells. *Development* **124**, 3651-62.

Oron, E., Mannervik, M., Rencus, S., Harari-Steinberg, O., Neuman-Silberberg, S., Segal, D. and Chamovitz, D. A. (2002). COP9 signalosome subunits 4 and 5 regulate multiple pleiotropic pathways in Drosophila melanogaster. *Development* **129**, 4399-409.

Ou, C. Y., Lin, Y. F., Chen, Y. J. and Chien, C. T. (2002). Distinct protein degradation mechanisms mediated by Cul1 and Cul3 controlling Ci stability in Drosophila eye development. *Genes Dev* **16**, 2403-14.

Parisi, M. J., Deng, W., Wang, Z. and Lin, H. (2001). The arrest gene is required for germline cyst formation during Drosophila oogenesis. *Genesis* **29**, 196-209.

Park, J. K., Liu, X., Strauss, T. J., McKearin, D. M. and Liu, Q. (2007). The miRNA pathway intrinsically controls self-renewal of Drosophila germline stem cells. *Curr Biol* **17**, 533-8.

Parks, A. L., Cook, K. R., Belvin, M., Dompe, N. A., Fawcett, R., Huppert, K., Tan, L. R., Winter, C. G., Bogart, K. P., Deal, J. E. et al. (2004). Systematic generation of high-resolution deletion coverage of the Drosophila melanogaster genome. *Nat Genet* **36**, 288-92.

Podust, V. N., Brownell, J. E., Gladysheva, T. B., Luo, R. S., Wang, C., Coggins, M. B., Pierce, J. W., Lightcap, E. S. and Chau, V. (2000). A Nedd8 conjugation pathway is essential for proteolytic targeting of p27Kip1 by ubiquitination. *Proc Natl Acad Sci U S A* **97**, 4579-84.

Ramalho-Santos, M., Yoon, S., Matsuzaki, Y., Mulligan, R. C. and Melton, D. A. (2002). "Stemness": transcriptional profiling of embryonic and adult stem cells. *Science* **298**, 597-600.

Read, M. A., Brownell, J. E., Gladysheva, T. B., Hottelet, M., Parent, L. A., Coggins, M. B., Pierce, J. W., Podust, V. N., Luo, R. S., Chau, V. et al. (2000). Nedd8 modification of cul-1 activates SCF(beta(TrCP))-dependent ubiquitination of IkappaBalpha. *Mol Cell Biol* **20**, 2326-33.

Richter, J. D. and Sonenberg, N. (2005). Regulation of cap-dependent translation by eIF4E inhibitory proteins. *Nature* **433**, 477-80.

Roegiers, F. and Jan, Y. N. (2000). Staufen: a common component of mRNA transport in oocytes and neurons? *Trends Cell Biol* **10**, 220-4.

Roy, G., Miron, M., Khaleghpour, K., Lasko, P. and Sonenberg, N. (2004). The Drosophila poly(A) binding protein-interacting protein, dPaip2, is a novel effector of cell growth. *Mol Cell Biol* **24**, 1143-54.

Saito, K., Ishizuka, A., Siomi, H. and Siomi, M. C. (2005). Processing of pre-microRNAs by the Dicer-1-Loquacious complex in Drosophila cells. *PLoS Biol* **3**, e235.

Sano, H., Nakamura, A. and Kobayashi, S. (2002). Identification of a transcriptional regulatory region for germline-specific expression of vasa gene in Drosophila melanogaster. *Mech Dev* **112**, 129-39.

Satterfield, T. F. and Pallanck, L. J. (2006). Ataxin-2 and its Drosophila homolog, ATX2, physically assemble with polyribosomes. *Hum Mol Genet* **15**, 2523-32.

Schwechheimer, C., Serino, G., Callis, J., Crosby, W. L., Lyapina, S., Deshaies, R. J., Gray, W. M., Estelle, M. and Deng, X. W. (2001). Interactions of the COP9 signalosome with the E3 ubiquitin ligase SCFTIRI in mediating auxin response. *Science* **292**, 1379-82.

Serano, T. L., Karlin-McGinness, M. and Cohen, R. S. (1995). The role of fs(1)K10 in the localization of the mRNA of the TGF alpha homolog gurken within the Drosophila oocyte. *Mech Dev* **51**, 183-92.

Snee, M. J. and Macdonald, P. M. (2004). Live imaging of nuage and polar granules: evidence against a precursor-product relationship and a novel role for Oskar in stabilization of polar granule components. *J Cell Sci* **117**, 2109-20.

Sonoda, J. and Wharton, R. P. (1999). Recruitment of Nanos to hunchback mRNA by Pumilio. *Genes Dev* **13**, 2704-12.

Spradling, A., Drummond-Barbosa, D. and Kai, T. (2001). Stem cells find their niche. *Nature* **414**, 98-104.

St Johnston, D. (2002). The art and design of genetic screens: Drosophila melanogaster. *Nat Rev Genet* **3**, 176-88.

St Johnston, D., Beuchle, D. and Nusslein-Volhard, C. (1991). Staufen, a gene required to localize maternal RNAs in the Drosophila egg. *Cell* **66**, 51-63.

Szakmary, A., Cox, D. N., Wang, Z. and Lin, H. (2005). Regulatory relationship among piwi, pumilio, and bag-of-marbles in Drosophila germline stem cell self-renewal and differentiation. *Curr Biol* **15**, 171-8.

Tomari, Y., Matranga, C., Haley, B., Martinez, N. and Zamore, P. D. (2004). A protein sensor for siRNA asymmetry. *Science* **306**, 1377-80.

Tomoda, K., Kubota, Y., Arata, Y., Mori, S., Maeda, M., Tanaka, T., Yoshida, M., Yoneda-Kato, N. and Kato, J. Y. (2002). The cytoplasmic shuttling and subsequent degradation of p27Kip1 mediated by Jab1/CSN5 and the COP9 signalosome complex. *J Biol Chem* **277**, 2302-10.

Van Buskirk, C., Hawkins, N. C. and Schupbach, T. (2000). Encore is a member of a novel family of proteins and affects multiple processes in Drosophila oogenesis. *Development* **127**, 4753-62.

Van Doren, M., Williamson, A. L. and Lehmann, R. (1998). Regulation of zygotic gene expression in Drosophila primordial germ cells. *Curr Biol* **8**, 243-6.

Vanzo, N. F. and Ephrussi, A. (2002). Oskar anchoring restricts pole plasm formation to the posterior of the Drosophila oocyte. *Development* **129**, 3705-14.

Verrotti, A. C. and Wharton, R. P. (2000). Nanos interacts with cup in the female germline of Drosophila. *Development* **127**, 5225-32.

Wang, S. and Hazelrigg, T. (1994). Implications for bcd mRNA localization from spatial distribution of exu protein in Drosophila oogenesis. *Nature* **369**, 400-03.

Wang, X., Kang, D., Feng, S., Serino, G., Schwechheimer, C. and Wei, N. (2002). CSN1 N-terminal-dependent activity is required for Arabidopsis development but not for Rub1/Nedd8 deconjugation of cullins: a structure-function study of CSN1 subunit of COP9 signalosome. *Mol Biol Cell* **13**, 646-55.

Wei, N. and Deng, X. W. (1998). Characterization and purification of the mammalian COP9 complex, a conserved nuclear regulator initially identified as a repressor of photomorphogenesis in higher plants. *Photochem Photobiol* **68**, 237-41.

Wei, N. and Deng, X. W. (2003). The COP9 signalosome. *Annu Rev Cell Dev Biol* **19**, 261-86.

Wilhelm, J. E., Buszczak, M. and Sayles, S. (2005). Efficient protein trafficking requires trailer hitch, a component of a ribonucleoprotein complex localized to the ER in Drosophila. *Dev Cell* **9**, 675-85.

Wilhelm, J. E., Hilton, M., Amos, Q. and Henzel, W. J. (2003). Cup is an eIF4E binding protein required for both the translational repression of oskar and the recruitment of Barentsz. *J Cell Biol* **163**, 1197-204.

Wilhelm, J. E., Mansfield, J., Hom-Booher, N., Wang, S., Turck, C. W., Hazelrigg, T. and Vale, R. D. (2000). Isolation of a ribonucleoprotein complex involved in mRNA localization in Drosophila oocytes. *J Cell Biol* **148**, 427-40.

Williamson, A. and Lehmann, R. (1996). Germ cell development in Drosophila. *Annu Rev Cell Dev Biol* **12**, 365-91.

Wilsch-Brauninger, M., Schwarz, H. and Nusslein-Volhard, C. (1997). A sponge-like structure involved in the association and transport of maternal products during Drosophila oogenesis. *J Cell Biol* **139**, 817-29.

Wilson, J. E., Connell, J. E. and Macdonald, P. M. (1996). aubergine enhances oskar translation in the Drosophila ovary. *Development* **122**, 1631-9.

Wolf, D. A., Zhou, C. and Wee, S. (2003). The COP9 signalosome: an assembly and maintenance platform for cullin ubiquitin ligases? *Nat Cell Biol* **5**, 1029-33.

Xie, T. and Spradling, A. C. (1998). decapentaplegic is essential for the maintenance and division of germline stem cells in the Drosophila ovary. *Cell* **94**, 251-60.

Xu, T. and Rubin, G. M. (1993). Analysis of genetic mosaics in developing and adult Drosophila tissues. *Development* **117**, 1223-37.

Yang, L., Duan, R., Chen, D., Wang, J., Chen, D. and Jin, P. (2007). Fragile X mental retardation protein modulates the fate of germline stem cells in Drosophila. *Hum Mol Genet*.

Yi, R., Qin, Y., Macara, I. G. and Cullen, B. R. (2003). Exportin-5 mediates the nuclear export of pre-microRNAs and short hairpin RNAs. *Genes Dev* **17**, 3011-6.

Zamore, P. D., Williamson, J. R. and Lehmann, R. (1997). The Pumilio protein binds RNA through a conserved domain that defines a new class of RNA-binding proteins. *Rna* **3**, 1421-33.

Zappavigna, V., Piccioni, F., Villaescusa, J. C. and Verrotti, A. C. (2004). Cup is a nucleocytoplasmic shuttling protein that interacts with the eukaryotic translation initiation factor 4E to modulate Drosophila ovary development. *Proc Natl Acad Sci U S A* **101**, 14800-5.

Zeng, Y. and Cullen, B. R. (2004). Structural requirements for pre-microRNA binding and nuclear export by Exportin 5. *Nucleic Acids Res* **32**, 4776-85.

Zhang, W., Wang, Y., Long, J., Girton, J., Johansen, J. and Johansen, K. M. (2003). A developmentally regulated splice variant from the complex lola locus encoding multiple different zinc finger domain proteins interacts with the chromosomal kinase JIL-1. *J Biol Chem* **278**, 11696-704.

Zhou, G., Li, H., DeCamp, D., Chen, S., Shu, H., Gong, Y., Flaig, M., Gillespie, J. W., Hu, N., Taylor, P. R. et al. (2002). 2D differential in-gel electrophoresis for the identification of esophageal scans cell cancer-specific protein markers. *Mol Cell Proteomics* **1**, 117-24.